

RELATIONSHIP BETWEEN RESILIENT MODULUS AND SOIL INDEX
PROPERTIES OF UNBOUND MATERIALS

A THESIS SUBMITTED TO
THE GRADUATE SCHOOL OF NATURAL AND APPLIED SCIENCES
OF
MIDDLE EAST TECHNICAL UNIVERSITY

BY

ERDEM ÇÖLERİ

IN PARTIAL FULFILLMENT OF THE REQUIREMENTS
FOR
THE DEGREE OF MASTER OF SCIENCE
IN
CIVIL ENGINEERING

AUGUST 2007

Approval of the Thesis:

**RELATIONSHIP BETWEEN RESILIENT MODULUS AND SOIL INDEX
PROPERTIES OF UNBOUND MATERIALS**

submitted by **ERDEM ÇÖLERİ** in partial fulfillment of the requirements for the degree of **Master of Science in Civil Engineering Department, Middle East Technical University** by,

Prof. Dr. Canan Özgen
Dean, Graduate School of **Natural and Applied Sciences** _____

Prof. Dr. Güney Özcebe
Head of Department, **Civil Engineering** _____

Asst. Prof. Dr. Murat Güler
Supervisor, **Civil Engineering Dept., METU** _____

Examining Committee Members:

Assoc. Prof. Dr. Kemal Önder Çetin
Civil Engineering Dept., METU _____

Asst. Prof. Dr. Murat Güler
Civil Engineering Dept., METU _____

Assoc. Prof. Dr. İsmail Özgür Yaman
Civil Engineering Dept., METU _____

Dr. Soner Osman Acar
Civil Engineering Dept., METU _____

Asst. Prof. Dr. Hikmet Bayırtepe
Civil Engineering Dept., Gazi University _____

Date: _____

I hereby declare that all information in this document has been obtained and presented in accordance with academic rules and ethical conduct. I also declare that, as required by these rules and conduct, I have fully cited and referenced all material and results that are not original to this work.

Name, Last name: Erdem Çöleri

Signature:

ABSTRACT

RELATIONSHIP BETWEEN RESILIENT MODULUS AND SOIL INDEX PROPERTIES OF UNBOUND MATERIALS

ÇÖLERİ, Erdem

M.S., Department of Civil Engineering

Supervisor: Asst. Prof. Dr. Murat Güler

August 2007, 154 pages

In the mechanistic design approach, which has already been started to utilize in several countries, the variations in material properties are better taken into account based on fundamental engineering principles. Resilient modulus is the most important material property that is used in the mechanistic design since it describes the true martial performance of unbound pavement layers under traffic loading. In this thesis, the objective is to determine the resilient modulus, used in the mechanistic design of pavement structures, for the unbound material types used in Turkey and develop linear and nonlinear prediction models to determine resilient response of unbound layers based on soil index properties, California Bearing Ratio (CBR) and Light Falling Weight Deflectometer (LFWD) test results. Application of genetic algorithm and curve shifting methodology to estimate design resilient modulus at various stress states is also investigated using the test results for fine-grained soils. Resilient modulus estimation for a constant stress state based on genetic algorithm and curve shifting methodolgy is quite promising for fine-grained soils since nonlinear constitutive models do not have the capability of representing resilient responses under different conditions. Furthermore, tree-based modeling is

discussed as an alternative way to develop resilient modulus prediction models. The outcome of the study will be a basis for the performance based design specifications of flexible pavements.

Keywords: Resilient modulus, California bearing ratio test, light falling weight deflectometer test, genetic algorithm

ÖZ

ESNEKLİK MODÜLÜ İLE ZEMİN İNDEKS ÖZELLİKLERİ ARASINDAKİ İLİŞKİ

ÇÖLERİ, Erdem

Yüksek Lisans, İnşaat Mühendisliği Bölümü

Tez Yöneticisi: Yr. Doç. Dr. Murat Güler

Ağustos 2007, 154 sayfa

Birçok ülkede kullanılmaya başlanan mekanistik dizayn yaklaşımlarına göre yol dizaynında malzeme özelliklerindeki çeşitliliğin genel mühendislik prensiplerine göre göz önüne alınması gerekmektedir. Bilinen malzeme özellikleri arasında esneklik modülü trafik yükü altındaki üst yapı zemin elemanlarının performansını temsil eden ve dizayn aşamasında kullanılabilecek en önemli değişken olarak görülmektedir. Bu tez çalışmasında, ana amaç Türkiyedeki üst yapı zeminlerinin üst yapı mekanistik dizaynında kullanılmak üzere esneklik modüllerinin belirlenmesi ve esneklik durumlarının tayini için zemin indeks özelliklerine, California taşıma oranı ve düşen hafif yük deformasyon deney sonuçlarına bağlı olarak lineer ve lineer olmayan tahmin modellerinin elde edilmesidir. İnce daneli zeminlerin değişik gerilme seviyelerindeki dizayn esneklik modüllerinin saptanması için genetik algoritma ve eğri kaydırma metotlarının uygulanabilirliği de araştırılmıştır. Belirli bir gerilme seviyesindeki esneklik modülünün genetik algoritma ve eğri kaydırma methodlarıyla tayini ince daneli zeminler için başarılı sonuçlar verirken, linear olmayan genel esas modelleri esneklik durumunun belirlenmesinde yetersiz

kalmaktadır. Bunlara ek olarak, esneklik modülü tahmin modellerinin oluşturulmasında alternatif bir yöntem olarak ağaç modellemesi yöntemi de ele alınmaktadır. Bu çalışmanın sonuçları performansa bağlı esnek üst yapı dizayn şartnamelerinin oluşturulmasında bir temel niteliği taşıyacaktır.

Anahtar Sözcükler: Esneklik modülü, Kaliforniya taşıma oranı deneyi, düşen hafif yük deformasyon deneyi, genetik algoritma

To *Erdoğan, Semra, Didem, Sinem*
and
my wife Selin

ACKNOWLEDGMENTS

I would like to express my deepest appreciation and gratitude to my supervisor, Asst. Prof. Dr. Murat Güler, whose expertise, understanding, and patience, added considerably to my graduate experience.

I owe my special thanks to Turkish General Directorate of Highways (TGDH) pavement division director, Ahmet Gürkan Güngör, for his continual encouragement and endless help during the project.

I would also like to thank Prof. Carl L. Monismith, Dr. Bor-Wen Tsai and all the pavement research center personnel for their guidance, inspiration, and unwavering support during my internship in UC Berkeley.

I am thankful to all the TGDH laboratory personnel, Ali Kahraman, Şimşek Sinan, Şükrü Çalıklı, Necati Ardağ, Ömer Güven and Elvan Ünal, in carrying out the experiments.

I would also like to thank TGDH engineers Cihat Avşar and Onur Özyay for their great assistance through the experiments.

I am deeply indebted to Mustafa and Sinem Ergen for their assistance, guidance and, encouragements during my graduate study.

I am also grateful to my family for their invaluable support without which it is impossible for me to finish my thesis.

Finally, I would also like to thank my wife Selin for her encouragements, unwavering support and intellectual advices.

TABLE OF CONTENTS

ABSTRACT	iv
ÖZ.....	vi
ACKNOWLEDGMENTS	ix
TABLE OF CONTENTS	x
LIST OF TABLES	xiv
LIST OF FIGURES.....	xvi
LIST OF ABBREVIATIONS	xx
CHAPTER	
1. INTRODUCTION.....	1
1.1 General	1
1.2 Problem Statement.....	2
1.3 Research Objectives	4
1.4 Research Scope.....	5
2. LITERATURE REVIEW.....	6
2.1 Introduction	6
2.2 Definition of Resilient Modulus.....	6
2.3 Resilient Modulus Testing.....	8
2.3.1 Factors Affecting Resilient Modulus.....	11
2.3.2 Models Correlating Resilient Modulus with Soil Index Properties.....	15
2.3.2.1 Soil Index Parameters.....	15
2.3.2.2 Proposed Correlation Models for Resilient Modulus in the Literature	18
2.4 CBR Testing	21

2.4.1	Models Correlating Resilient Modulus with CBR	23
2.5	Light Falling Weight Deflectometer (LFWD) Test.....	26
2.5.1	Models Correlating Resilient Modulus with LFWD Test	
Results	28
2.6	Genetic Algorithm and Applications for Mechanistic Empirical	
Design Procedures	28
3.	EXPERIMENTAL STUDY	31
3.1	Introduction	31
3.2	Experimental Design	32
3.2.1	Experiment Set 1 for Correlations between Soil Index Properties	
and Resilient Modulus	32
3.2.2	Experiment Set 2 for Correlations between CBR and Resilient	
Modulus	35
3.2.3	Experiment Set 3 for Correlations between LFWD and Resilient	
Modulus	37
3.3	General Characteristics of Test Specimens	42
3.4	Test Setup and Procedure for Resilient Modulus Testing	45
3.4.1	Resilient Modulus Test Setup.....	45
3.4.2	Resilient Modulus Test Procedure.....	50
3.4.2.1	Specimen Preparation.....	50
3.4.2.2	Conducting Tests	52
3.4.3	Loading Wave Form for Resilient Modulus Testing.....	56
3.5	Test Setup and Procedure for CBR Testing	57
3.5.1	CBR Test Setup	57
3.5.2	CBR Test Procedure	58
3.6	Test Setup and Procedure for LFWD Testing	61
4.	STATISTICAL MODELS FOR RESILIENT MODULUS	
PREDICTION	63
4.1	Introduction	63

4.2	Resilient Modulus, CBR and LFWD Test Results	66
4.3	Development of Conventional Constitutive Models Based on Resilient Modulus Test Results	73
4.4	Models Correlating Resilient Modulus with Soil Index Properties (Experiment Set 1).....	75
4.4.1	Statistical Analysis Procedure Used for Model Development (Demonstration Example)	76
4.4.1.1	Pairs Plots	77
4.4.1.2	Correlation Matrix	78
4.4.1.3	ANOVA Table.....	79
4.4.1.4	Mallow’s C_p	81
4.4.1.5	Regression Analysis and Residual Plots for Model Development.....	84
4.4.2	Linear Model Correlating Resilient Modulus with Soil Index Properties and Stress Levels	88
4.4.3	Linear Model Correlating Universal Constitutive Model Regression Coefficients with Soil Index Properties.....	90
4.4.4	Nonlinear Model Correlating Resilient Modulus with Soil Index Properties.....	93
4.4.4.1	Model Validation Using an Independent Data Set.....	96
4.5	Application of Genetic Algorithm and Curve Shifting Methodology as an Alternative to Constitutive Nonlinear Models (Experiment Set 1).....	97
4.5.1	Demonstration Example	109
4.6	Models Correlating Resilient Modulus with CBR Test Results (Experiment Set 2).....	110
4.6.1	One-to-one Correlation between Resilient Modulus and CBR Test Results	112
4.6.2	Correlation between Resilient Modulus and CBR Test Results Considering the Category Covariate “TYPE”	113
4.6.3	Correlation between Resilient Modulus and CBR Test Results Considering the Soil Index Properties	115

4.6.4	Tree-Based Approach for Model Development	116
4.7	Models Correlating Resilient Modulus with LFWD Test Results (Experiment Set 3).....	122
4.7.1	One-to-one Correlation between Resilient Modulus and LFWD Test Results	123
4.7.2	Correlation between Resilient Modulus and LFWD Test Results Considering the Category Covariate “TYPE”	124
4.7.3	Correlation between Resilient Modulus and LFWD Test Results Considering the Soil Index Properties	126
5.	SUMMARY AND CONCLUSIONS	128
5.1	Summary.....	128
5.2	Conclusions	132
5.3	Recommendations	134
	REFERENCES.....	135
APPENDIX		
A.	Circlly Results for the Typical Pavement Section.....	143
B.	Universal Model Coefficients for Experiment Set 1	146
C.	Genetic Algorithm Code for Curve Shifting (S-PLUS)	149

LIST OF TABLES

TABLES

Table 3.1 Design for the Experiment Set 1 (Total Number of Tests = 75)	34
Table 3.2 Design for the Experiment Set 2 (Total Number of Tests = 104)	39
Table 3.3 Design for the Experiment Set 3 (Total Number of Tests = 39)	41
Table 3.4 Testing Sequence for Granular Materials.....	53
Table 3.5 Testing Sequence for Fine-Grained Materials.....	54
Table 4.1 Tests Results for Experiment Set 1	67
Table 4.2 Tests Results for Experiment Set 2	69
Table 4.3 Tests Results for Experiment Set 3	72
Table 4.4 Independent and Dependent Variables Used for Model Development..	76
Table 4.5 Correlation Matrix Results for the Experiment Set 1 Test Results	79
Table 4.6 ANOVA Table for the Experiment Set 1 Test Results and Soil Index Variables	81
Table 4.7 The Summary Statistics of Experimental Set 1 Linear Model Independent Variables	84
Table 4.8 Factor W_c , Contrast Table.....	85
Table 4.9 Ranges of Independent Stress State Variables	89
Table 4.10 Summary of the Data Set Used for the Validation of the Developed Nonlinear Model.....	96
Table 4.11 Resilient Modulus Master Curve Parameters	106
Table 4.12 Independent and Dependent Variables Used for Model Development (Experiment Set 2).....	111
Table 4.13 Independent and Dependent Variables Used for Model Development (Experiment Set 3).....	123

Table 5.1 Summary of Developed Models for Resilient Modulus Prediction Based on Soil Index Properties	130
Table 5.2 Summary of Developed Models for Resilient Modulus Prediction Based on Strength Test Results and Soil Index Properties	131
Table A.1 Typical CIRCLY Output	143
Table B.1 Universal Model Coefficients for Experiment Set 1	146

LIST OF FIGURES

FIGURES

Figure 2.1 Elastic and Plastic Responses under Repeated Loads [Huang, 1993] ..	7
Figure 2.2 Variation of Resilient Modulus at Different Moisture Contents for Fine-Grained Soils (A-2-4) [Maher, 2000]	12
Figure 2.3 AASHTO Type 2 Resilient Modulus Test Results at Optimum Water Content (Test Results – Solid Line : Model – Dotted Line) [Maher, 2000]	13
Figure 2.4 AASHTO Type 1 Resilient Modulus Test Results at Optimum Water Content (Test Results – Solid Line : Model – Dotted Line) [Maher, 2000]	13
Figure 2.5 Seasonal Variations in Subgrade Resilient Modulus [Huang, 1993]..	15
Figure 2.6 Variation of Dry-Density with Water Content [Atkins, 2002]	17
Figure 2.7 Correlation Chart for Estimating Resilient Modulus of Subgrade Soils [Huang, 1993].....	24
Figure 2.8 Correlation Chart for Estimating Resilient Modulus of Base/Subbase Soils (a) Untreated (b) Bituminous Treated (c) Cement Treated [Huang, 1993] ...	25
Figure 2.9 LFWD Test Results for 20 Different Locations [Mehta, 2003].....	28
Figure 3.1 Dry-Density and Plasticity Index Variation for the Experiment Set 1 Specimens [(K6-5 : City – Kayseri, Region – 6-5), (AC: Ankara Çankırı), (DS: Diyarbakır Silvan), (DKV: Diyarbakır Kızıltepe Viranşehir), (DB: Diyarbakır Bismil)].....	33
Figure 3.2 Dry-Density and Plasticity Index Variation for the Experiment Set 2 Granular (Type 1) Specimens [(B14/2 : City – Bursa, Region – 14/2), (K: Kayseri), (DB: Diyarbakır Bismil), (KAS: Kastamonu), (KD: Kırıkkale Delice), (KON: Konya)].....	36
Figure 3.3 Dry-Density and Plasticity Index Variation for the Experiment Set 2 Fine-Grained (Type 2) Specimens.....	37

Figure 3.4 Dry-Density and Plasticity Index Variation for the Experiment Set 3 Specimens.....	38
Figure 3.5 Gradation Characteristics for the Experiment Set 1 Soil Types	43
Figure 3.6 Gradation Characteristics for the Experiment Set 2 Granular (Type 1) Soil Types.....	44
Figure 3.7 Gradation Characteristics for the Experiment Set 2 Fine-Grained (Type 2) Soil Types.....	44
Figure 3.8 Gradation Characteristics for the Experiment Set 3 Soil Types	45
Figure 3.9 System for Resilient Modulus Testing.....	48
Figure 3.10 Typical Output for a Resilient Modulus Test.....	49
Figure 3.11 Specimen Preparation Procedure for Granular Materials	51
Figure 3.12 Specimen Preparation Procedure for Fine-Grained Soil Types.....	52
Figure 3.13 User-interface of the Software Used for Resilient Modulus Testing..	55
Figure 3.14 Loading Wave Form for Resilient Modulus Testing [NCHRP, 2004]	57
Figure 3.15 System for CBR Testing	58
Figure 3.16 Saturation Pool for Soaked CBR Specimen Preparation	59
Figure 3.17 Data Output for a Single CBR Test	60
Figure 3.18 LFWD Test Setup	62
Figure 4.1 Summary of the Developed Models.....	65
Figure 4.2 Typical Pavement Section Characteristics.....	75
Figure 4.3 Pairs Plot for the Demonstration of the Interactions between Soil Index Parameters and Resilient Modulus	78
Figure 4.4 Residual Plots for the Linear Regression Model Correlating M_R with Soil Index Parameters.....	86
Figure 4.5 Comparison of Predicted and Measured Resilient Modulus for a Certain Stress State.....	88
Figure 4.6 Comparison of Predicted and Measured Resilient Modulus for Varying Stress State.....	90
Figure 4.7 Comparison of Predicted and Measured Resilient Modulus for Constant Stress State (Based on Universal Constitutive Model Coefficients).....	92

Figure 4.8 Comparison of Predicted and Measured Resilient Modulus for Varying Stress State (Based on Universal Constitutive Model Coefficients)	92
Figure 4.9 Comparison of Nonlinear Model Predicted and Measured Resilient Modulus	94
Figure 4.10 Residuals versus Fitted Values for the Developed Nonlinear Model	95
Figure 4.11 Residuals Histogram for the Estimation of the Deviation from Measured Resilient Modulus (Developed Nonlinear Model)	95
Figure 4.12 Comparison of Nonlinear Model Predicted and Measured Resilient Modulus Value (Based on the Independent Data Set).....	97
Figure 4.13 Deviator Stress vs. Resilient Modulus Curves at Three Different Confining Pressure Levels for a Certain Test.....	98
Figure 4.14 Initial Shift Amount Estimation	99
Figure 4.15 The Residual Standard Error Convergence Trend for Increasing Generations.....	100
Figure 4.16 General Flow Chart for the Application of the Genetic Algorithm ..	101
Figure 4.17 Gamma Fitting Curves with the Shape Parameter $n = 3$, Scale Parameter (B) = 10 , A = -0.2, -0.4, -0.6, -0.8, -1.0, C = $\ln(47139) = 10.76$	103
Figure 4.18 Gamma Fitting Curves with the Shape Parameter $n = 3$, Scale Parameters (B) = 3, 6, 9, 12, 15 , A = -0.5 , C = $\ln(47139) = 10.76$	104
Figure 4.19 Gamma Fitting Curves with the Shape Parameter $n = 3$, Scale Parameter (B) = 13.5, A = -0.5 and C = 11.2	104
Figure 4.20 Final Gamma Fitting Curve for the Representation of the Shifted Test Results (A = -0.39782, B = 13.91460, C = 11.18780 (Eqn. 4.4))	108
Figure 4.21 The Relationship between Confining Pressure and Confining Pressure Shift Factor (Eqn. 4.6)	108
Figure 4.22 Comparison of Predicted and Measured Soaked CBR	112
Figure 4.23 Comparison of Predicted and Measured Resilient Modulus based on One-to-one M_R vs. CBR Model.....	113
Figure 4.24 Comparison of Predicted and Measured Resilient Modulus based on M_R vs. CBR + TYPE Model.....	114

Figure 4.25 Comparison of Predicted and Measured Resilient Modulus based on M_R vs. CBR + Soil Index Parameters Model	116
Figure 4.26 Initial Form of a Regression Tree	117
Figure 4.27 Uniform Regression Tree with the Corresponding Independent Variables.....	118
Figure 4.28 Tree model residual plots: (a) residuals vs. fitted values, (b) normal propability plot of residuals, (c) histogram of residuals.....	119
Figure 4.29 Pruned Regression Tree and Model Fitting Results for Each Interval.....	121
Figure 4.30 Comparison of Predicted and Measured Resilient Modulus based on One-to-one M_R vs. LFWD Model	124
Figure 4.31 Comparison of Predicted and Measured Resilient Modulus based on M_R vs. LFWD + TYPE Model	125
Figure 4.32 Comparison of Predicted and Measured Resilient Modulus based on M_R vs. LFWD + Soil Index Parameters Model.....	127

LIST OF ABBREVIATIONS

TGDH: Turkish General Directorate of Highways

STRCT: Scientific and Technological Research Council of Turkey

METU: Middle East Technical University

LFWD: Light Falling Weight Deflectometer

AASHTO: American Association of State Highway and Transportation Officials

NCHRP: National Cooperative Highway Research Program

CBR: California Bearing Ratio Test

LTPP: Long-Term Pavement Performance

PID: Proportional Gain, Integral Gain, Derivative Gain

LVDT: Linear Variable Displacement Transducers

CHAPTER 1

INTRODUCTION

1.1 General

The reliability of pavement design depends on the success in determining the material properties required for the development of performance prediction models. However, due to technical difficulties, specifications for testing unbound materials have been modified several times in the last decade to achieve reliable estimates of the material properties. Consequently, the lack of well-established test procedures drove researchers to find empirical relations between resilient modulus and the index properties of unbound materials. This thesis presents methodology and findings of a laboratory testing program to seek possible correlations between the resilient modulus, simple field strength tests and the soil index properties of a range of unbound pavement materials based on statistical analyses.

The data for this study were obtained as a part of a research project entitled “Adaptation of Resilient Modulus to Mechanistic-Empirical Design Specifications of Flexible Pavements”. This project is a collaboration between the Middle East Technical University (METU) and the Turkish General Directorate of Highways (TGDH), and is financed by the Scientific and Technological Research Council of Turkey (STRCT). In the laboratory testing program, materials are divided into two types: (a) type1- granular soils (b) type 2 – fine-grained soils. Genetic algorithm applications based on the current AASHTO procedures are also utilized for model development in order to minimize the estimation errors. Validation of the derived

models is performed by back calculating the resilient modulus for extra samples not used for the model development. The outline of the thesis can be summarized as follows: Chapter 1 presents problem statement, objectives and scope of this study. Chapter 2 gives information about the literature and background of the resilient modulus testing and its relation to various laboratory determined soil properties. Chapter 3 presents the methodology used by other researchers for performing the laboratory tests in accordance to AASHTO standards. Chapter 4 discusses the results of analyses and the developed prediction models for resilient modulus. Chapter 5 presents the summary and conclusions about the research.

1.2 Problem Statement

The characteristics and behavior of subgrade, base and subbase soils have a major impact on the performance of flexible pavement systems. Pavement design based on field performance requires using realistic material properties that can simulate the in-situ behavior of unbound layers. There are many empirical methods proposed in the literature which could not successfully characterize the in-situ behavior of unbound layers under traffic loading. The most common test used for the estimation of the unbound layers performance in most of the design specifications is the California Bearing Ratio (CBR) Test. There are, however, certain problems in using the CBR test in the design process of flexible pavements. First, CBR is a quasi-static test that cannot effectively model the types of stresses experienced by the unbound pavement layers. Second, neither the test conditions nor the specimens prepared do not represent the actual field conditions of the materials. In order to reflect the dynamic response of pavement layers to vehicular traffic loads, highway engineers developed new techniques to perform dynamic tests. Resilient modulus test is one of the most common and reliable experiment for the estimation of the unbound layers' response to dynamic traffic loads. The pavement loads on the unbound layers are simulated by the application of a confining pressure and a repeated axial haversine loading which represents the dynamic wheel loads.

Resilient modulus is accepted to be an appropriate measure of stiffness for unbound materials in a pavement structure. Although resilient modulus testing gives the best representation of the in-situ pavement characteristics, resilient modulus for different subgrade soils at different seasonal and construction conditions should be determined for better performance estimation. The lifetime of the pavement depends on the condition of the whole pavement system which is composed of asphalt, subgrade, base and subbase layers. During the construction period, moisture content fluctuations in the base, subbase and subgrade soils change the resilient modulus in the pavement structure. Hence, any correlation that relates the resilient modulus to some other soil properties should account for changes in the general structure of the pavement layers for different soil types in order to estimate a realistic value of design modulus. In addition, the geological characteristics of area from which the test samples are obtained have important effects on the resilient modulus displaying significant variability in Turkey. In order to simulate the geological variations, test results collected from different regions of Turkey are utilized for developing correlation models which can be used during the mechanistic-empirical pavement design process.

Since the laboratory determination of resilient modulus is rather complex in terms of data acquisition and analysis, correlations of resilient modulus with different simple strength and index tests could simplify the design process of both flexible and rigid pavements. Correlations with CBR testing can result in acceptable estimates for the determination of resilient modulus for certain soil index intervals. These correlations would be useful to use by reducing the testing time and costs for pavements with low traffic volumes.

Since conducting resilient modulus and CBR tests during the construction process is time consuming, light falling weight deflectometers (LWD) are also used for in-situ measurement of resilient modulus. However, LWD results can not be directly used for design resilient modulus estimations since they cannot simulate the in-situ traffic loading conditions. Thus, models correlating laboratory and field resilient

modulus values are determined in order to achieve reliable estimates for in-situ performance prediction of unbound layers.

In this research project, the objective is to determine the resilient modulus, used in the mechanistic-empirical design of pavement structures, for the material types used in Turkey, and develop correlation models with soil index properties and specifications to incorporate the resilient modulus in the pavement design process. The outcome of the study will be a basis for the performance based design specifications of flexible pavements in Turkey.

1.3 Research Objectives

The research objectives for this thesis can be summarized as follows:

- Determine whether it is possible to predict the laboratory resilient modulus of unbound materials through simple field strength tests and the index properties using statistical correlation functions.
- Estimate the effects of different environmental and structural factors on the resilient modulus of various unbound materials in Turkey.
- Investigate the applicability of genetic algorithm and curve shifting methodology for the estimation of resilient modulus at various stress states.
- Propose resilient modulus – CBR relationships, if exist, that can be used in the mechanistic-empirical design of flexible pavements.
- Propose a test procedure for the measurement of resilient modulus to be used as a design specification for flexible pavements.
- Evaluate the utilized test procedure for the measurement of resilient modulus in terms of its applicability in Turkey.

1.4 Research Scope

The scope of this study includes conducting resilient modulus, LFWD, CBR and soil index tests to determine the elastic response of unbound pavement layers under in-situ traffic loads. Tests were conducted on a wide range of materials from various regions of Turkey in order to develop reliable correlation functions for resilient modulus. Resilient modulus tests were conducted according to AASHTO T307 specification [2000]. A total of 32 different soil types from different regions of Turkey were collected and divided into two groups as Type 1 and Type 2. This research involves both field investigation and laboratory investigation of these soil types. In the field investigation, LFWD tests were conducted to collect data about the elastic response of pavement sections on the construction site. In the laboratory investigation, simple strength, resilient modulus and soil index tests were conducted in the TGDH laboratories. The laboratory and the simple field strength test results were compared with the resilient modulus test results in order to develop reliable statistical correlation functions for resilient modulus. The results of the 232 LFWD, 132 CBR and 155 resilient modulus tests were analyzed to develop resilient modulus prediction models. Several linear and nonlinear correlation functions were proposed to estimate the laboratory resilient modulus of the tested materials. In addition, application of the genetic algorithm and the curve shifting methodology to determine the resilient modulus for a certain stress state was proved to give better estimates than the statistical based methods for fine-grained soils. An evaluation of the test method for resilient modulus and its applicability as a design specification in Turkey was also discussed. Conclusions and results of this study were presented, accordingly.

CHAPTER 2

LITERATURE REVIEW

2.1 Introduction

This chapter presents information about the resilient modulus and its correlations with simple field strength tests and soil index properties in the literature. In addition, information about the CBR and LFWD tests are also presented. The history of these tests and the existing correlations for different environmental and structural conditions are also emphasized in order to present an overview about the subject.

2.2 Definition of Resilient Modulus

The loading wave form used in the resilient modulus testing should simulate the actual loads in pavements during the service conditions. When a vehicle is approaching to a certain point on the pavement, the amount of load increases from zero to a maximum value. The maximum load level will be reached when the edge of the tire is just above the reference point according to the pseudo-energy simulations [Sousa et al., 1994 ; Monismith et al., 2000]. Thus, the haversine load pulse is proposed for conducting the test since it better simulates the stress state under a wheel load.

The actual resilient response of a material under repeated loading can be determined after a certain number of load applications since there would be considerable permanent deformation within the early stages. As the number of load applications

increases, the plastic strain due to load repetition decreases [Huang, 1993]. Thus, the resilient modulus for a certain sequence is determined using the last 5 measurements out of 100. Resilient modulus is defined as the ratio of the applied deviatoric stress to the elastic vertical strain. Figure 2.1 shows the elastic and plastic responses under the repeated loads. It can be observed from the figure that the permanent deformation rate approaches to zero with the increasing number of repetitions.

$$M_R = \frac{\sigma_d}{\epsilon_r} \quad (2.1)$$

where

σ_d : repeated deviatoric stress;

ϵ_r : resilient recoverable strain.

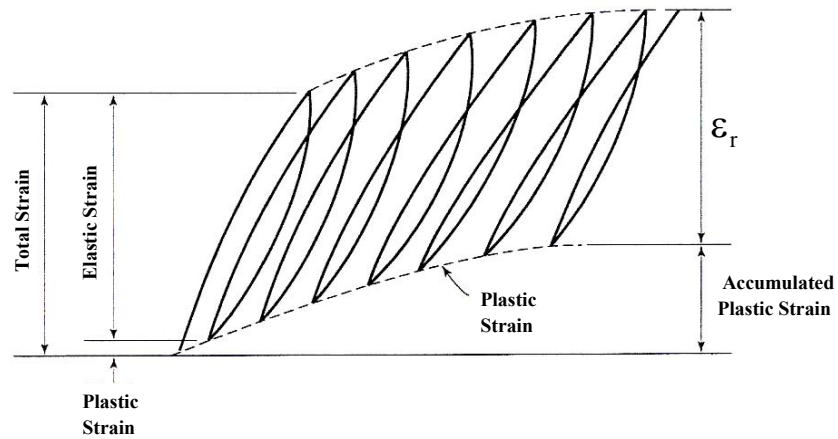
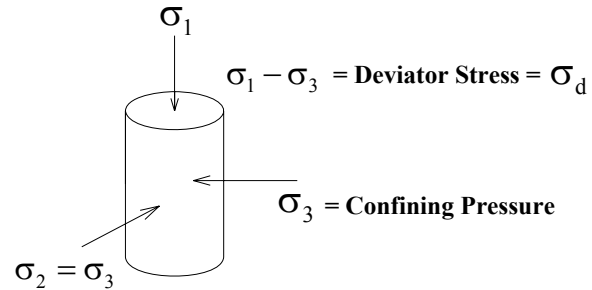


Figure 2.1 Elastic and Plastic Responses under Repeated Loads [Huang, 1993]

2.3 Resilient Modulus Testing

Resilient modulus testing, developed by Seed et al. (1962), aims to determine an index that describes the nonlinear stress-strain behavior of soils under cyclic loading. Resilient modulus is simply the ratio of the dynamic deviatoric stress to the recovered strain under a standard haversine pulse loading. Mechanistic design procedures for pavements and overlays require resilient modulus of unbound pavement layers to determine layer thickness and the overall system response to traffic loads. In AASHTO specification T-274 (1982) based on the mechanistic methods, resilient modulus is considered as an important design input parameter. After this specification, AASHTO TP46, T292, T294 and T307 specifications were also published as improvements were made over the years in the test procedures.

Many nonlinear constitutive models were proposed to describe the phenomenon of stiffness variations of unbound layers under different traffic loads. Accordingly, many equations were developed to define the resilient response of unbound layers as a function of various stress variables as shown in the following:

$$\text{AASHTO Model: } M_R = k_1 (\theta)^{k_2} \quad (2.2)$$

$$\text{Hicks and Monismith [1971]: } \frac{M_R}{\sigma_{\text{atm}}} = k_1 \left(\frac{\theta}{\sigma_{\text{atm}}} \right)^{k_2} \quad (2.3)$$

$$\text{Uzan (Universal) [1985]: } \frac{M_R}{\sigma_{\text{atm}}} = k_1 \left(\frac{\theta}{\sigma_{\text{atm}}} \right)^{k_2} \left(\frac{\sigma_d}{\sigma_{\text{atm}}} \right)^{k_3} \quad (2.4)$$

$$\text{Johnson [1986]: } M_R = k_1 \left(\frac{J_2}{\tau_{\text{oct}}} \right)^{k_2} \quad (2.5)$$

$$\text{Rafael Pezo [1993]: } M_R = k_1 \sigma_d^{k_2} \sigma_3^{k_3} \quad (2.6)$$

$$\text{Louay [1999]: } \frac{M_R}{\sigma_{\text{atm}}} = k_1 \left(\frac{\sigma_{\text{oct}}}{\sigma_{\text{atm}}} \right)^{k_2} \left(\frac{\tau_{\text{oct}}}{\sigma_{\text{atm}}} \right)^{k_3} \quad (2.7)$$

where:

M_R = resilient modulus

$\theta = \sigma_1 + \sigma_2 + \sigma_3$ (bulk stress)

k_1, k_2, k_3 = regression coefficients

σ_d = deviator stress

σ_3 = confining pressure

σ_{atm} = atmospheric pressure

$\tau_{oct} = (1/3)[(\sigma_1 - \sigma_2)^2 + (\sigma_1 - \sigma_3)^2 + (\sigma_2 - \sigma_3)^2]$ (octahedral shear stress)

$J_2 = \sigma_1 \sigma_2 + \sigma_2 \sigma_3 + \sigma_1 \sigma_3 = 2 \sigma_3 (\sigma_3 + \sigma_d) + \sigma^2$ (second stress invariant)

Over the past three decades, various models were developed to determine the resilient response of unbound layers in terms of various soil properties. The AASHTO design procedure developed in 1960 is based on the empirical tests through which the variations in the structural and functional properties of pavements are modeled by using the covariates of terminal serviceability index (p_t), structural number of pavement (SN) and 80-kN total load application at the end of time t (W_{t18}). Later, the general AASHTO model was modified to perform reliable performance estimates by the inclusion of the soil support term (S_i). This covariate is added to the model in order to predict the effect of variations in the subgrade soil. In the AASHTO design guide (1993), the soil support term was changed with the effective resilient modulus covariate [Huang, 1993] which is a single value accounting for the annual variations in the relative damage values. The general relationship for the estimation of pavement performance and the thickness of asphalt layers is as follows:

$$\log W_{t18} = 9.36 \log(SN + 1) - 0.20 + \frac{\log[(4.2 - p_t)/(4.2 - 1.5)]}{0.40 + [1094/(SN + 1)^{5.19}]} + 2.32 \log M_R - 8.07$$

(2.8)

Mechanistic-empirical design procedures for pavements and overlays require the specification of base, subbase and subgrade resilient modulus to determine layer thickness and the overall system response to the traffic loads. In the AASHTO specification T-274 (1982) based on mechanistic-empirical methods, resilient modulus is considered as an important design input parameter. Subsequently, the AASHTO TP46, T292, T294, T307 specifications and the national cooperative highway research program (NCHRP) research results (2004) were published providing important guidelines for the resilient modulus testing. According to these specifications, the main objective of the resilient modulus testing is the evaluation of the support characteristics of unbound layers in terms of resilient modulus values. In this research project, the tests were performed according to the NCHRP research report (2004) guidelines and the AASHTO T307 (2000) specifications proposing the latest guidelines for laboratory determination of resilient modulus. The deficiencies improved in the recent specifications were reported by previous authors [AASHTO TP46, 1994; Pezo et al., 1991; Nazarian, 1993] as:

- Serious flaws in the test results
- Deformation fluctuations during the tests
- Incompatible deformation and load impulse times
- Problems in the LVDT measurements and haversine load applications
- Complex and expensive testing procedures
- Lack of equipment standardization
- Difficulty in training the personnel to prepare specimens and conduct resilient modulus tests
- Inadequacy of controlling the deviatoric stress and the confining pressure levels

In addition, the possible problems during resilient modulus testing addressed by the latest studies are as follows: [AASHTO TP46, 1994 ; Pezo et al., 1991 ; Nazarian, 1993]

- number of load applications during the preconditioning stage
- grouting of the end platens to the sample to decrease the undesirable effects of surface irregularity
- accuracy in controlling the deviatoric stress and the confining pressure
- location of LVDT's (inside or outside the chamber)
- maintaining contact between specimen and end-platens.

2.3.1 Factors Affecting Resilient Modulus

The effects of confining pressure, deviator stress and moisture content on the resilient response of unbound layers have been studied over the past years. Based on these studies, it is known that the variation in the interparticle frictions due to the applied deviatoric stress, confining pressure, moisture content and the degree of compaction affect the stiffness of unbound materials. Granular and fine-grained soils exhibit different behaviors under the resilient modulus testing because of their different interparticular structures.

Fine-grained soils exhibit a stress - softening behavior with the increasing load applications. In addition, they are highly affected from the deviator stress and moisture content variations [Hardcastle, 1992]. The effect of confining pressure on the resilient response of fine-grained soils is generally insignificant [Seed et al., 1962; Thompson, 1976; Pezo, 1994]. For non-cohesive granular soils, the effect of the degree of saturation on the resilient response depends on the fine particles present in the soil matrix. Clean gravels and sands are less sensitive to moisture content variations due to the absence of suction developing voids in the soil structure. Figure 2.2 illustrates the variation of the resilient modulus for a fine-grained soil with different moisture contents [Maher et al., 2000]. In Figure 2.3, the effects of confining pressure and the deviator stress on fine-grained soils are presented based on the tests performed for the same soil type [Maher et al., 2000].

On the other hand, the interparticular friction increases with the increasing load applications for granular materials hence increasing the confining pressure becomes important [Rada, 1981]. Figure 2.4 illustrates this concept for different confining pressure levels [Maher, 2000]. Thus, the bulk stress (θ), which is the summation of the principal stresses, is proposed to be used for model development according to the AASHTO T- 274 (1982). The reason for the stress-hardening behavior is due to the reorientation of the grains into a denser state. In addition, many studies showed that the size of specimen and the stress pulse shape are other important factors affecting the resilient response of unbound materials. [Monismith, 1989; Nataatmadja, 1989]

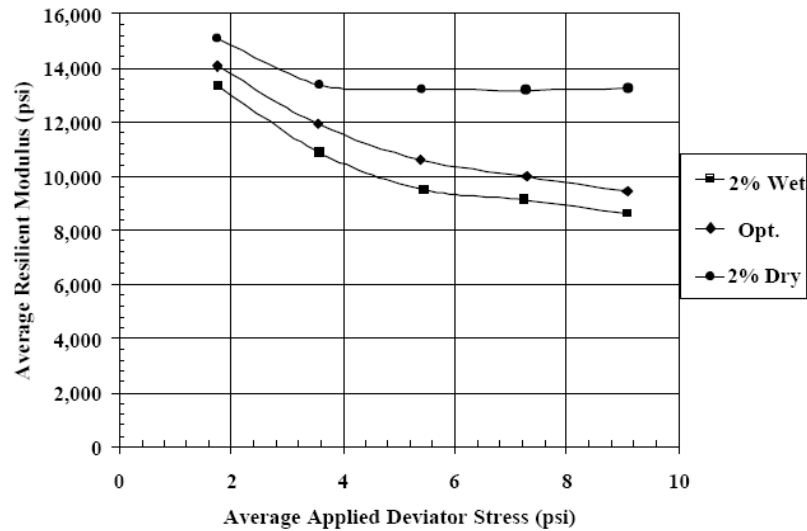


Figure 2.2 Variation of Resilient Modulus at Different Moisture Contents for Fine-Grained Soils (A-2-4) [Maher et al., 2000]

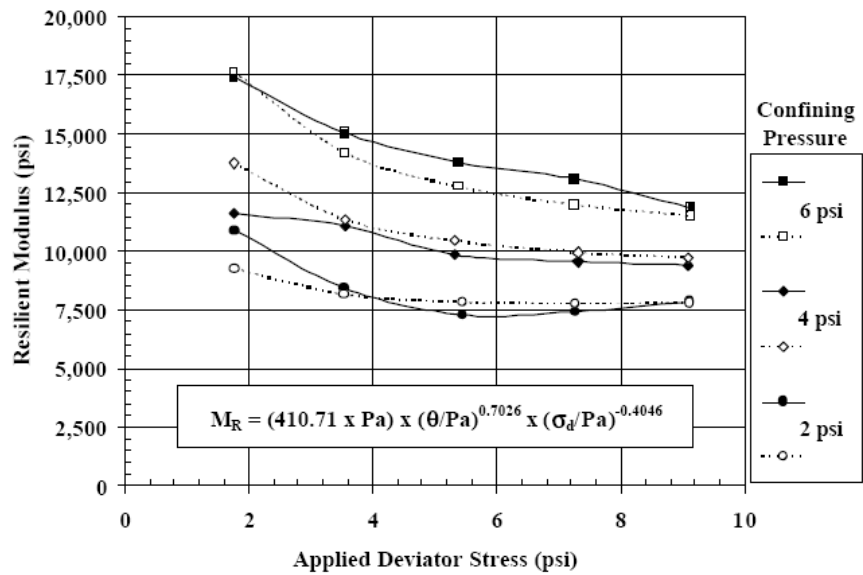


Figure 2.3 AASHTO Type 2 Resilient Modulus Test Results at Optimum Water Content (Test Results – Solid Line : Model – Dotted Line) [Maher et al., 2000]

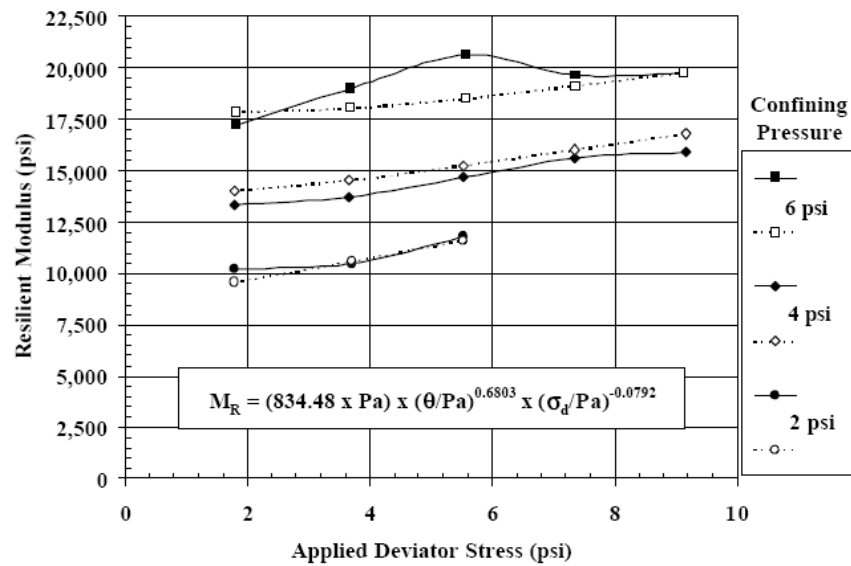


Figure 2.4 AASHTO Type 1 Resilient Modulus Test Results at Optimum Water Content (Test Results – Solid Line : Model – Dotted Line) [Maher et al., 2000].

Temperature effects also have a great influence on the resilient modulus of pavement layers. Freezing of fine-grained and granular soils increases the resilient modulus compared to the unfrozen conditions. In addition, the resilient modulus of recently thawed soils exhibit a significant decrease compared to the unfrozen and frozen conditions. Variations in the resilient modulus of subgrades according to the seasonal changes are given in Figure 2.5 [Huang, 1993]. The most critical time period for the resilient modulus is the end of thaw at which a minimum modulus value can be attained. The critical value of the resilient modulus should be considered during the design of flexible pavements in order to minimize early failures in the life time of pavement structures.

For fine-grained soils, compaction method may affect the variations in the resilient modulus. Static compaction method may result in higher resilient modulus compared to the method of proctor type compaction. In addition, the number of load applications can affect the resilient modulus during the pre-conditioning stage. The number of load applications during the pre-conditioning stage is recommended a minimum of 1000 cycles for fine-grained soils in order to achieve the minimum permanent deformation rate.

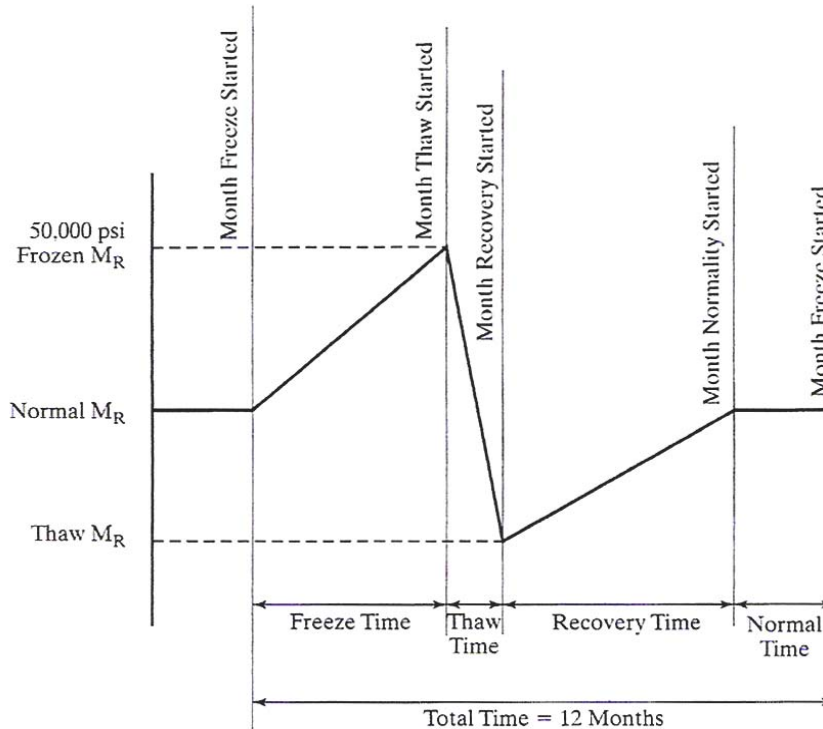


Figure 2.5 Seasonal Variations in Subgrade Resilient Modulus [Huang, 1993]

2.3.2 Models Correlating Resilient Modulus with Soil Index Properties

2.3.2.1 Soil Index Parameters

Since the resilient modulus test is complex and time consuming, design resilient modulus can be estimated based on correlations with the soil index properties. Soil index parameters used for this purpose are given as follows:

Liquid Limit (LL) and Plastic Limit (PL): AASHTO T-89 (2000) and AASHTO T-90 (2004) specifications are used to determine the liquid limit and the plastic limit of different soils, respectively. Liquid limit of a soil sample is determined as follows:

1. Determine the mass of three metal containers
2. Calibrate the Casagrande's liquid limit device
3. Put a 250 g of dried soil passing from sieve number 4 and add some water until the soil looks like a uniform paste
4. Place the specimen in the Casagrande's liquid limit device and smoothen the surface with a spatula until the maximum depth is 8mm.
5. Cut a groove on the sample by using the standard grooving tool
6. Turn the crank at a rate of 2 turn per second until the width of the groove approaches to 0.5 inch. Record the number of blows and determine the moisture content of the tested specimen if number of blows is between 15 and 40.
7. Draw the blow vs. moisture content curves. The water content of the tested specimen simply gives the liquid limit. If number of blows is higher than 40, add more water and repeat the procedure.

Plastic limit of a soil sample is determined as follows:

1. Take 20g of oven dried soil and add some water
2. Prepare some sphere-shaped soil masses
3. Roll the thread between fingers until the diameter is around 3mm.
4. Repeat the procedure with specimens at different moisture contents until the specimen reaches the crumbling point at 3mm diameter.
5. The moisture content of the specimen is the plastic limit.

Sieve Analysis: AASHTO T27-99 (2006) standard test method is utilized for the determination of gradation characteristics of soils. The general sieve sizes utilized for the test are 75, 50, 37.5, 25, 19, 9.5, 4.75, 2, 0.425, 0.075 mm. The most important sieve sizes for the estimation of the resilient response of unbound layers are 2, 0.425 and 0.075 mm [George, 2004].

Optimum Water Content (W_c) and Maximum Dry-Density (γ_{dmax}) : AASHTO T99-01 (2004) standard test method is utilized for the determination of the optimum water content and the maximum dry-density of soils. The dry-density of a soil changes with its water content. A dry-compacted soil can reach a certain density achieved under a certain amount of compaction effort and water content. If the same soil is compacted again with a higher compaction effort and amount of water, the dry-density will increase. This is the result of the lubrication effect of water causing higher compaction. The increase in the dry-density will continue until the maximum dry-density is reached. However, when the maximum dry-density is achieved, adding more water to the mixture results in a lower dry-density. The optimum water content and the maximum dry-density can be determined by using the water content-dry-density curves (Figure 2.6) [Atkins, 2002].

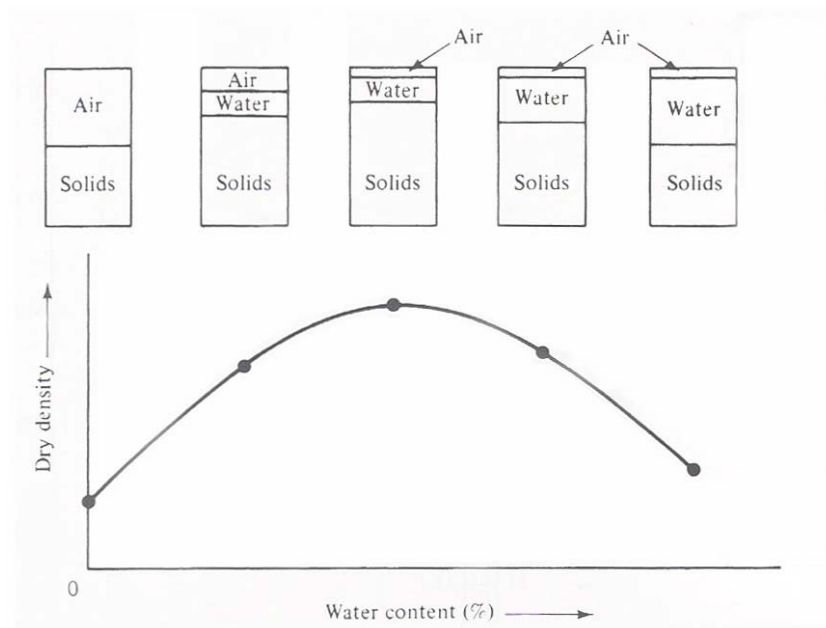


Figure 2.6 Variation of Dry-Density with Water Content [Atkins, 2002]

2.3.2.2 Proposed Correlation Models for Resilient Modulus in the Literature

Previous studies show that resilient modulus can be successfully estimated based on correlations with the certain soil index properties. Estimations are performed in two ways: using the bulk stress, confining pressure and deviator stress as independent variables or assuming these variables as constant and determining the resilient modulus for each test according to the constitutive models. George (2004) proposed linear and nonlinear models as:

Linear models: (Changes in the test stress levels are used as independent variables)

For granular soils:

$$\text{Log } M_R = 0.523 - 0.025(W_c) + 0.544(\log \theta) + 0.173(SM) + 0.197(GR) \quad (2.9)$$

where

M_R = resilient modulus, ksi

W_c = moisture content, %

θ = bulk stress ($\sigma_1 + \sigma_2 + \sigma_3$), psi

SM = 1 for SM soils (Unified Soil Classification)

= 0 otherwise

GR = 1 for GR soils (GM, GW, GC or GP)

= 0 otherwise.

For fine-grained soils:

$$M_R = 37.431 - 0.4566(PI) - 0.6179(W_c) - 0.1424(P_{200}) + 0.1791(\sigma_3) - 0.3248(\sigma_d) + 36.722(CH) + 17.097(MH) \quad (2.10)$$

where

PI = plasticity index, %;

P_{200} = percentage passing #200 sieve;

σ_3 = confining stress, psi;

σ_d = deviator stress, psi;

CH = 1 for CH soil

= 0 otherwise (for MH, ML or CL soil); and

MH = 1 for MH soil

= 0 otherwise (for CH, ML or CL soil).

Nonlinear models: (Resilient modulus for each test is calculated according to the constitutive models for a certain stress state)

For granular soils:

$$M_R \text{ (MPa)} = 307.4 \cdot \left(\left(\frac{\gamma_{dr}}{W_c} \right)^{0.86} + \left(\frac{P_{200}}{\log(c_u)} \right)^{-0.46} \right) \quad (2.11)$$

where

γ_{dr} = dry density/maximum dry density

c_u = uniformity coefficient

For fine-grained soils:

$$M_R \text{ (MPa)} = 16.75 \cdot \left(\left(\frac{LL}{W_c \gamma_{dr}} \right)^{2.06} + \left(\frac{P_{200}}{100} \right)^{-0.59} \right) \quad (2.12)$$

There are many studies in the literature correlating the soil index properties with the coefficients of constitutive equations. Coefficients of the nonlinear constitutive equations are also modeled in order to capture the effects of stress sensitivity and physical properties on resilient modulus. The correlations with good statistics were generally confined to specific soil types. On the other hand, correlations developed using the test results of various soil types did not result in satisfactory estimates for the resilient modulus of unbound pavement layers. George (2004) conducted regression analysis between the constitutive equation coefficients and the soil index properties. Based on his results, he proposed the following relationships:

Constitutive equation used for coefficient determination:

$$M_R = k_1 \sigma_{atm} (\theta / \sigma_{atm})^{k_2} [(\tau_{oct} / \sigma_{atm}) + 1]^{k_3} \quad (2.13)$$

Correlations for the estimation of the k_1 , k_2 and k_3 using soil index properties:

For coarse-grained sand soils,

$$k_1 = 3.2868 - 0.0412 \cdot P_{3/8} + 0.0267 \cdot P_4 + 0.0137 \cdot (\%Clay) + 0.0083 \cdot LL - 0.0379 \cdot w_{opt} - 0.0004 \cdot \gamma_s \quad (2.14)$$

$$k_2 = 0.5670 + 0.0045 \cdot P_{3/8} - (2.98 \times 10^{-5}) \cdot P_4 - 0.0043 \cdot (\%Silt) - 0.0102 \cdot (\%Clay) - 0.0041 \cdot LL + 0.0014 \cdot w_{opt} - (3.41 \times 10^{-5}) \cdot \gamma_s - 0.4582 \cdot (\gamma_s / \gamma_{opt}) + 0.1779 \cdot (w_c / w_{opt}) \quad (2.15)$$

$$k_3 = -3.5677 + 0.1142 \cdot P_{3/8} - 0.0839 \cdot P_4 - 0.1249 \cdot P_{200} + 0.1030 \cdot (\%Silt) + 0.1191 \cdot (\%Clay) - 0.0069 \cdot LL - 0.0103 \cdot w_{opt} - 0.0017 \cdot \gamma_s + 4.3177 \cdot (\gamma_s / \gamma_{opt}) - 1.1095 \cdot (w_c / w_{opt}). \quad (2.16)$$

Fine-grain silt soils:

$$k_1 = 1.0480 + 0.0177 \cdot (\%Clay) + 0.0279 \cdot PI - 0.0370 \cdot w_c \quad (2.17)$$

$$k_2 = 0.5097 - 0.0286 \cdot PI \quad (2.18)$$

$$k_3 = -0.2218 + 0.0047 \cdot (\%Silt) + 0.0849 \cdot PI - 0.1399 \cdot w_c \quad (2.19)$$

Fine-grain clay soils:

$$k_1 = 1.3577 + 0.0106 \cdot (\%Clay) - 0.0437 \cdot w_c \quad (2.20)$$

$$k_2 = 0.5193 - 0.0073 \cdot P_4 + 0.0095 \cdot P_{40} - 0.0027 \cdot P_{200} - 0.003 \cdot LL - 0.0049 \cdot w_{opt} \quad (2.21)$$

$$k_3 = 1.4258 - 0.0288 \cdot P_4 + 0.0303 \cdot P_{40} - 0.0521 \cdot P_{200} + 0.0251 \cdot (\% \text{Silt}) + 0.0535 \cdot \text{LL} - 0.0672 \cdot w_{\text{opt}} - 0.0026 \cdot \gamma_{\text{opt}} + 0.0025 \cdot \gamma_s - 0.6055 \cdot (w_c / w_{\text{opt}}) \quad (2.22)$$

where,

M_R = resilient modulus, MPa;

$P_{3/8}$ = percentage passing sieve #3/8;

P_4 = percentage passing #4 sieve;

P_{40} = percentage passing #40 sieve;

w_c = moisture content of the specimen, %;

w_{opt} = optimum moisture content of the soil, %;

γ_s = dry density of the sample, kg/m^3 ; and

γ_{opt} = optimum dry density, kg/m^3 .

LL = liquid limit

2.4 CBR Testing

The California Bearing Ratio (CBR) test is a penetration test used for the evaluation of mechanical strength of unbound pavement layers. It was first developed by the California Department of Transportation. A standardized piston with an area of 3 square inches is penetrated into a compacted soil specimen at a standard rate of 0.05 in/min. The applied pressure at every 0.1 in. increments is recorded during the test. The ratio of the recorded pressure values to the standard test results of a high-quality crushed-stone specimen simply gives the CBR values for a certain test.

The standard pressure values for the high-quality crushed-stone specimens are as follows:

Penetration	Pressure
0.1 in.	1000 psi
0.2 in.	1500 psi
0.3 in.	1900 psi
0.4 in.	2300 psi
0.5 in.	2600 psi

The highest pressure ratio for the 0.1 in. penetration increments is accepted as the design CBR according to the test results. For fine-grained soils, CBR values usually decreases with increasing penetration. In contrast, test results for granular soils may exhibit an increase in CBR values during a certain test. Tests are conducted at two different conditions in order to simulate the in-situ conditions for unbound soils which are unsoaked and soaked. For the soaked tests, the compacted specimen is saturated for 4 days by placing the specimen in a water pool. Surcharge weights are also utilized during soaking and testing in order to simulate the actual weight of in-service pavements above the unbound layers. The diameter of the cylindrical specimens is standardized as 6 in. where the height is 4.58 in.

CBR testing procedures are modified by the application of controlled lateral pressure since there are concerns about the simulation ability of the test [Livneh, 1978; Franco, 1987]. Clegg et. al. (1980) also proposed impact soil tests as an alternative to CBR in order to decrease the experimental effort. In addition, statistical correlations between the resilient modulus and CBR are also established based on the results of various research studies [Zaman et al., 1994; Mohammad et al, 1999]. Since the resilient modulus test aims to estimate the elastic response of the pavement layers, the correlations based on penetration tests are realized to give unreliable estimates [Bandara, 2002]. Furthermore, elasticity based field performance tests are

proposed to develop reliable models for resilient modulus estimations [Tanyu et al., 2002].

2.4.1 Models Correlating Resilient Modulus with CBR

The studies conducted on the estimation of resilient modulus from CBR test results showed that the reliability of prediction models are not statistically satisfactory which is a result of the structural differences between these two tests. The correlation charts for the estimation of the resilient modulus from simple performance tests for subgrade, base and subbase soils are given in Figures 2.7 and 2.8 [Huang, 1993]. The general function which is proposed by AASHTO design guide for fine-grained soils is also as follows [Heukelom. 1962]:

$$M_R (\text{psi}) = 1500 \cdot \text{CBR} \quad (2.23)$$

This correlation appears to be effective for CBR values less than about 20 which restrict the use of this equation for pavement design.

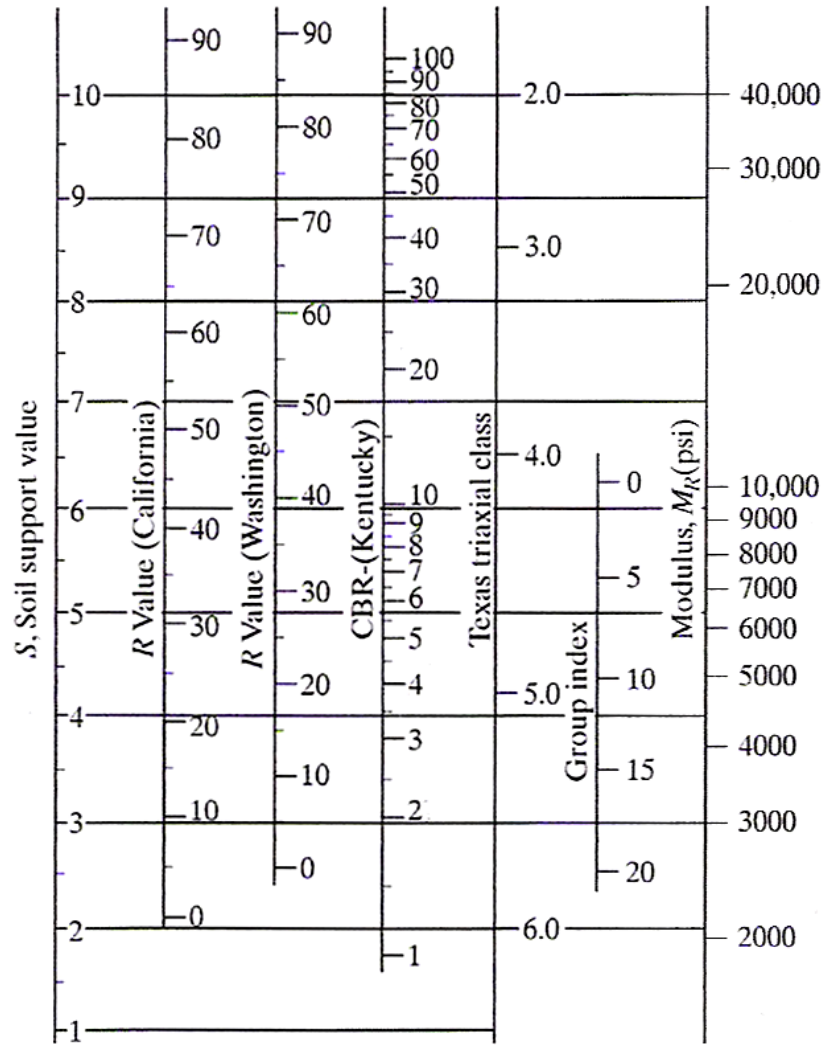


Figure 2.7 Correlation Chart for Estimating Resilient Modulus of Subgrade Soils [Huang, 1993]

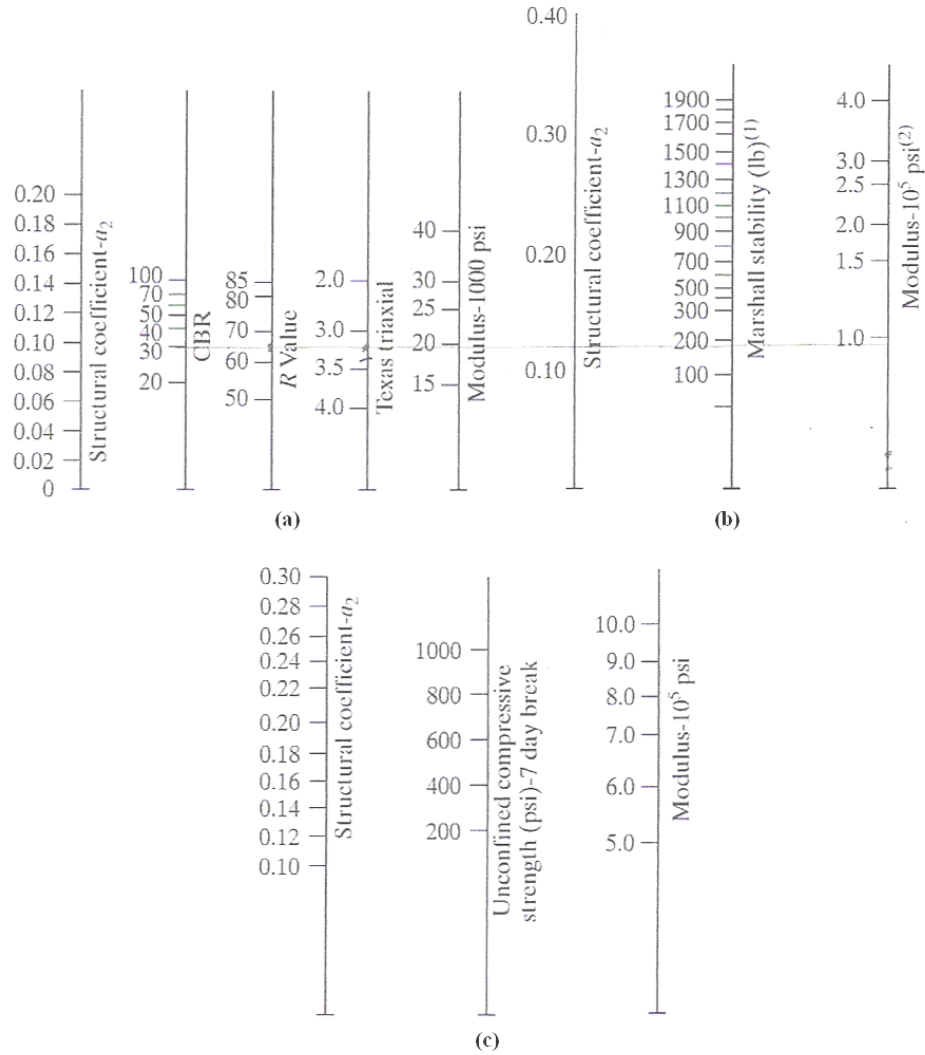


Figure 2.8 Correlation Chart for Estimating Resilient Modulus of Base/Subbase Soils (a) Untreated (b) Bituminous Treated (c) Cement Treated [Huang, 1993]

In addition, there are also various other equations used for estimating the resilient modulus based on the CBR test results:

U.S. Army Corps of Engineers (Green and Hall 1975)

$$M_R \text{ (psi)} = 5,409 \text{ CBR}^{0.71} \tag{2.24}$$

South African Council on Scientific and Industrial Research (CSIR)

$$M_R \text{ (psi)} = 3,000 \text{ CBR}^{0.65} \quad (2.25)$$

Transportation and Road Research Laboratory (TRRL)

$$M_R \text{ (psi)} = 2,555 \text{ CBR}^{0.64} \quad (2.26)$$

Lotfi et al. (1988) also proposed an empirical equation that is valid only for CBR values ranging from 2 to 21:

The relationship for M_R is given as follows:

$$M_R = k_1 \cdot \sigma_d^{k_2} \quad (2.27)$$

$$k_1 = 10^{(1.0016 + 0.043 \text{ CBR})} \quad (2.28)$$

$$k_2 = -\left(\frac{1.9557}{\text{CBR}} + 0.1705\right) \quad (2.29)$$

2.5 Light Falling Weight Deflectometer (LFWD) Test

Light falling weight deflectometer (LFWD) test is a test system for performing non-destructive testing of pavements. It was developed as an alternative to the plate bearing test to estimate the field elasticity of unbound layers. LFWD is accepted to be a reliable equipment for the estimation of the in-situ resilient response of unbound pavement layers. LFWD test results can be also used for the validation of laboratory test results in order to achieve the most realistic design parameters.

The equipment used consists of three main parts, a metal load, a loading plate and a deflection measuring sensor. The load is freely dropped from a constant height on to

a loading plate. The impulse occurring on the compacted soil structure generates a certain deflection which is measured by the deflection sensor. The measured deflection values are converted to the modulus based on the Boussinesq's theory [Alshibli et al., 2005]. The general back-calculation equation is given as:

$$E_{\text{LFWD}} = \frac{k\sigma_0 R}{\Delta}(1 - \nu^2) \quad (2.30)$$

where

$k = \pi/2$ or 2 for rigid and flexible plates, respectively

σ_0 = pressure applied to the surface of the loading plate

R = radius of the plate (6in.)

Δ = deflection of the plate associated with the pressure

ν = poisson's ratio

Computer-based LFWD systems are effective means of determining the resilient modulus that can directly convert the measured deflections to the modulus values. An example output of LFWD test can be seen in Figure 2.9 [Mehta, 2003]. Using the LFWD systems, field engineers can directly decide on the thickness of the asphalt layers according to the test results without performing any laboratory testing. On the other hand, the reliability of the test should be validated by using laboratory models in order to avoid estimation errors during the design [Ping et al., 2002]. Development of effective correlations between laboratory and field test results for certain soil index properties may provide satisfactory estimates in the pavement design process.

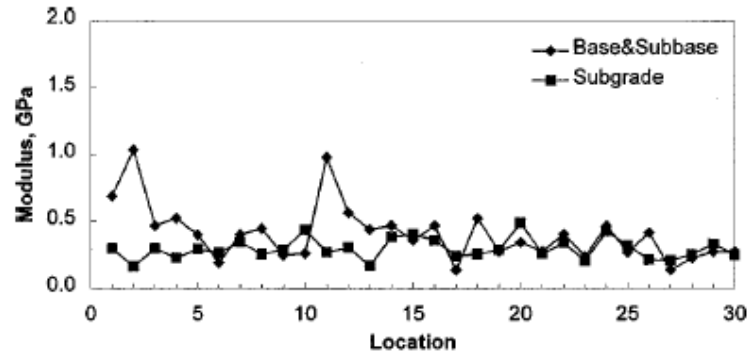


Figure 2.9 LFWD Test Results for 20 Different Locations [Mehta, 2003]

2.5.1 Models Correlating Resilient Modulus with LFWD Test Results

According to the literature review, there are many models which correlate resilient modulus with the falling weight deflectometer results [Mehta, 2003]. The models determined for fine-grained and granular soils are as follows: [Rahim, 2003]

$$M_R (\text{Lab.}) = E_{\text{FWD}} \cdot 0.71 \quad (\text{Fine-grained soils}) \quad (2.31)$$

$$M_R (\text{Lab.}) = E_{\text{FWD}} \cdot 0.50 \quad (\text{Granular soils}) \quad (2.32)$$

Another correlation which is developed by K.P George [2003] is given as:

$$M_R (\text{Lab.}) = 10275.7 + 0.462262 E_{\text{FWD}} \quad (R^2 = 0.56) \quad (2.33)$$

2.6 Genetic Algorithm and Applications for Mechanistic-Empirical Design Procedures

Genetic algorithm is a method originally developed to evaluate the fitness of a population at the end of a number of trial solutions. The method is based on the generation of new genes with the goal of evolving to a better solution each time in order to achieve the best solution at the end. The genetic algorithm is a computer

simulation of evolution where the user provides the environment (function) in which the population must evolve.

The first genetic algorithm simulation is performed by Nils Aall Barricelli in 1954 where his publication was not widely noticed. In particular, genetic algorithms become popular through the work of John Holland in the early 1970s. In 1989, genetic algorithm softwares are started to be used in many commercial areas as an optimization tool. The primary applications of the algorithm are related to solving difficult scheduling, data fitting, trend spotting and budgeting problems.

Although genetic algorithm has many applications in the literature, little has been done to use for civil engineering problems. Scheduling of construction projects, back-calculation of asphalt layer moduli and pavement design are the primary applications of genetic algorithm in pavement engineering. Genetic algorithm has been used to predict the fatigue performance of asphalt pavements in recent studies [Tsai et. al., (2003); Tsai et. al., (2004); Tsai et. al., (2005)]. The time vs. stiffness ratio Weibull curves are separated in to two parts by using genetic algorithm in order to determine the crack initiation and propagation stages. The regression equations obtained for these stages are also integrated into the accelerated pavement test results to determine the calibration factors utilized for the asphalt pavement design. In addition, Liu-Wang [2003] used genetic algorithm for the design of asphalt pavements. Kameyama et al. [1997] also developed a methodology which uses genetic algorithm to backcalculate pavement layer moduli from the surface deflections. In addition to these studies, Shekharan [2000] used genetic algorithm to model the pavement deterioration process and Attoh-Okine [1998] applied genetic algorithm for the prediction of the roughness progression in flexible pavements.

In this research, genetic algorithm is proposed as an alternative to conventional constitutive nonlinear models. Since these models present unreliable results for fine-grained soils, the application of genetic algorithm and curve shifting methodology is

strongly recommended for better estimation of the resilient modulus. Further information about the application of genetic algorithm and the curve shifting methodology is presented in Section 4.5.

CHAPTER 3

EXPERIMENTAL STUDY

3.1 Introduction

The main objective of this study is to determine the resilient modulus, used in the mechanistic design of pavement structures, for the material types used in Turkey, and develop methods and specifications to incorporate the resilient modulus in the pavement design process. The correlations between resilient modulus and other performance tests were also investigated in order to develop reliable models for asphalt pavement design.

The materials tested in this study are composed of disturbed samples with different geological origin and engineering properties. The soil samples were taken from the highway construction sites by the TGDH engineers where the construction of the base, subbase or subgrade pavement layers was started. In the laboratory, the general soil index properties of the materials were determined in order to perform classifications. For this purpose, liquid limit, plastic limit, gradation characteristics, optimum water content and maximum dry-density of the specimens were determined according to the AASHTO specifications. The summary of the test procedures for the estimation of these soil index parameters are given in part 2.3.2.1. Specimens are also classified according to the AASHTO soil classification system [ASTM M 145, 1986] based on the determined soil index parameters.

The primary objective of the analysis undertaken in this study is to obtain reliable resilient modulus prediction models in order to estimate design resilient modulus values with minimum cost and maximum accuracy. For this purpose, 155 resilient modulus and 132 CBR tests were conducted following the AASHTO specifications and the NCHRP Research Results (No. 285) in the TGDH's laboratories. In addition, 232 LFWD field strength tests were also conducted at 11 different regions of Turkey. Technicians and engineers of TGDH also participated in the project at the specimen collection, preparation and testing stages.

This chapter provides information about the material types utilized for resilient modulus, CBR and LFWD testing, experimental design and the results of the conducted tests.

3.2 Experimental Design

3.2.1 Experiment Set 1 for Correlations between Soil Index Properties and Resilient Modulus

According to the literature, the influence of soil index properties on resilient modulus testing is extremely important. The correlations based on these independent variables result in successful estimates for the determination of the resilient response of unbound soils [George, 2004]. Thus, correlations based on soil index properties are developed in this study for better resilient modulus estimations. In addition, genetic algorithm and curve shifting methodology are applied for this experiment set in order to obtain reliable models as an alternative to conventional constitutive correlations. In this study, soil index parameters analyzed for model development are as follows: water content, maximum dry-density, degree of saturation, gradation characteristics, plasticity index and liquid limit. 75 resilient modulus tests were conducted for four different compaction and water content sets which are: (1) W_{opt} - 100% compaction, (2) $W_{opt} - 95\%$ compaction, (3) $(W_{opt} - 2)$, 100% compaction, (4)

($W_{opt} + 2$), 100% compaction. In addition, Atterberg limits, optimum water content, maximum dry-density and gradation characteristics of the specimens are determined according to the corresponding AASHTO specifications. Table 3.1 presents the general experimental design for each soil type with the corresponding soil index properties. Soil types with different soil index properties are chosen for this experimental set in order to develop reliable models. Maximum dry-density and plasticity index values of the experiment set 1 specimens are graphically presented in Figure 3.1.

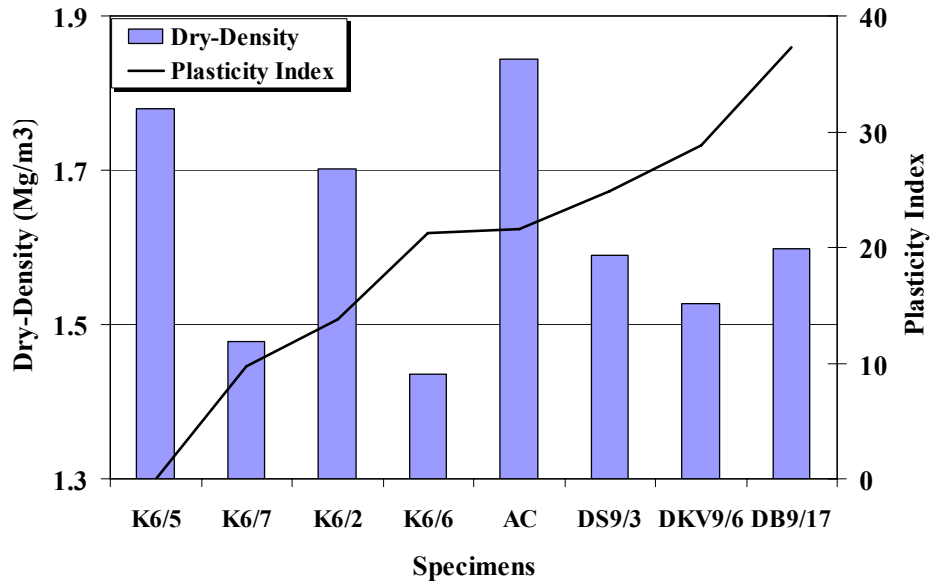


Figure 3.1 Dry-Density and Plasticity Index Variation for the Experiment Set 1 Specimens [(K6-5 : City – Kayseri, Region – 6-5), (AC: Ankara Çankırı), (DS: Diyarbakır Silvan), (DKV: Diyarbakır Kızıltepe Viranşehir), (DB: Diyarbakır Bismil)]

Table 3.1 Design for the Experiment Set 1 (Total Number of Tests = 75)

City	Type	Region	AASHTO	Number of Tests						PP10	PP40	PP200	LL	PI	W _{opt} (stnd)	γ _{d,max} (stnd)
				C 100%			C 95%									
				opt-2	opt	opt+2	opt	opt+2	opt							
Kayseri	2	6//2	A-7-5	2	3	2	2	2	82.8	71.8	48.3	44.7	13.8	19.2	1.702	
	2	6//5	A-2-4	2	4	3	2	2	87.3	73.1	33.0	NP	NP	15.8	1.780	
	2	6//6	A-2-7	3	3	2	2	2	43.0	26.1	18.3	59.2	21.2	28.4	1.436	
	2	6//7	A-5	2	3	2	2	2	81.5	71.8	48.5	42.0	9.7	24.8	1.478	
Diyarbakır- Bismil	2	9//17	A-7-6	2	3	3	2	2	96.8	90.9	83.7	61.1	37.3	22.5	1.599	
Diyarbakır- Silvan	2	9//3	A-7-6	2	3	2	2	2	91.4	88.0	76.1	50.4	24.9	22.8	1.590	
Diyarbakır Kızıltepe	2	9//6	A-7-6	2	3	2	2	2	99	96.6	94.2	57.2	28.8	25.8	1.527	
Viranşehir																
Ankara -Çankırı	2	-	A-6	2	2	2	2	2	62.3	50.5	41.3	39.9	21.6	14.8	1.844	

Note: PP10: Percent passing No. 10 sieve
 PP40: Percent passing No. 40 sieve
 PP200: Percent passing No. 200 sieve
 LL: Liquid Limit
 PI: Plastic Index
 W_{opt}: Optimum Water Content
 γ_{d,max}: Maximum Dry-density

Stnd: Standard Proctor Compaction
 NP: Non-plastic
 C 95% :95 % compaction
 C 100% :100 % compaction
 opt-2: compaction performed at (W_{opt}-2)% water content level
 opt: compaction performed at (W_{opt})/% water content level
 opt+2: compaction performed at (W_{opt}+2)% water content level

3.2.2 Experiment Set 2 for Correlations between CBR and Resilient Modulus

In this experiment set, the aim is to develop prediction models which correlate CBR with resilient modulus. For this purpose, 104 resilient modulus and 132 CBR tests (soaked and unsoaked) were conducted at the optimum water content. Materials with different soil index properties were chosen for the development of the experiment data set in order to determine correlations which present the characteristics of the soils in Turkey. Figure 3.2 and 3.3 present the variation of the plasticity index and maximum dry-density for the tested granular and fine-grained soil specimens. The models are developed by considering the effects of Type 1 and Type 2 category covariates and using the complete data set. In addition, soil index properties of the specimens are also determined in order to analyze for model development since one-to-one correlations between resilient modulus and CBR did not give satisfactory results [Heukelom 1962]. The most important soil index properties and their statistical strength for data classification are also determined according to the tree-based approach in order to develop separate models for different soil index parameter intervals. The design for the experiment set 2 is given in Table 3.2.

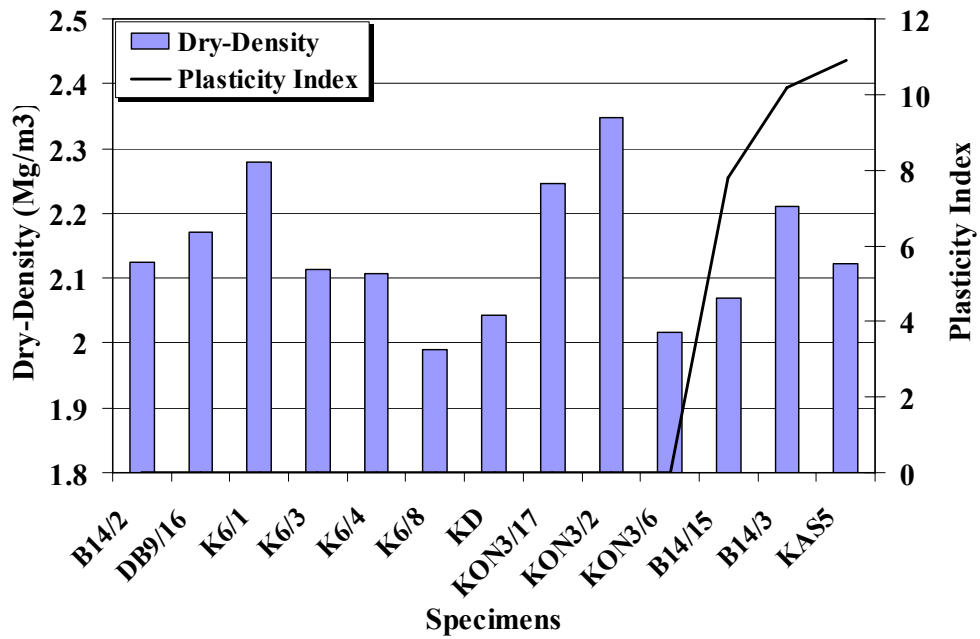


Figure 3.2 Dry-Density and Plasticity Index Variation for the Experiment Set 2 Granular (Type 1) Specimens [(B14/2 : City – Bursa, Region – 14/2), (K: Kayseri), (DB: Diyarbakır Bismil), (KAS: Kastamonu), (KD: Kırıkkale Delice), (KON: Konya)]

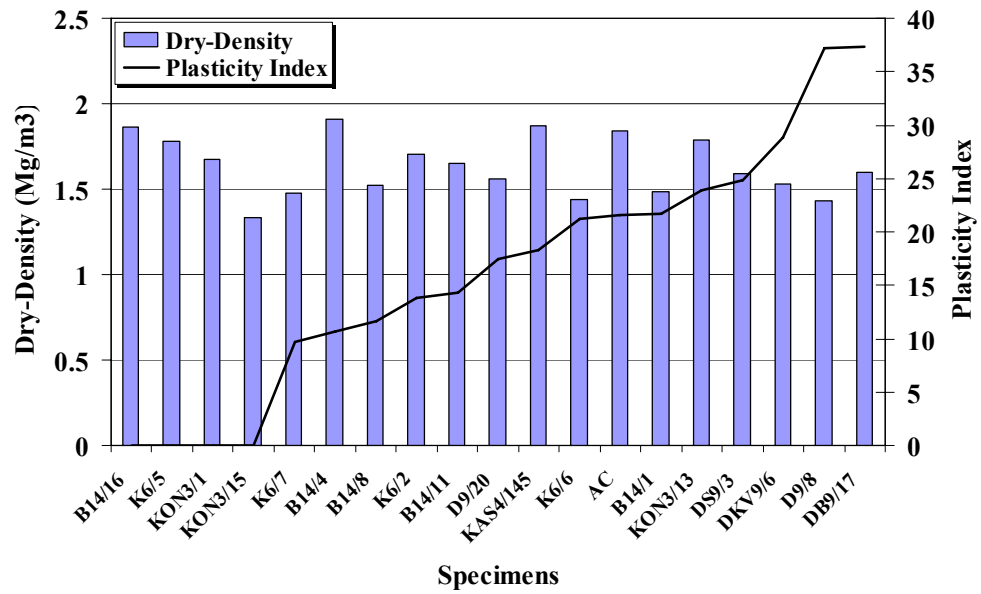


Figure 3.3 Dry-Density and Plasticity Index Variation for the Experiment Set 2 Fine-Grained (Type 2) Specimens

3.2.3 Experiment Set 3 for Correlations between LFWD and Resilient Modulus

LFWD tests were conducted for the compacted base, subbase (granular soil types) and subgrade (fine-grained soil types) highway layers from 11 different regions of Turkey. Standardized TGDH roller compacters were utilized for this purpose. Five measurements were taken on a 1 m² section (at the middle of the square and at four corners) in order to reduce the experimental errors. Tests were conducted on three to four sections along the highway in order to reduce the outliers for statistical analysis. Soil samples were also collected from the tested areas to use in the resilient modulus testing. In addition, soil index properties of the specimens were also determined in order to improve the statistical strength of the correlations. The variation of maximum dry-density and plasticity index are shown in Figure 3.4. Since LFWD tests were conducted in order to determine the resilient response of the in-situ

pavement layers, one-to-one correlations with resilient modulus tests results in more reliable estimates. The main purpose of the tests was to achieve satisfactory correlations between LFWD and resilient modulus test results. The experimental design developed for this purpose is given in Table 3.3.

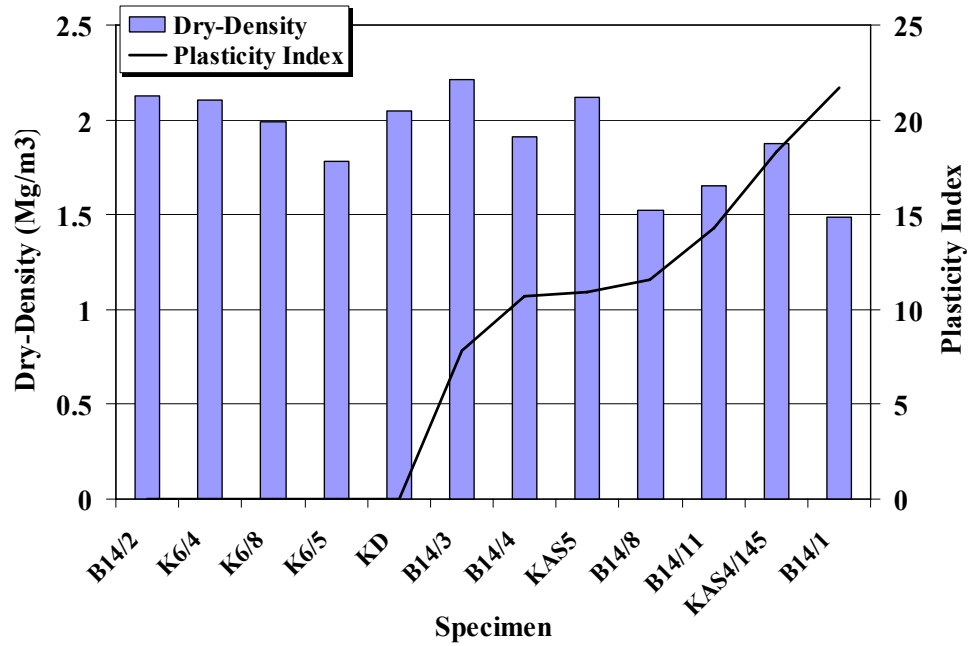


Figure 3.4 Dry-Density and Plasticity Index Variation for the Experiment Set 3 Specimens

Table 3.2 Design for the Experiment Set 2 (Total Number of M_R Tests = 104)

City	Type	Region	AASHTO	Number of Tests at W_{opt}	PP4	PP10	PP40	PP200	LL	PI	W_{opt}	γ_{dmax}
Bursa	1	14//2	A-1-a	3	51.6	38.4	20.4	10.8	NP	NP	8.6	2.124
	1	14//3	A-2-4	3	56.0	41.8	23.3	12.4	23.3	7.8	7.3	2.210
	2	14//4	A-2-4	3	46.4	38.1	26.2	17.1	35.7	10.7	12.7	1.912
	1	14//15	A-2-4	3	60.6	50.2	31.4	18.7	28.0	10.2	9.7	2.070
	2	14//1	A-2-7	3	50.9	44.2	34.5	26.4	55.9	21.7	26.0	1.485
	2	14//8	A-6	3	100	95.5	81.6	48.8	40.2	11.6	23.6	1.521
	2	14//11	A-6	3	100	99.7	97.9	67.5	36	14.3	19.8	1.655
	2	14//16	A-2-4	3	96.1	88.1	60.0	18.6	NP	NP	13.8	1.862
	1	6//1	A-1-a	6	43.3	32.0	14.9	4.3	NP	NP	4.9	2.280
	1	6//3	A-1-b	5	69.1	53.0	21.4	7.7	NP	NP	7.8	2.113
Kayseri	1	6//4	A-1-b	5	71.2	55.2	27.0	14.3	NP	NP	8.7	2.106
	1	6//8	A-1-b	3	65.2	50.9	24.0	9.3	NP	NP	11.5	1.989
	2	6//2	A-7-5	3	85.9	82.8	71.8	48.3	44.7	13.8	19.2	1.702
	2	6//5	A-2-4	4	92.5	87.3	73.1	33.0	NP	NP	15.8	1.780
	2	6//6	A-2-7	3	60.8	43.0	26.1	18.3	59.2	21.2	28.4	1.436
	2	6//7	A-5	3	86.8	81.5	71.8	48.5	42.0	9.7	24.8	1.478

Table 3.2 Design for the Experiment Set 2 (Total Number of M_R Tests = 104) (Continued)

City	Type	Region	AASHTO	Number of Tests at W_{opt}	PP4	PP10	PP40	PP200	LL	PI	W_{opt}	γ_{dmax}
Diyar.-Bismil	1	9//16	A-1-a	3	37.4	29.0	16.4	7.4	NP	NP	9.0	2.170
	2	9//17	A-7-6	3	98.7	96.8	90.9	83.7	61.1	37.3	22.5	1.599
Diyar.-Silvan	2	9//3	A-7-6	3	93.2	91.4	88.0	76.1	50.4	24.9	22.8	1.590
	2	9//6	A-7-6	3	99.7	99.0	96.6	94.2	57.2	28.8	25.8	1.527
Ank.-Çan.	2	-	A-6	3	72.5	62.3	50.5	41.3	39.9	21.6	14.8	1.844
Kastamonu	1	5	A-2-4	3	54.0	38.8	19.4	11.6	25.8	10.9	8.5	2.122
	2	4//145	A-2-6	3	86.2	77.0	54.6	35.1	34.6	18.3	13.6	1.872
Kırıkkale	1	-	A-1-a	3	54.6	40.9	16.3	8.1	NP	NP	8.6	2.044
	2	9//8	A-6	3	100	99.9	99.7	97.9	67.2	37.2	28.8	1.430
Diyarbakır	2	9//20	A-7-6	3	100	98.3	94.0	78.5	43.2	17.5	23.0	1.564
	1	3//2	A-1-a	3	58.2	37.7	17.6	11.8	NP	NP	4.8	2.348
Konya	1	3//6	A-1-b	3	58.8	51.6	34.8	19.8	NP	NP	11.3	2.016
	1	3//17	A-1-a	3	43.4	30.6	18.0	10.7	NP	NP	7.8	2.247
	2	3//1	A-3	3	94.7	82.4	65.2	1.1	NP	NP	13.6	1.673
	2	3//13	A-6	3	67.7	56.4	46.0	39.7	40.6	23.9	17.4	1.789
	2	3//15	A-2-4	3	95.4	87.3	62.5	28.9	NP	NP	20.1	1.335

Table 3.3 Design for the Experiment Set 3 (Total Number of M_R Tests = 39)

City	Type	Region	AASHTO	Number of Lab. Tests at W_{opt}	Number of Field Tests	PP4	PP10	PP40	PP200	LL	PI	W_{opt}	γ_{dmax}
Bursa	1	14//2	A-1-a	3	17	51.6	38.4	20.4	10.8	NP	NP	8.6	2.124
	1	14//3	A-2-4	3	18	56.0	41.8	23.3	12.4	23.3	7.8	7.3	2.210
	2	14//4	A-2-4	3	18	46.4	38.1	26.2	17.1	35.7	10.7	12.7	1.912
	2	14//1	A-2-7	3	23	50.9	44.2	34.5	26.4	55.9	21.7	26.0	1.485
	2	14//8	A-6	3	17	100	95.5	81.6	48.8	40.2	11.6	23.6	1.521
	2	14//11	A-6	3	20	100	99.7	97.9	67.5	36.0	14.3	19.8	1.655
Kayseri	1	6//4	A-1-b	5	23	71.2	55.2	27.0	14.3	NP	NP	8.7	2.106
	1	6//8	A-1-b	3	16	65.2	50.9	24.0	9.3	NP	NP	11.5	1.989
	2	6//5	A-2-4	4	20	92.5	87.3	73.1	33.0	NP	NP	15.8	1.780
Kastamonu	1	5	A-2-4	3	15	54.0	38.8	19.4	11.6	25.8	10.9	8.5	2.122
	2	4//145	A-2-6	3	20	86.2	77.0	54.6	35.1	34.6	18.3	13.6	1.872
Kırıkkale	1	-	A-1-a	3	25	54.6	40.9	16.3	8.1	NP	NP	8.6	2.044

3.3 General Characteristics of Test Specimens

According to the AASHTO T307 specification [2000], soils from different regions of Turkey are classified as Type 1 and Type 2 based on their gradation and plasticity characteristics for resilient modulus testing:

Type 1: all untreated granular base and subbase material and all untreated subgrade soils which meet the criteria of less than 70 percent passing the No.10 (2 mm) sieve and less than 20 percent passing the No.200 (75 μm) sieve, and which have a plasticity index of 10 or less. Type 1 soils will be molded in cylindrical 150 mm – 315 mm dimension molds. The compaction method strongly recommended for Type 1 specimen preparation is the vibratory compaction which is also the compaction method used for Type 1 soil compaction in this study.

Type 2: all untreated granular base/subbase and untreated subgrade soils not meeting the criteria for material Type 1. Type 2 soils will be molded in cylindrical 100 mm – 210 mm dimension molds. The recommended compaction methods for Type 2 soils are static, vibratory and standard proctor. In this study standard proctor type compaction is used during the preparation of the Type 2 specimens.

The optimum water content and the maximum dry-density of the tested specimens are determined according to the AASHTO T99 [2004] specification. Since this procedure is only valid for soil types which totally pass from No. 4 sieve, the effect of coarse particles on the moisture density relationships is corrected according to the AASHTO T224 specification [2001].

Sieve analyses of the specimens were performed according to the AASHTO T27 specification [1999]. Since gradation has considerable effects on the resilient modulus test results, soil types with different gradation characteristics are chosen in order to perform successful model estimations. Gradation characteristics of the

experiment set 1, 2 and 3 soil types are given in Figures 3.5, 3.6, 3.7, 3.8 respectively.

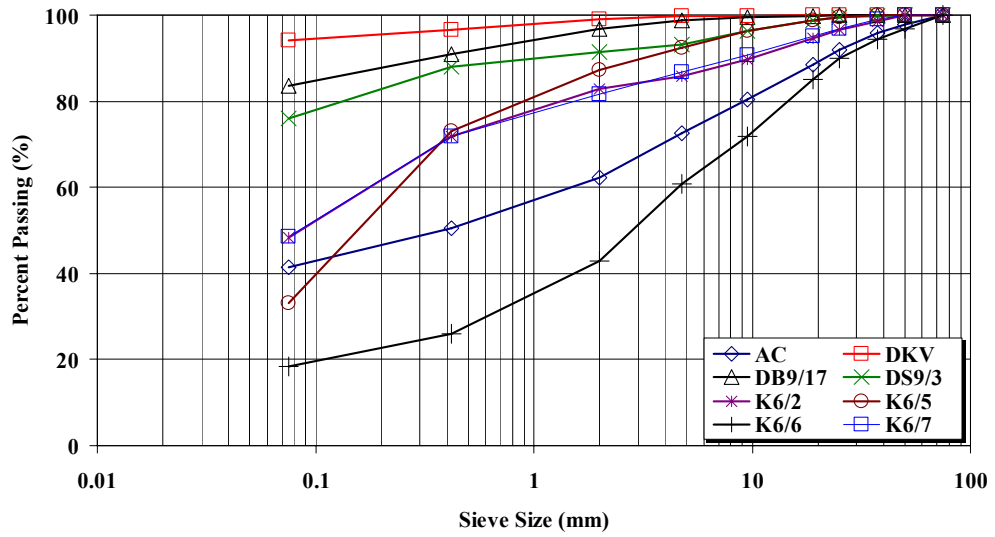


Figure 3.5 Gradation Characteristics for the Experiment Set 1 Soil Types

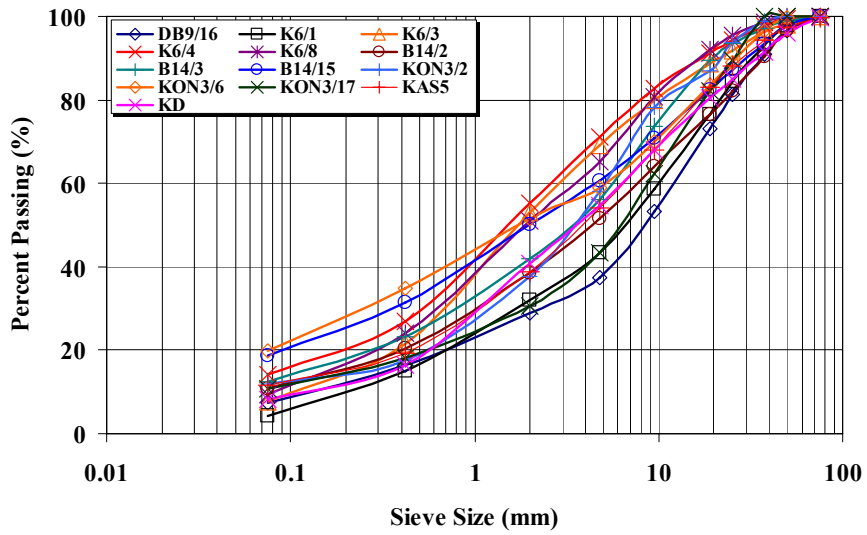


Figure 3.6 Gradation Characteristics for the Experiment Set 2 Granular (Type 1) Soil Types

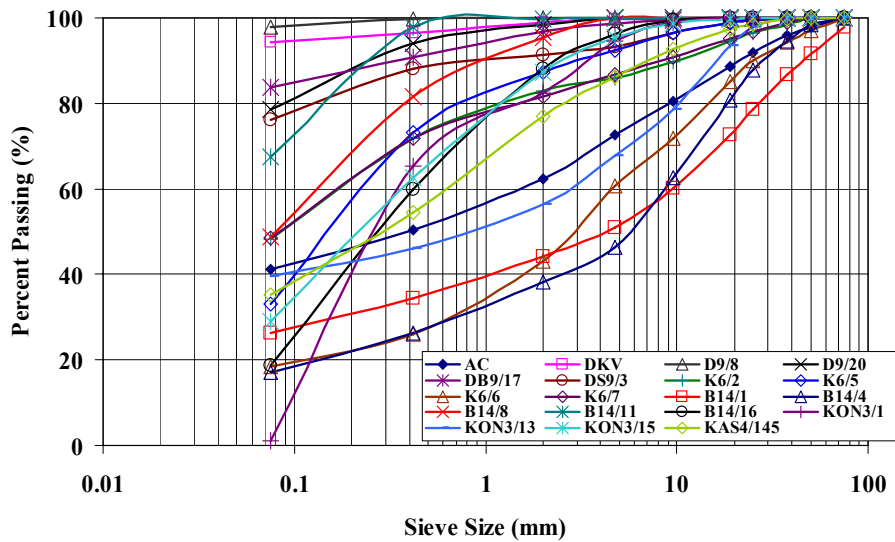


Figure 3.7 Gradation Characteristics for the Experiment Set 2 Fine-Grained (Type 2) Soil Types

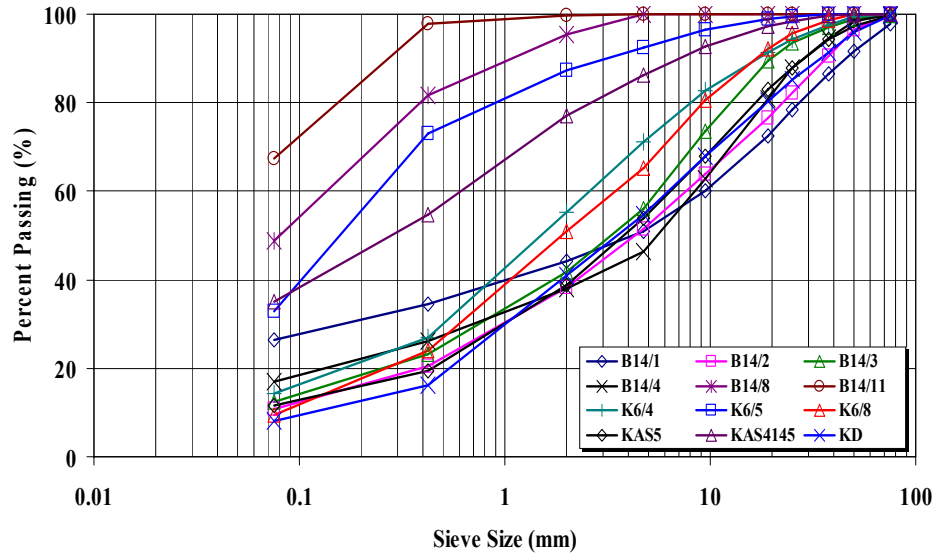


Figure 3.8 Gradation Characteristics for the Experiment Set 3 Soil Types

3.4 Test Setup and Procedure for Resilient Modulus Testing

3.4.1 Resilient Modulus Test Setup

Resilient modulus test equipment used in this study is the Load-Trac II operated in the highway materials laboratory at the TGDH. The system is capable of conducting resilient modulus tests according to AASHTO T292, T307, and LTPP Protocol P46. The system composed of seven distinct parts. The function of each part as described in Load Trac II User's Manual (2005) are as follows:

Load Frame: Unit that contains the embedded control system and the components to apply the force on a specimen and to measure the force and the displacements. The operation of the load frame can be controlled using the LCD panel and the keyboard on the front panel.

Test Chamber: Chamber that confines the specimen to be tested in the load frame includes load cell/piston coupling and two optional proximeters for lateral strain measurements.

Hydraulic Power Unit: Produces fluid power to operate hydraulic actuator at up to 2.5 gpm and a pressure up to 40000 kPa (3000 psi); adjustable flow and pressure.

Servo-valve controller: Provides commands to produce sinusoidal loading from the hydraulic actuator.

E/P controller: Electro-pneumatic pressure controller to automatically apply the air cell pressure.

Signal Conditioning Unit: Contains electronics for sensor excitation and sensor signal conditioning. It also contains an interface card with power supply for the servo-valve and solenoid valve.

Computer: PC computer, operating system, network card, A/D card, hard disk and disk drive.

The equipment setup utilized for resilient modulus testing in TGDH is given in Figure 3.9.

The system software runs the test, collects data for the test, stores data in a single file, performs necessary calculations, and prepares the final tables and graphs of the test results. Figure 3.10 illustrates the typical out for a resilient modulus test. The definitions of the columns in the test output table are as follows:

Confining Stress, S3 (kPa): The average of the applied confining pressures for the last 5 cycles of a certain sequence.

Nom. Max. Deviator Stress (kPa): The input deviator stress values as stated in the AASHTO T307 specification [2000].

Mean Deviator Stress, σ_d (kPa): The average of the applied deviator stresses for the last 5 cycles of a certain sequence.

Std. Dev. Deviator Stress (kPa): Standard deviation of the last 5 cycles' applied deviator stresses for a certain sequence.

Mean Bulk Stress, θ (kPa): The summation of the principal stresses (confining and mean deviator stress).

$$\theta = 3 \cdot S_3 + \sigma_d \quad (3.1)$$

Mean Resilient Strain (%): The average of the accumulated resilient strain for the last 5 cycles of a certain sequence.

Std. Dev. Resilient Strain (%): Standard deviation of the last 5 cycles' accumulated resilient strains for a certain sequence.

Mean Resilient Modulus (kPa): The average of the measured resilient modulus values for the last 5 cycles of a certain sequence.

Std. Dev. Resilient Modulus (kPa): Standard deviation of the last 5 cycles' measured resilient modulus values for a certain sequence.

Since the PID unit controls the load application sensitivity based on the stiffness of the specimens, all the soil index properties of the specimens (moisture content, plastic limit, liquid limit etc.) should be entered to the software in order to gather the

most reliable results from the tests. In addition, dimensions of the specimens should be also entered in order to determine the accumulated strain during the tests.

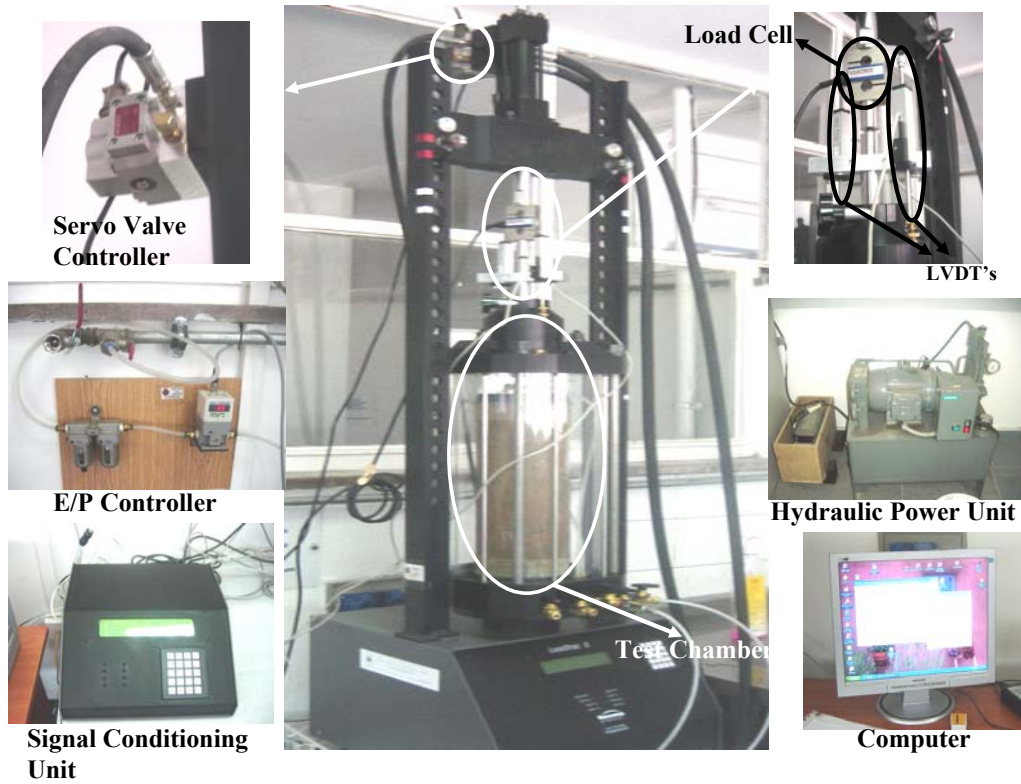
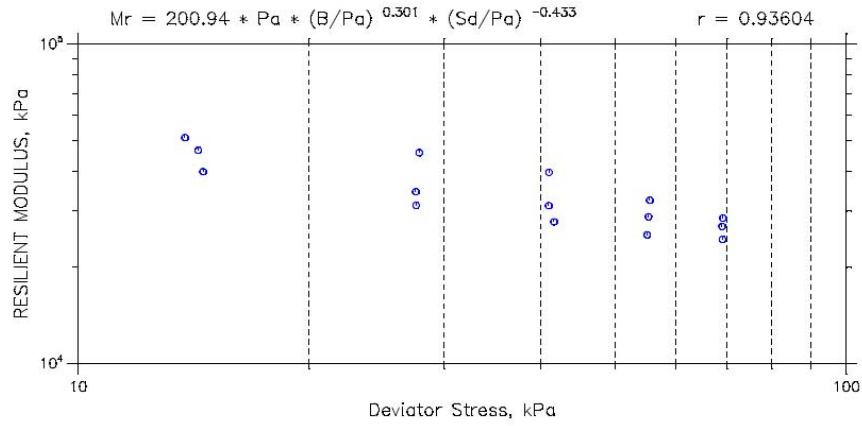


Figure 3.9 System for Resilient Modulus Testing

RESILIENT MODULUS TEST DATA
SUMMARY REPORT



Confining Stress S3 (kPa)	Nom. Max. Deviator Stress (kPa)	Mean Deviator Stress (kPa)	Std. Dev. Deviator Stress (kPa)	Mean Bulk Stress (kPa)	Mean Resilient Strain (%)	Std. Dev. Resilient Strain (%)	Mean Resilient Modulus (kPa)	Std. Dev. Resilient Modulus (kPa)
41.42	13.79	13.78	0.2546	138	0.02	0.00	50926	229.61
41.51	27.58	27.8	0.5298	152.3	0.05	0.00	45706	161.87
41.99	41.37	41.02	2.0138	167	0.09	0.01	39670	130.07
41.49	55.16	55.51	1.0578	180	0.15	0.00	32440	99.469
42.01	68.95	69.08	0.7520	195.1	0.22	0.00	28519	41.1
28.04	13.79	14.55	1.0871	98.66	0.03	0.00	39870	805.82
28.59	27.58	27.52	0.6628	113.3	0.07	0.00	34480	146.16
28.01	41.37	41	1.5809	125	0.12	0.01	31181	348.23
28.6	55.16	55.27	0.5866	141.1	0.17	0.00	28809	80.924
28.16	68.95	68.92	0.4698	153.4	0.23	0.00	26866	23.429
13.82	13.79	14.33	0.8474	55.8	0.03	0.00	46496	1295.3
13.94	27.58	27.55	0.2791	69.37	0.08	0.00	31261	43.77
14.03	41.37	41.64	1.4033	83.73	0.13	0.00	27773	46.621
14.1	55.16	55.04	0.4296	97.34	0.19	0.00	25287	27.602
14.14	68.95	69.01	0.1690	111.4	0.25	0.00	24458	24.463

Project: Diyarbakır-Silvan 9/3	Location: tck	Project No.:
Boring No.:	Tested By: ERDEM COLER	Checked By:
Sample No.:	Test Date: 05/05/2007	Depth:
Test No.:	Sample Type:	Elevation:
Description: Diyarbakır-Silvan 9/3 Proc100 Wopt+2 2. Numune		
Remarks:		
File: C:\Software\NEW\RM DATA\RM_New\RM\Diyarbakır-Silvan Yolu\DS93100opt+22.dat		

Mon, 18-JUN-2007 13:51:10

Figure 3.10 Typical Output for a Resilient Modulus Test

3.4.2 Resilient Modulus Test Procedure

3.4.2.1 Specimen Preparation

The steps given in AASHTO T307 specification [2000] are followed for specimen preparation. Since the dimensions and the cohesion properties of the Type 1 and Type 2 specimens are different, different procedures are recommended for the preparation of these soil specimens.

Granular Soil Specimens: The most challenging point in the specimen preparation of this soil type is the difficulty of handling due to low cohesion between the soil particles. AASHTO T307 specification [2000] recommends using membranes for compaction in order to minimize possible problems during transferring specimens to the test chamber. Vibratory compaction is preferred for specimen preparation to minimize membrane deteriorations during compaction. Specimens are compacted in 2 inch lift thicknesses in order to maintain uniformity in the specimen structure. The height of the compacted part is determined by using electronic calipers. The difference between the target and the achieved dry density and the water content is kept in acceptable limits for all the specimens in order to minimize variations between replicates. In the final lift, the top surface of the specimen is smoothed by using the fine-grained part of the soil mixture in order to avoid holes which will affect the load applications. After the test, specimen is broken into pieces and the final moisture content is determined in order to estimate the moisture loss during the test. Figure 3.11 summarizes the specimen preparation procedure for granular materials.



Figure 3.11 Specimen Preparation Procedure for Granular Materials

Fine-Grained Soil Specimens: Fine-grained soils are aerated and oven dried in order to remove existing water. After oven-drying, the specimen is mixed to achieve homogeneity. Finally, the mixed material is blended with water and bagged for 14 hours to maintain homogenous absorption. After 14 hours, the soil sample is compacted at five layers according to the AASHTO T307 specification [2000]. Standard proctor type compaction is preferred for fine-grained soil compaction. The difference between the target and the achieved dry density and the water content is again kept in the acceptable limits for all the fine-grained soil specimens in order to minimize variations between replicates. Figure 3.12 illustrates the specimen preparation process for fine-grained soils.



Figure 3.12 Specimen Preparation Procedure for Fine-Grained Soil Types

3.4.2.2 Conducting Tests

Resilient modulus tests are conducted at 16 different confining pressure and deviator stress sets to simulate the most realistic load model for in-service pavements. The confining pressure and the deviator stress sets can change for Type 1 and Type 2 soil specimens, depending on the locations of these materials along the highway cross-sections. Lower confining pressures and deviator stresses are utilized for Type 2 tests since the soils of this type are generally located at the subgrade level (bottom) of the pavement. The testing sequences specified in AASHTO T307 specification for Type 1 and Type 2 soil specimens are utilized for the resilient modulus testing. At the first sequence, the specimens are conditioned by applying 1000 repetitions in order to avoid variations from specimen compaction and minimize the imperfect contacts between the end platens and the specimen.

Tests for Granular Soil Specimens (Base/Subbase): The most important problem encountered during Type 1 resilient modulus testing is the high deviations between the applied and target load levels. This phenomenon is a result of high stiffness levels for these materials. The PID control unit in the Load-Trac II software is utilized in order to decrease the deviations from the target load level. The PID is the abbreviation for three important control parameters which are proportional, integral and derivative gain. The proportional value determines the reaction to the current error, the integral determines the reaction based on the recent errors and the derivative determines the reaction based on the rate of change of the current error. By adjusting these three parameters to acceptable ranges, the deviations in the load applications are minimized. After the adjustment, resilient modulus tests are conducted according to the AASHTO T307 Type 1 loading sequence table which is given in Table 3.4.

Table 3.4 Testing Sequence for Granular Materials

Sequence No.	Confining Pressure (kPa)	Max. Axial Stress (kPa)	Cyclic Stress (kPa)	Constant Stress (0.1 × Max. Axial)	No. of Load Applications
0	103.4	103.4	93.1	10.3	500-1000
1	20.7	20.7	18.6	2.1	100
2	20.7	41.4	37.3	4.1	100
3	20.7	62.1	55.9	6.2	100
4	34.5	34.5	31	3.5	100
5	34.5	68.9	62	6.9	100
6	34.5	103.4	93.1	10.3	100
7	68.9	68.9	62	6.9	100
8	68.9	137.9	124.1	13.8	100
9	68.9	206.8	186.1	20.7	100
10	103.4	68.9	62	6.9	100
11	103.4	103.4	93.1	10.3	100
12	103.4	206.8	186.1	20.7	100
13	137.9	103.4	93.1	10.3	100
14	137.9	137.9	124.1	13.8	100
15	137.9	275.8	248.2	27.6	100

Tests for Fine-Grained Soil Specimens (Subgrade): The same testing procedure is used for testing the fine-grained and granular soils except for the loading sequence and PID control. The loading sequence proposed by the AASHTO T307 is given in Table 3.5.

Table 3.5 Testing Sequence for Fine-Grained Materials

Sequence No.	Confining Pressure (kPa)	Max. Axial Stress (kPa)	Cyclic Stress (kPa)	Constant Stress (0.1 × Max. Axial)	No. of Load Application
0	41.4	27.6	24.8	2.8	500-1000
1	41.4	13.8	12.4	1.4	100
2	41.4	27.6	24.8	2.8	100
3	41.4	41.4	37.3	4.1	100
4	41.4	55.2	49.7	5.5	100
5	41.4	68.9	62.0	6.9	100
6	27.6	13.8	12.4	1.4	100
7	27.6	27.6	24.8	2.8	100
8	27.6	41.4	37.3	4.1	100
9	27.6	55.2	49.7	5.5	100
10	27.6	68.9	62.0	6.9	100
11	13.8	13.8	12.4	1.4	100
12	13.8	27.6	24.8	2.8	100
13	13.8	41.4	37.3	4.1	100
14	13.8	55.2	49.7	5.5	100
15	13.8	68.9	62.0	6.9	100

Running a Test with Load-Trac II: The user interface of the software used for resilient modulus testing is given in Figure 3.13. The steps followed for computer – based resilient modulus testing is as follows:

- Place the resilient modulus cell containing the specimen onto the bottom platen

- Check the alignment of the loading piston and the resilient modulus cell piston to apply the axial load without any eccentricity.
- Connect the external cell pressure from E/P to the cell.
- Initialize the LVDT and load cell readings
- Control the calibration factors with the previous calibration measurements
- Start the test

Figure 3.13 User-interface of the Software Used for Resilient Modulus Testing

The system automatically applies the specified loads and electro-pneumatic pressure. The steps followed by the resilient modulus testing system for a certain load application are as follows:

- Signal conditioning unit produces the electronic signals to start the test according to the data entered in the software
- The electro-pneumatic controller receives the signals and starts applying the specified confining pressure
- The servo-valve controller receives the signals and decreases the 20000 kPa hydraulic pressure to the specified levels to apply the deviator stress.
- LVDT's measure the elastic deflections (200 data point readings for each LVDT for a certain cycle) for each repetition in the electronic signal format and transfer to the signal conditioning unit.
- Load cell measures the applied load in the electronic signal format and transfers to the signal conditioning unit.
- Signal conditioning unit converts the electronic signals to numerical values and saves into the related test file in the computer.

3.4.3 Loading Wave Form for Resilient Modulus Testing

Test specimens are loaded using a haversine type load pulse as given in Figure 3.14. The axial load applied on the specimen to maintain a contact between the loading piston and the specimen is called the contact load (P_{contact}). The maximum total load applied to the sample is called the maximum applied load (P_{max}). Each cycle of the load application is composed of 0.1 sec. loading and 0.9 sec. rest period. The capacity of the hydraulic pump (3000 psi) must be high enough to achieve this rapid load pulse. The load pulse function for resilient modulus testing is as follows:

$$\text{Haversine Load Pulse} = \frac{(1 - \cos \theta)}{2} \quad (3.2)$$

where

θ : time

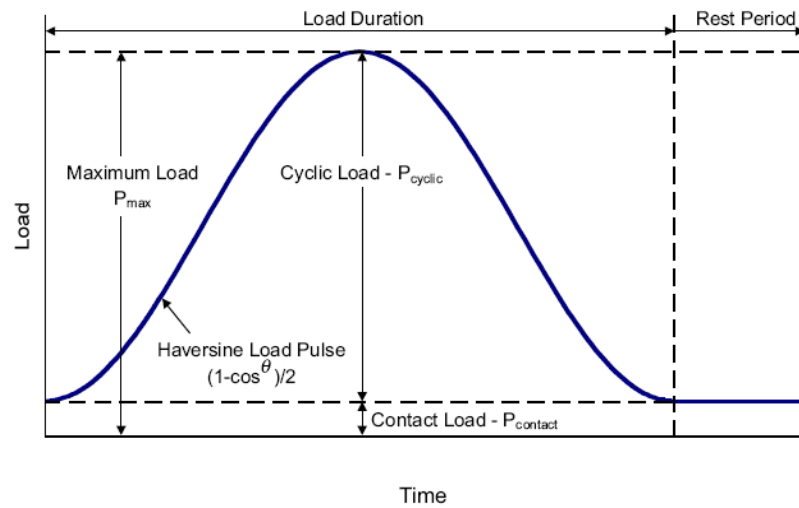


Figure 3.14 Loading Wave Form for Resilient Modulus Testing [NCHRP, 2004]

3.5 Test Setup and Procedure for CBR Testing

In this study, the guidelines given in the AASHTO T193 (2003) specifications are followed for CBR testing.

3.5.1 CBR Test Setup

The hardware for CBR testing consists of two distinct parts:

Load frame: Unit that contains an embedded control system and the components to generate the pressure on a specimens and to measure the force and the displacement.

Computer: PC computer, operating system, network card and hard disk.

TGDH CBR testing equipment utilized in this project is given in Figure 3.15.



Figure 3.15 System for CBR Testing

3.5.2 CBR Test Procedure

The same procedure is followed during specimen preparation and testing for granular and fine-grained soil types. Specimens are compacted with the standard proctor compaction equipment at optimum water contents. The diameter of the cylindrical specimens is standardized as 6 in. where the height is 4.58 in. Compacted specimens for the soaked CBR tests are saturated in the water pool for four days. (Figure 3.16) Simple deflection gauges are used in order to determine the swell amounts for each specimen. The procedure for conducting CBR tests is as follows:

- Place the CBR mold containing the specimen onto the bottom platen
- Place the first surcharge load on the specimen

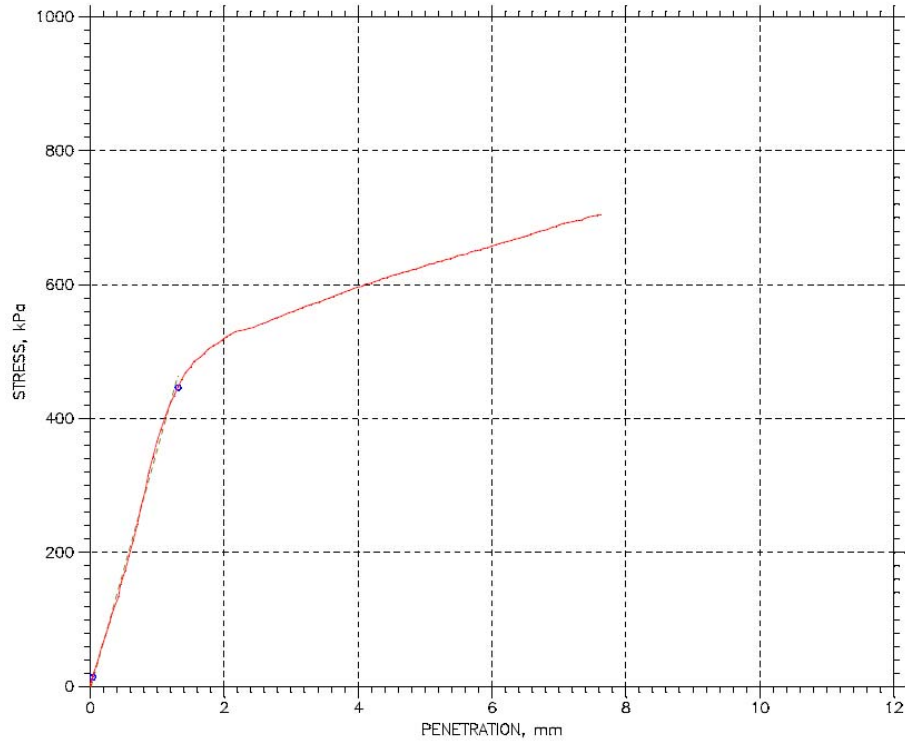
- Apply the initial 44 N load to maintain a contact between the specimen and the loading piston.
- Place the other three surcharge loads.
- Initialize the LVDT and load cell readings
- Start the test

Load frame starts to rise at a constant speed of 1.27mm/min. Load cell measures the amount of applied load at every 1.67×10^{-2} min. The final output of a single CBR test with the corresponding penetration-stress graph is given in Figure 3.17.



Figure 3.16 Saturation Pool for Soaked CBR Specimen Preparation

CALIFORNIA BEARING RATIO TEST REPORT



Sample Height: 116.4 mm	California Bearing Ratio			
Sample Area: 18241 mm ²	at 2.54 mm: 8	at 7.62 mm: N/A	at 12.7 mm: N/A	
Sample Volume: 2123.3 cc	at 5.08 mm: 6	at 10.16 mm: N/A		
Sample Mass: 4.2002 kg				
Sample Condition: Soaked	Water Content	Before	Top	Average
Swell: -98.63 %	Tare ID			
Surcharge: 9.144 kg	Tare Mass, kg	0	0	0
Void Ratio: 0.00	Mass Tare + Wet Soil, kg	0	0	0
Wet Unit Weight: 0 N/m ³	Mass Tare + Dry Soil, kg	0	0.097	0
Dry Unit Weight: 0 N/m ³	Water Content, %	0.00	0.00	0.00

	Project: Diyarbakir Bismil 9/17	Location: TCK, ANKARA	Project No.:
	Boring No.:	Tested By: Erdem Coler	Checked By:
	Sample No.: KALIP NO:11	Test Date: 15/05/2007	Depth:
	Test No.:	Sample Type:	Elevation:
	Description: Diyarbakir Bismil 9/17 Yas CBR Kalip No 11		
Remarks:			

Mon, 18-JUN-2007 20:38:42

Figure 3.17 Data Output for a Single CBR Test

3.6 Test Setup and Procedure for LFWD Testing

The reliability of elastic response evaluation based on deflection measurements and back-calculation procedures is still debatable. Currently, the Keros Prima 100, a Danish device, is under consideration as the standard test to measure the elastic response of unbound materials and used also in this project. However, well-defined specifications for this device are not still available.

The system is composed of three main parts:

- 1) the center sensor and the signal conditioning unit
- 2) 10 kg falling weight
- 3) a pocket pc for data processing

The test is conducted by freely dropping the 10 kg weight on to the loading platen of the device. The center sensor located at the center of the bottom platen measures the deflection resulting from the applied impact load. The information from the sensor is transferred to the signal conditioning unit and the processed signals are sent to the pocket pc. The received data are saved in the Excel format for further analysis.

LFWD tests are conducted for the constructed base, subbase and subgrade pavement layers to estimate the optimum design asphalt thicknesses. Figure 3.18 demonstrates the test setup for LFWD testing.



Figure 3.18 LFWD Test Setup

CHAPTER 4

STATISTICAL MODELS FOR RESILIENT MODULUS PREDICTION

4.1 Introduction

This chapter discusses the results of resilient modulus, CBR and LFWD tests for granular and fine grained soils. In addition, procedure to develop statistical models for estimating the resilient modulus of laboratory specimens is discussed. The reliability of prediction models is also determined based on statistical analyses. The applicability of genetic algorithm and curve shifting methodology for the estimation of resilient modulus is also investigated for various states of stresses.

In this chapter, first the results of resilient modulus, CBR and LFWD tests are presented (Section 4.2). Then, the estimation of the resilient modulus for a typical pavement section according to the constitutive Uzan model and layered elastic analysis is discussed (Section 4.3). In Section 4.4, statistical analysis procedure for model development is presented and the developed linear and nonlinear models are discussed based on the results of experiment set 1 to investigate the effects of various soil index properties on the resilient response of test specimens. Furthermore, application of the genetic algorithm and the curve shifting methodology as an alternative to conventional constitutive nonlinear models is presented based on the experiment set 1. Test results for specimen K67100opt1 (City: Kayseri, Region: 6/7, Compaction: 100%, Water content: optimum, Test

number: 1) is utilized to demonstrate the application procedure of the genetic algorithm and the curve shifting methodology (Section 4.5). Deviator stress – resilient modulus curves at different confining pressures are shifted in order to obtain a final gamma or polynomial type curve by using genetic algorithm. Shift amounts are also modeled using gamma type functions in order to use for the back-calculation of resilient modulus at different stress states. In addition, models correlating resilient modulus with CBR test results are also introduced based on statistical analyses (Section 4.6). For this purpose, four different correlations are investigated: (1) One-to-one correlation: resilient modulus vs. CBR, (2) Inclusion of category covariate “TYPE”: resilient modulus vs. CBR – TYPE, (3) Inclusion of soil index parameters: resilient modulus vs. CBR – Soil index parameters, (4) Separation of test results according to the tree-based approach: resilient modulus vs. CBR – Soil index parameters. Finally, correlations between resilient modulus and LFWD test results are determined (Section 4.7). Three different models are analyzed: (1) One-to-one correlation: resilient modulus vs. LFWD, (2) Inclusion of category covariate “TYPE”: resilient modulus vs. LFWD – TYPE, (3) Inclusion of soil index parameters: resilient modulus vs. LFWD – Soil index parameters. Summary of the developed models is given in Figure 4.1.

The primary objective of this chapter is to determine prediction models for resilient modulus that can be used in the mechanistic-empirical design of flexible pavements in Turkey. For this purpose, laboratory tests are performed for materials from different regions of Turkey. Thus, the developed statistical models are aimed to represent the general resilient response of unbound pavement layers under different conditions.

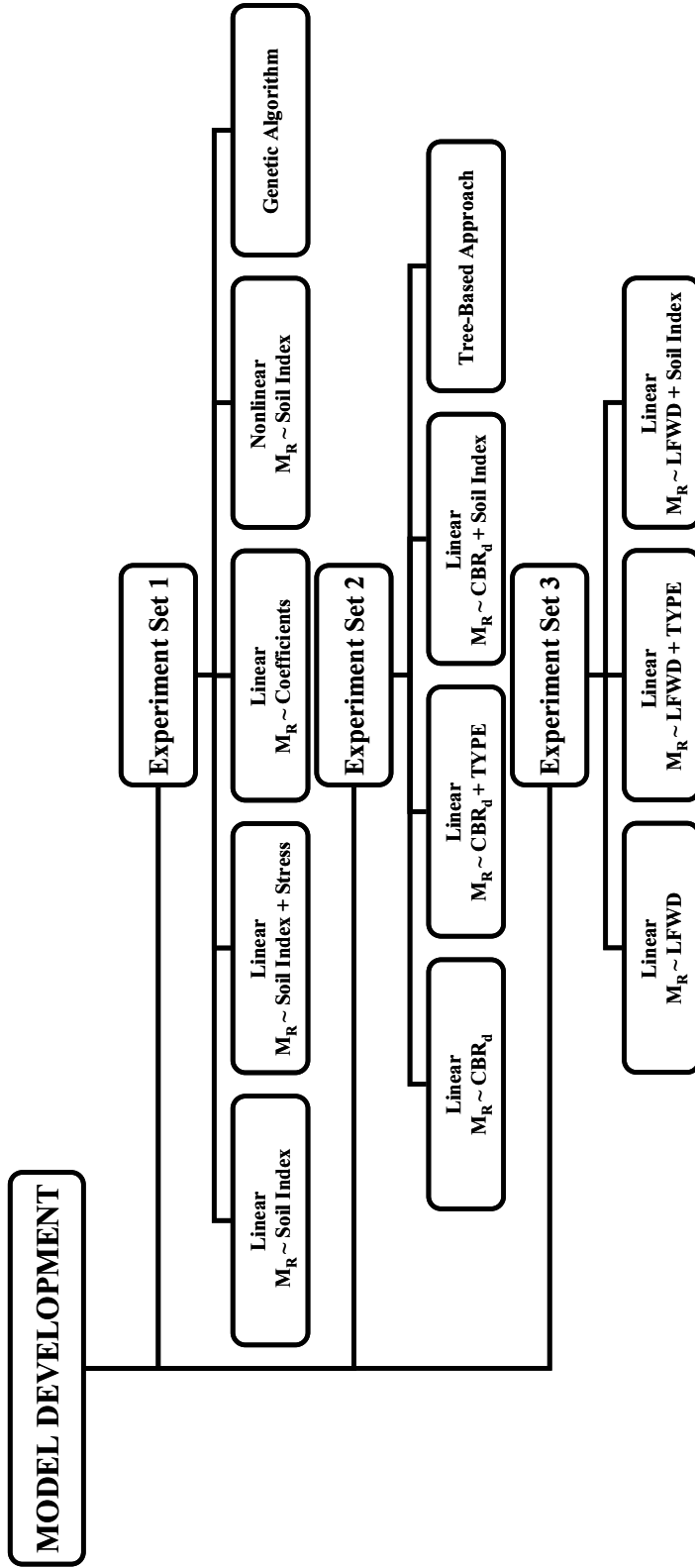


Figure 4.1 Summary of the Developed Models

4.2 Resilient Modulus, CBR and LFWD Test Results

Three types of data sets are utilized for the development of the prediction models:

1. Experiment Set 1: Test for the experiment set 1 were conducted in order to determine the effects of moisture content, compaction percentage and soil index properties for model development purposes. The tests were performed at W_{opt} , $W_{opt}-2$ and $W_{opt}+2$. In addition, tests are also performed for 95% compaction level at optimum water content. Hence, a total of 8 tests were conducted for each specimen in order to monitor the effects of compaction level and moisture content on the resilient modulus. Since the compaction level and the moisture content cannot be maintained at a standard level during the specimen preparation process, effects of variations in these variables should be determined in order to justify the reliability of design modulus selected for pavement design problems. For this experimental set, the genetic algorithm and the curve shifting methodology are also applied in order to estimate resilient modulus at constant stress levels. Table 4.1 illustrates the results of resilient modulus tests for the experiment set 1 specimens. In this table, k_1 , k_2 and k_3 constants are the nonlinear constitutive model coefficients which are described in section 4.3. The naming convention for specimens in this set is as follows:

k62100opt+23 : k: Kayseri, 6/2: section, 100: compaction percentage, opt+2: compaction water content, 3: replicate

Table 4.1 Tests Results for Experiment Set 1

Region	Test	AASHTO	k1	k2	k3	M _R (kPa)
Kayseri 6/2	k6295opt1	A-7-5	493.80	0.2230	-0.0787	53008
Kayseri 6/2	k6295opt2	A-7-5	453.99	0.2220	-0.1350	51490
Kayseri 6/2	k62100opt1	A-7-5	708.43	0.2860	-0.1700	82685
Kayseri 6/2	k62100opt2	A-7-5	768.23	0.0949	-0.0291	79436
Kayseri 6/2	k62100opt3	A-7-5	693.05	0.2360	-0.1440	79201
Kayseri 6/2	k62100opt-21	A-7-5	779.04	0.1130	-0.1340	89094
Kayseri 6/2	k62100opt-22	A-7-5	987.99	0.1440	-0.0792	106827
Kayseri 6/2	k62100opt+21	A-7-5	512.73	0.1510	-0.1170	57487
Kayseri 6/2	k62100opt+23	A-7-5	637.35	0.0245	-0.1590	75254
Kayseri 6/5	k6595opt1	A-2-4	351.81	0.7450	-0.1110	37278
Kayseri 6/5	k6595opt2	A-2-4	360.52	0.7520	-0.1860	41075
Kayseri 6/5	k65100opt1	A-2-4	426.72	0.7050	-0.0712	43643
Kayseri 6/5	k65100opt2	A-2-4	368.98	0.8290	-0.0838	37802
Kayseri 6/5	k65100opt3	A-2-4	320.33	0.5630	0.1410	26962
Kayseri 6/5	k65100opt4	A-2-4	306.78	0.9760	-0.2610	36893
Kayseri 6/5	k65100opt-21	A-2-4	551.76	0.5470	-0.2340	67038
Kayseri 6/5	k65100opt-22	A-2-4	438.93	0.7400	-0.3290	57551
Kayseri 6/5	k65100opt+21	A-2-4	347.34	0.7590	0.0349	31885
Kayseri 6/5	k65100opt+22	A-2-4	384.14	0.3130	0.3360	27309
Kayseri 6/5	k65100opt+23	A-2-4	328.49	0.3370	0.3380	23260
Kayseri 6/6	k6695opt1	A-2-7	356.22	0.7560	-0.1820	40413
Kayseri 6/6	k6695opt2	A-2-7	369.12	0.6980	-0.1710	41635
Kayseri 6/6	k66100opt1	A-2-7	408.21	0.6690	-0.2220	48513
Kayseri 6/6	k66100opt2	A-2-7	357.55	0.8770	-0.2900	44607
Kayseri 6/6	k66100opt3	A-2-7	293.51	0.9180	-0.3690	39412
Kayseri 6/6	k66100opt-21	A-2-7	551.57	0.5250	-0.2000	64951
Kayseri 6/6	k66100opt-22	A-2-7	573.49	0.5480	-0.1950	67072
Kayseri 6/6	k66100opt-23	A-2-7	546.81	0.5140	-0.1450	61085
Kayseri 6/6	k66100opt+21	A-2-7	355.26	0.7830	-0.1520	39052
Kayseri 6/6	k66100opt+22	A-2-7	422.10	0.7380	-0.0788	43369
Kayseri 6/7	k6795opt1	A-5	425.39	0.2710	-0.2060	51489
Kayseri 6/7	k6795opt2	A-5	353.09	0.4630	-0.2180	42539
Kayseri 6/7	k67100opt1	A-5	417.01	0.4170	-0.2250	50783
Kayseri 6/7	k67100opt2	A-5	435.83	0.4360	-0.2140	52424
Kayseri 6/7	k67100opt3	A-5	242.46	0.6260	-0.2660	30188
Kayseri 6/7	k67100opt-21	A-5	602.25	0.2310	-0.1130	66804
Kayseri 6/7	k67100opt-22	A-5	513.81	0.2970	-0.0658	54124

Table 4.1 Tests Results for Experiment Set 1 (Continued)

Region	Test	AASHTO	k1	k2	k3	M _R (kPa)
Kayseri 6/7	k67100opt+21	A-5	446.46	0.3670	-0.1070	48666
Kayseri 6/7	k67100opt+22	A-5	413.67	0.3430	-0.1830	48661
A.C	ac95opt1	A-6	940.23	0.2350	-0.0574	98755
A.C	ac95opt2	A-6	899.03	0.2430	-0.1080	99137
A.C	ac100opt3	A-6	886.88	0.5000	-0.1130	96145
A.C	ac100opt4	A-6	998.28	0.2570	-0.0624	105168
A.C	ac100opt-21	A-6	1686.9	0.0468	0.1330	149535
A.C	ac100opt-22	A-6	1575.8	0.2320	0.0809	144665
A.C	ac100opt+21	A-6	539.66	0.4470	-0.2570	67629
A.C	ac100opt+22	A-6	689.82	0.4140	-0.2020	82163
D.S	ds9395opt1	A-7-6	434.98	0.2610	-0.1700	50877
D.S	ds9395opt2	A-7-6	467.21	0.3380	-0.2260	57337
D.S	ds93100opt1	A-7-6	537.42	0.1950	-0.2300	67023
D.S	ds93100opt2	A-7-6	611.88	0.1690	-0.0616	64896
D.S	ds93100opt3	A-7-6	648.59	0.1430	-0.0477	68013
D.S	ds93100opt-21	A-7-6	648.99	0.2100	-0.0845	70140
D.S	ds93100opt-22	A-7-6	746.67	0.0966	0.0570	70978
D.S	ds93100opt+21	A-7-6	186.62	0.2980	-0.3740	26549
D.S	ds93100opt+22	A-7-6	200.94	0.3010	-0.4330	30271
D.K.V	dkv9695opt1	A-7-6	625.33	0.1210	-0.0729	67332
D.K.V	dkv9695opt2	A-7-6	729.95	0.2050	-0.0481	76171
D.K.V	dkv96100opt1	A-7-6	589.54	0.1440	-0.0838	64031
D.K.V	dkv96100opt2	A-7-6	552.73	0.1670	-0.0525	58114
D.K.V	dkv96100opt3	A-7-6	603.80	0.2670	-0.1890	71907
D.K.V	dkv96100opt-21	A-7-6	1158.4	0.1790	-0.00157	115774
D.K.V	dkv96100opt-22	A-7-6	1046.9	0.3120	-0.0730	110914
D.K.V	dkv96100opt+21	A-7-6	430.47	0.1790	-0.1840	51400
D.K.V	dkv96100opt+22	A-7-6	434.02	0.2370	-0.1110	48025
D.B	db91795opt1	A-7-6	674.79	0.0852	0.0369	65479
D.B	db91795opt2	A-7-6	535.54	0.3100	-0.3800	76555
D.B	db917100opt1	A-7-6	823.71	0.2630	-0.0713	87488
D.B	db917100opt2	A-7-6	758.05	0.2120	-0.0808	81618
D.B	db917100opt3	A-7-6	912.60	0.1550	0.1380	79764
D.B	db917100opt-21	A-7-6	913.16	0.2740	0.0594	85302
D.B	db917100opt-22	A-7-6	947.89	0.1880	-0.00405	94892
D.B	db917100opt+21	A-7-6	505.95	0.1880	-0.0531	53132
D.B	db917100opt+22	A-7-6	526.92	0.2150	-0.0762	56464

2. Experiment Set 2: Tests for the experiment set 2 were conducted in order to develop resilient modulus prediction models based on simple strength test (CBR) results. In addition, models correlating resilient modulus with soil index parameters and simple strength test results were also developed in order to minimize the model residual errors. For this purpose, a total of three tests were conducted for each soil type at the optimum water content and 100% compaction level. The results of the simple strength and resilient modulus tests that were performed are given in Table 4.2.

Table 4.2 Tests Results for Experiment Set 2

Region	Test	AASHTO	CBR _w	CBR _d	M _R (kPa)
B142	B142OPT1	A-1-a	31.5	29.5	123493
B142	B142OPT2	A-1-a	31.5	29.5	169398
B142	B142OPT3	A-1-a	31.5	29.5	148043
B1415	B1415OPT1	A-2-4	12.0	21.0	154273
B1415	B1415OPT2	A-2-4	12.0	21.0	140399
B1415	B1415OPT3	A-2-4	12.0	21.0	152724
B143	B143OPT1	A-2-4	26.5	28.0	163744
B143	B143OPT2	A-2-4	26.5	28.0	147227
B143	B143OPT3	A-2-4	26.5	28.0	131107
K61	K61OPT1	A-1-a	128.0	137.0	259015
K61	K61OPT2	A-1-a	128.0	137.0	127000
K61	K61OPT3	A-1-a	128.0	137.0	338462
K61	K61OPT4	A-1-a	128.0	137.0	286471
K61	K61OPT5	A-1-a	128.0	137.0	269991
K63	K63OPT1	A-1-b	64.0	64.0	278292
K63	K63OPT2	A-1-b	64.0	64.0	124129
K63	K63OPT3	A-1-b	64.0	64.0	162962
K63	K63OPT4	A-1-b	64.0	64.0	289499
K63	K63OPT5	A-1-b	64.0	64.0	216446
K64	K64OPT1	A-1-b	62.0	70.0	159918
K64	K64OPT2	A-1-b	62.0	70.0	179437
K64	K64OPT3	A-1-b	62.0	70.0	249186
K64	K64OPT4	A-1-b	62.0	70.0	220868
K64	K64OPT5	A-1-b	62.0	70.0	222635
K68	K68OPT1	A-1-b	45.5	47.0	90448
K68	K68OPT2	A-1-b	45.5	47.0	95224
K68	K68OPT3	A-1-b	45.5	47.0	93742
DB916	DB916OPT1	A-1-a	32.5	28.0	117602
DB916	DB916OPT2	A-1-a	32.5	28.0	132995

Table 4.2 Tests Results for Experiment Set 2 (Continued)

Region	Test	AASHTO	CBR _w	CBR _d	M _R (kPa)
DB916	DB916OPT3	A-1-a	32.5	28.0	113332
KAS5	KAS5OPT1	A-2-4	36.0	39.0	140001
KAS5	KAS5OPT2	A-2-4	36.0	39.0	140876
KAS5	KAS5OPT3	A-2-4	36.0	39.0	136460
KD	KDOPT1	A-1-a	54.0	57.0	119540
KD	KDOPT2	A-1-a	54.0	57.0	129848
KD	KDOPT3	A-1-a	54.0	57.0	106265
KON32	KON32OPT1	A-1-a	106.0	109.0	297574
KON32	KON32OPT2	A-1-a	106.0	109.0	359442
KON32	KON32OPT3	A-1-a	106.0	109.0	318465
KON36	KON36OPT1	A-1-b	12.0	16.5	67871
KON36	KON36OPT2	A-1-b	12.0	16.5	70414
KON36	KON36OPT3	A-1-b	12.0	16.5	66575
KON317	KON317OPT1	A-1-a	120.0	122.5	111863
KON317	KON317OPT2	A-1-a	120.0	122.5	95652
KON317	KON317OPT3	A-1-a	120.0	122.5	140424
AC	ACOPT1	A-6	8.0	21.0	70438
AC	ACOPT2	A-6	8.0	21.0	98757
AC	ACOPT3	A-6	8.0	21.0	96148
B141	B141OPT1	A-2-7	12.0	17.0	105169
B141	B141OPT2	A-2-7	12.0	17.0	92372
B141	B141OPT3	A-2-7	12.0	17.0	89411
B1411	B1411OPT1	A-6	7.5	17.5	69233
B1411	B1411OPT2	A-6	7.5	17.5	67117
B1411	B1411OPT3	A-6	7.5	17.5	71514
B1416	B1416OPT1	A-2-4	28.0	31.0	66462
B1416	B1416OPT2	A-2-4	28.0	31.0	50165
B1416	B1416OPT3	A-2-4	28.0	31.0	55968
B148	B148OPT1	A-6	20.0	24.5	56385
B148	B148OPT2	A-6	20.0	24.5	44529
B148	B148OPT3	A-6	20.0	24.5	47924
B144	B144OPT1	A-2-4	15.0	27.0	43827
B144	B144OPT2	A-2-4	15.0	27.0	71290
B144	B144OPT3	A-2-4	15.0	27.0	95060
D98	D98OPT1	A-6	9.0	17.5	84492
D98	D98OPT2	A-6	9.0	17.5	38242
D98	D98OPT3	A-6	9.0	17.5	42609
D920	D920OPT1	A-7-6	14.0	14.0	50580
D920	D920OPT2	A-7-6	14.0	14.0	34236
D920	D920OPT3	A-7-6	14.0	14.0	34730
DB917	DB917OPT1	A-7-6	8.0	14.0	36469

Table 4.2 Tests Results for Experiment Set 2 (Continued)

Region	Test	AASHTO	CBR _w	CBR _d	M _R (kPa)
DB917	DB917OPT2	A-7-6	8.0	14.0	87490
DB917	DB917OPT3	A-7-6	8.0	14.0	81619
DKV96	DKV96OPT1	A-7-6	5.5	13.5	79765
DKV96	DKV96OPT2	A-7-6	5.5	13.5	64032
DKV96	DKV96OPT3	A-7-6	5.5	13.5	58115
DS93	DS93OPT1	A-7-6	9.0	13.5	71908
DS93	DS93OPT2	A-7-6	9.0	13.5	67024
DS93	DS93OPT3	A-7-6	9.0	13.5	64896
K62	K62OPT1	A-7-5	9.5	16.0	68014
K62	K62OPT2	A-7-5	9.5	16.0	82686
K62	K62OPT3	A-7-5	9.5	16.0	79437
K65	K65OPT1	A-2-4	13.0	21.0	79202
K65	K65OPT2	A-2-4	13.0	21.0	43645
K65	K65OPT3	A-2-4	13.0	21.0	37804
K65	K65OPT4	A-2-4	13.0	21.0	26963
K66	K66OPT1	A-2-7	29.0	31.5	36896
K66	K66OPT2	A-2-7	29.0	31.5	48515
K66	K66OPT3	A-2-7	29.0	31.5	44610
K67	K67OPT1	A-5	17.5	22.0	39415
K67	K67OPT2	A-5	17.5	22.0	50784
K67	K67OPT3	A-5	17.5	22.0	52401
KAS4145	KAS4145OPT1	A-2-6	10.5	17.5	30190
KAS4145	KAS4145OPT2	A-2-6	10.5	17.5	99813
KAS4145	KAS4145OPT3	A-2-6	10.5	17.5	103863
KON31	KON31OPT1	A-3	36.0	31.0	119085
KON31	KON31OPT2	A-3	36.0	31.0	63557
KON31	KON31OPT3	A-3	36.0	31.0	68313
KON313	KON313OPT1	A-6	16.0	18.0	76066
KON313	KON313OPT2	A-6	16.0	18.0	69344
KON313	KON313OPT3	A-6	16.0	18.0	70559
KON315	KON315OPT1	A-2-4	87.0	93.5	94015
KON315	KON315OPT2	A-2-4	87.0	93.5	48157
KON315	KON315OPT3	A-2-4	87.0	93.5	48811

3. Experiment Set 3: Tests for the experiment set 3 were conducted in order to develop resilient modulus prediction models based on the field strength test (LFWD) results. In addition, models correlating resilient modulus with field strength tests were improved by including various soil index parameters. Since the LFWD is a simple test to evaluate the resilient response of in-situ unbound pavement layers, design resilient modulus values can be directly estimated based

these correlation functions without performing laboratory resilient modulus tests. The results of the field strength and resilient modulus tests are given in Table 4.3.

Table 4.3 Tests Results for Experiment Set 3

Region	Test	AASHTO	LFWD (kPa)	k1	k2	k3	M _R (kPa)
B142	B142OPT1	A-1-a	155000	534.74	0.961	-0.1230	123493
B142	B142OPT2	A-1-a	155000	891.85	0.698	-0.1630	169398
B142	B142OPT3	A-1-a	155000	827.15	0.660	-0.0922	148043
B143	B143OPT1	A-2-4	214000	813.30	0.741	-0.2210	163744
B143	B143OPT2	A-2-4	214000	889.73	0.575	-0.0676	147227
B143	B143OPT3	A-2-4	214000	826.21	0.543	-0.0280	131107
K64	K64OPT1	A-1-b	178000	1147.4	0.522	0.2490	159918
K64	K64OPT2	A-1-b	178000	594.12	1.270	-0.1710	179437
K64	K64OPT3	A-1-b	178000	1229.1	0.822	-0.0780	249186
K64	K64OPT4	A-1-b	178000	1171.5	0.763	-0.0163	220868
K64	K64OPT5	A-1-b	178000	836.37	1.100	-0.1970	222635
K68	K68OPT1	A-1-b	151000	435.64	0.842	-0.0969	90448
K68	K68OPT2	A-1-b	151000	499.37	0.755	-0.0600	95224
K68	K68OPT3	A-1-b	151000	463.54	0.808	-0.0995	93742
KAS5	KAS5OPT1	A-2-4	116000	617.78	0.934	-0.1300	140001
KAS5	KAS5OPT2	A-2-4	116000	679.42	0.848	-0.0818	140876
KAS5	KAS5OPT3	A-2-4	116000	644.81	0.850	-0.1280	136460
KD	KDOPT1	A-1-a	112000	568.20	0.883	-0.0483	119540
KD	KDOPT2	A-1-a	112000	553.76	0.987	-0.1090	129848
KD	KDOPT3	A-1-a	112000	409.79	1.110	-0.1130	106265
B141	B141OPT1	A-2-7	56000	956.60	0.153	0.0360	92372
B141	B141OPT2	A-2-7	56000	935.79	0.133	0.0486	89411
B141	B141OPT3	A-2-7	56000	713.36	0.279	0.0198	69233
B148	B148OPT1	A-6	76000	366.49	0.387	-0.2200	44529
B148	B148OPT2	A-6	76000	381.37	0.438	-0.2590	47924
B148	B148OPT3	A-6	76000	362.56	0.401	-0.2160	43827
B1411	B1411OPT1	A-6	103000	625.15	0.225	-0.0790	67117
B1411	B1411OPT2	A-6	103000	619.05	0.258	-0.1570	71514
B1411	B1411OPT3	A-6	103000	595.66	0.311	-0.1260	66462
B144	B144OPT1	A-2-4	139000	574.16	0.533	-0.2550	71290
B144	B144OPT2	A-2-4	139000	695.63	0.301	-0.3330	95060
B144	B144OPT3	A-2-4	139000	670.86	0.114	-0.2330	84492
K65	K65OPT1	A-2-4	58000	426.72	0.705	-0.0712	43645
K65	K65OPT2	A-2-4	58000	368.98	0.829	-0.0838	37804
K65	K65OPT3	A-2-4	58000	320.33	0.563	0.1410	26963
K65	K65OPT4	A-2-4	58000	306.78	0.976	-0.2610	36896
KAS4145	KAS4145OPT1	A-2-6	115000	857.48	0.146	-0.1550	99813
KAS4145	KAS4145OPT2	A-2-6	115000	1383.6	0.0523	0.3030	103863
KAS4145	KAS4145OPT3	A-2-6	115000	996.41	0.134	-0.1810	119085

4.3 Development of Conventional Constitutive Models Based on Resilient Modulus Test Results

The universal (Uzan) constitutive model is utilized for the estimation of the resilient modulus at different layers of a typical pavement section (Equation 2.3). The nonlinear universal model should be normalized in order to perform linear regression:

$$\log\left(\frac{M_R}{\sigma_{atm}}\right) = \log(k_1) + k_2 \cdot \left(\log\left(\frac{\theta}{\sigma_{atm}}\right)\right) + k_3 \cdot \left(\log\left(\frac{\sigma_d}{\sigma_{atm}}\right)\right) \quad (4.1)$$

where:

M_R = resilient modulus

σ_d = deviator stress

σ_{atm} = atmospheric pressure

$\theta = \sigma_1 + \sigma_2 + \sigma_3$ (bulk stress)

k_1, k_2, k_3 = regression coefficients

The regression result for the universal model is as follows

(Specimen:DS93100opt+22)

```
> const.lm<-lm(logrm~logbatm+logdevatm,data=const)
> summary(const.lm)

Call: lm(formula = logrm ~ logbatm + logdevatm, data = const)
Residuals:
    Min       1Q   Median       3Q      Max
-0.06974 -0.01392 -0.007479  0.004611  0.06862

Coefficients:
            Value Std. Error t value Pr(>|t|)
(Intercept)  2.3030    0.0261  88.1497  0.0000
      logbatm  0.3005    0.0764   3.9316  0.0020
      logdevatm -0.4332    0.0472  -9.1841  0.0000

Residual standard error: 0.03848 on 12 degrees of freedom
Multiple R-Squared:  0.8761^2 = 0.94
F-statistic: 42.43 on 2 and 12 degrees of freedom, the p-value is 3.615e-006
Correlation of Coefficients:
      (Intercept) logbatm
      logbatm    -0.6024
      logdevatm   0.9081   -0.4959
```

The final universal constitutive model according to the regression analysis of the DS93100opt+22 test results is expressed as follows:

$$\frac{M_R}{\sigma_{atm}} = 200.91 \left(\frac{\theta}{\sigma_{atm}} \right)^{0.301} \left(\frac{\sigma_d}{\sigma_{atm}} \right)^{-0.433}$$

A typical pavement section with low elastic modulus values is chosen as a representative section in order to determine a single resilient modulus for a certain test. The deviator stress, confining pressure and bulk stress parameters at the middle of base layer and at the top of subgrade layer are determined based on the corresponding section properties, the elastic modulus values and the axle configurations using the layered-elastic program CIRCLY (Appendix A). The stress values at the most critical point, the edge of the tire, are determined in order to estimate the most secure design parameters. The typical pavement section and the representative axle configurations with the determined critical stresses are given in Figure 4.2. A representative resilient modulus for a certain test can be determined using this typical pavement section. The representative resilient modulus based on the regression results of DS93100opt+22 test results is calculated as follows:

$$\frac{M_R}{101.32501} = 200.91 \cdot \left(\frac{(3 \times 18.28 + 38.21)}{101.32501} \right)^{0.301} \left(\frac{38.21}{101.32501} \right)^{-0.433} = 30267.31 \text{ kPa}$$

The stresses occurring at the top of the subgrade layer are used in the estimation of resilient modulus since DS93 specimens are composed of Type 2 (fine-grained) subgrade soils. The resilient modulus for fine-grained and granular materials is determined for each test according to the selected stress state and the universal constitutive model. These values represent the measured resilient modulus for each test and will be used to estimate the reliability of the predicted models.

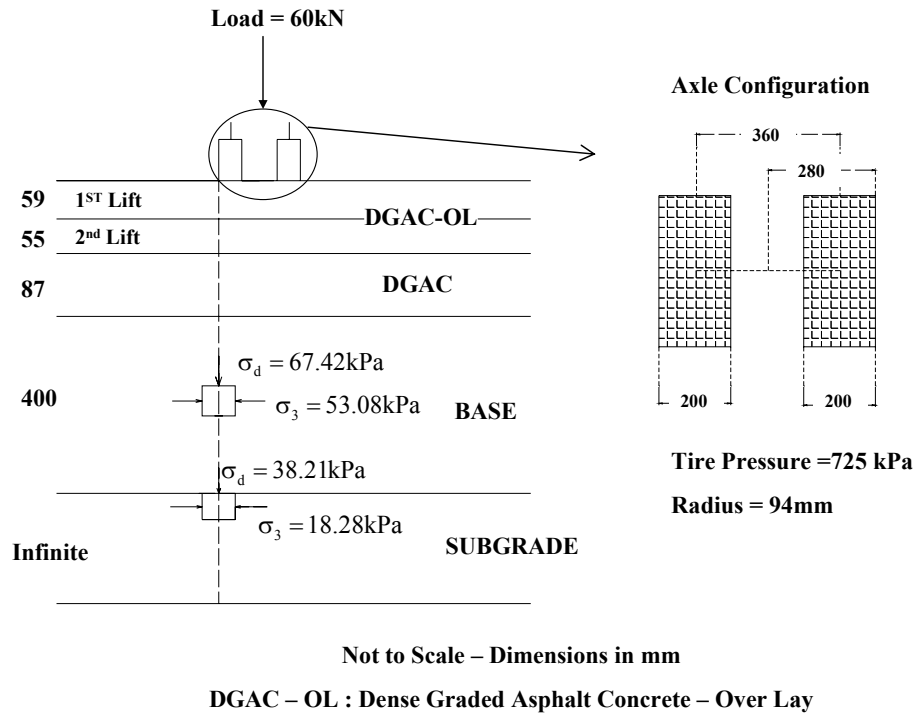


Figure 4.2 Typical Pavement Section Characteristics

4.4 Models Correlating Resilient Modulus with Soil Index Properties (Experiment Set 1)

The primary objective of this section is to develop reliable prediction models for the estimation of the resilient modulus from soil index parameters. In addition, genetic algorithm and curve shifting methodology is applied for this experiment set in order to develop reliable models as an alternative to conventional constitutive correlation functions. Resilient modulus prediction models are developed for two different cases: (1) selected stress state (2) variable stress state

4.4.1 Statistical Analysis Procedure Used for Model Development (Demonstration Example)

In this section, application of regression analysis is demonstrated to construct a linear model correlating the resilient modulus with soil index properties. In statistics, regression analysis examines the relation of a dependent variable (response variable) to specified independent variables (predictors). The mathematical model of their relationship is called the regression equation. In this study, the dependent variable used for model development is the resilient modulus and the independent variables are the index properties which may change according to the experiment sets. The detailed statistical analyses procedure followed for the regression model development is illustrated next for a certain stress state. In this section, only the experiment set 1 specimens were utilized for model development to construct possible relations between the resilient modulus and the corresponding soil index properties. All dependent and independent variables and their numerical ranges used for experimental set 1 model development are presented in Table 4.4.

Table 4.4 Independent and Dependent Variables Used for Model Development

Variable Type	Symbol	Description	Range
Dependent	M_R	Laboratory resilient modulus for a certain stress state	26549 – 149535 kPa
Independent	Comp	Compaction Percentage	95, 100 %
	LL	Liquid Limit	39.9 – 61.1
	PI	Plasticity Index	9.7 – 37.3
	Wopt	Optimum water content	14.8 – 28.4 %
	DDstd	Maximum dry-density	1.436 – 1.844 Mg/m ³
	PP10	Percent passing no. 10 sieve	43 – 99 %
	PP40	Percent passing no. 40 sieve	26.1 – 96.6 %
PP200	Percent passing no. 200 sieve	18.3 – 94.2 %	
Category independent	Wc	Water content levels for compaction	opt-2, opt, opt+2

The model selection procedure discussed here includes the following steps:

1. pairs plot to inspect the possible relationship amongst various variables,
2. correlation matrix of the independent and dependent variables,
3. ANOVA table to identify the significant terms,
4. Mallows' C_p [Ross, 1987] to choose the best subset of the covariates,
5. regression analysis,
6. residual plots, and
7. engineering judgment.

4.4.1.1 Pairs Plots

It is a statistical fact that high correlations between the independent variables improve the coefficient of determination (R^2) in a regression model. However, the increase in R^2 values can be sometimes unrealistic because of interactions between the similar independent variables. The colinearity between two independent variables improves the R^2 where the statistical strength of the model does not change. At this point, pairs plots can be considered as a handy tool to estimate the relationships and linearities between quantitative variables in a data set. It is possible to eliminate independent variables that increase the numerical noise (over-fit) in a regression model using pairs plots. Figure 4.3 is the pairs plot which demonstrates the interactions between dependent and independent variables for the experiment set 1 test results. The linearities between Wopt, DDstnd and PP10, PP40, PP200 soil index variables suggest that only the most effective of these terms be used to develop a model.

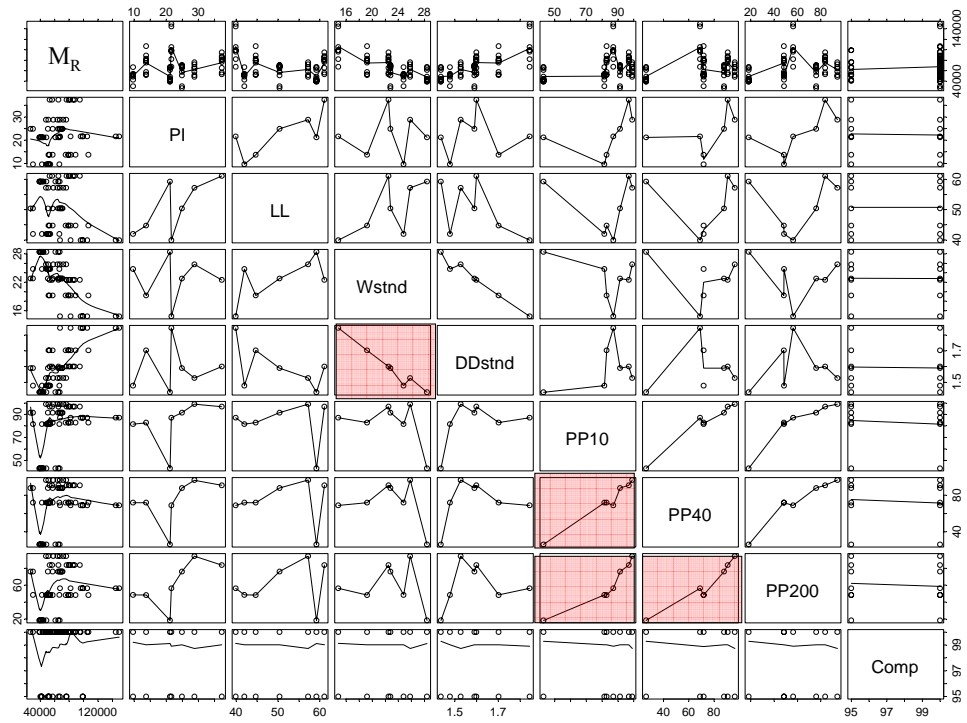


Figure 4.3 Pairs Plot for the Demonstration of the Interactions between Soil Index Parameters and Resilient Modulus

4.4.1.2 Correlation Matrix

Analysis of correlation matrix indicates the strength and direction of a linear relationship between two random variables. It is a reliable tool to determine the independent variables which are highly correlated with the dependent variable. In addition, it is possible to estimate the linear interactions between two independent variables by the analysis of the correlation matrix. Correlation values ranges from -1 to +1. Minus sign represents an inverse proportion between two variables whereas plus sign represents the direct proportion. The absolute value of the correlation coefficient closer to 1 represents a strong relationship between two variables. High correlations between two independent variables may indicate the possible noise in

the model. In this case, the parameter with higher statistical strength should be used for model development in order to avoid over-fitting. The correlation matrix for the representation of linear interactions between the soil index properties and the resilient modulus is given in Table 4.5.

Table 4.5 Correlation Matrix Results for the Experiment Set 1 Test Results

	M_R	PI	LL	Wopt	DDstd	PP10	PP40	PP200	Comp
M_R	1.000	0.165	-0.280	-0.689	0.715	0.316	0.197	0.185	0.103
PI	0.165	1.000	0.740	0.059	0.041	0.036	0.392	0.620	-0.014
LL	-0.280	0.740	1.000	0.649	-0.546	-0.182	-0.070	0.173	0.007
Wopt	-0.689	0.059	0.649	1.000	-0.984	-0.486	-0.337	-0.210	0.016
DDstd	0.715	0.041	-0.546	-0.984	1.000	0.459	0.313	0.230	-0.019
PP10	0.316	0.036	-0.182	-0.486	0.459	1.000	0.983	0.921	-0.037
PP40	0.197	0.392	-0.070	-0.337	0.313	0.983	1.000	0.952	-0.035
PP200	0.185	0.620	0.173	-0.210	0.230	0.921	0.952	1.000	-0.039
Comp	0.103	-0.014	0.007	0.016	-0.019	-0.037	-0.035	-0.039	1.000

4.4.1.3 ANOVA Table

The ANOVA table is the results of applying the basic principles of the analysis of variance technique. First, measured data points are decomposed in parts due to the differences between groups and residual effects. Secondly, this decomposition is analyzed for the estimation of variations between parameters and interaction effects. The general statistical terms in an ANOVA table can be expressed as follows:
[Seber, 1977]

Degrees of Freedom (DF): Total number of degrees of freedom is one less than the number of observations. Each sum of square value is associated with the degrees of freedom.

Sum of Squares: Sum of squares represents the total amount of variability in the data set that can be estimated by calculating the sum of the squared differences between each observation and the overall mean.

Mean Square: Mean square is simply the sum of squares divided by the corresponding degrees of freedom.

F Value: It is the most important term in the estimation of the statistical significance of independent variables. It also represents whether the model has significant predictive capability. F value is simply the ratio of the model mean square to the error mean square.

Pr(F) Value: It simply gives the percent error for a single independent variable in the representation of the dependent variable.

Table 4.6 presents the ANOVA table for the estimation of the effects of soil index variables on the dependent variable resilient modulus with the corresponding interaction terms based on the experiment set 1 test results.

Table 4.6 ANOVA Table for the Experiment Set 1 Test Results and Soil Index Variables

	Df	Sum of Sq	Mean Sq	F Value	Pr(F)
Comp	1	374258229	374258229	1.37154	0.2474515
LL	1	2747058358	2747058358	10.06708	0.0026605
PI	1	10817871912	10817871912	39.64402	0.0000001
Wopt	1	4811299367	4811299367	17.63186	0.0001184
DDstnd	1	250334242	250334242	0.91739	0.3430613
PP10	1	199340031	199340031	0.73052	0.3970515
PP40	1	1519932316	1519932316	5.57006	0.0224730
Comp:LL	1	169571562	16957156	0.62143	0.4344763
Comp:PI	1	96122787	96122787	0.35226	0.5556828
Comp:Wopt	1	962230549	962230549	3.52627	0.0666163
Comp:DDstnd	1	104619942	104619942	0.38340	0.5387800
Comp:PP10	1	5630136	5630136	0.02063	0.8863983
Comp: PP40	1	71844014	71844014	0.26329	0.6102757
Residuals	47	12825137587	272875268		

4.4.1.4 Mallows's C_p

Mallows' C_p method is proposed in order to choose the best independent variable subset which will develop the most reliable regression model with minimum numerical noise. This method is used as a subsetting criterion in selecting a reduced model without over-fitting problems. C_p is defined as:

$$C_p = \frac{SS_{res,p}}{\sigma^2} + 2p - n \quad (4.2)$$

where:

$SS_{res,p}$: residual sum of the squares of the p-parameter sub-model

σ^2 : residual mean square after regression

n: sample size

p: number of selected independent variables

The independent variable subset which will be used for model development is estimated based on the following guidelines:

- if no large systematic error exists, then $C_p \approx p$.
- if $C_p \gg p$, then it indicates a sub-model with large bias
- Consider a sub-model with small C_p and $C_p \approx p$.

The Mallows' C_p analysis result for the experiment set 1 test results and soil index properties is as follows:

4.4.1.5 Regression Analysis and Residual Plots for Model Development

The results of the statistical analysis (Table 4.7) suggest using PI, LL, Wopt and PP40 as model independent variables. In addition, the category covariate Wc should also be considered in model development since it reflects the effects of $\pm 2\%$ compaction water content. Since PI and LL represent similar properties of the experiment set 1 specimens, only the most effective PI variable is chosen for regression modeling based on the ANOVA table and correlation matrix results.

Table 4.7 The Summary Statistics of Experimental Set 1 Linear Model Independent Variables

	PI	LL	Wopt	DDstd	PP10	PP40	PP200	Comp
Pairs Plots	√	√	X ₂	X ₂	X ₃	X ₃	X ₃	√
Correlation Matrix	X ₁	X ₁	X ₂	X ₂	X ₃	X ₃	X ₃	√
ANOVA Tables	√	√	√	I	I	√	I	I
Mallow's C _p	√	√	√	√	√	√	I	√

Note: √: statistically effective
 I: statistically ineffective
 X : do not use with a certain independent variable

The final linear model which correlates laboratory resilient modulus test results for a certain stress state with soil index properties is as follows:

$$M_R = 155670.8879 + 752.7832 \cdot PI - 4262.4089 \cdot Wopt - 107.9602 \cdot PP40 - 7183.4191 \cdot Wc1 + 9073.0600 \cdot Wc2 \quad (R^2 = 0.7637)$$

(0.0000)
(0.0005)
(0.0000)
(0.1998)

(0.0005)
(0.0000)

where the contrast table of Wc category covariate is given in Table 4.8.

Table 4.8 Factor Wc, Contrast Table

	Wc1	Wc2
opt	-1	-1
opt+2	1	-1
opt-2	0	2

The number inside the parentheses is the standard error of regression coefficient. Since R^2 does not reflect the effects of colinearity in the model, residual plots of the model must be analyzed. The residual plots for the regression model are given in Figure 4.4.

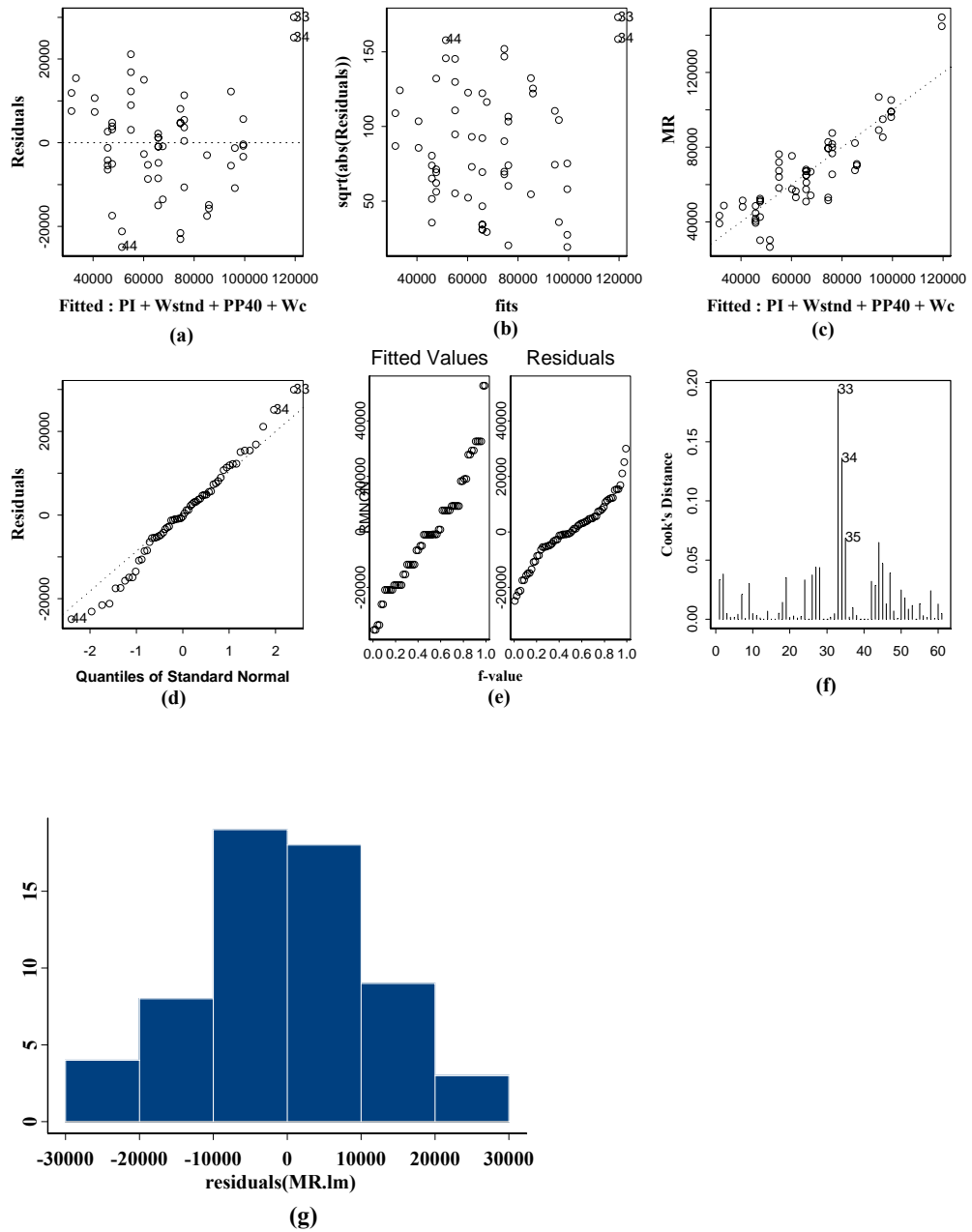


Figure 4.4 Residual Plots for the Linear Regression Model Correlating M_R with Soil Index Parameters

Figure 4.4 (a) illustrates the residual versus the fitted values. The residual values should be close to zero for a reliable model. In addition, if the residuals present a constant trend (linear, parabolic, hyperbolic etc.), the mathematical function used for model development must be changed. For this regression model, the pattern of the residual plot is acceptable. Figure 4.4 (b) shows the same residual plot where the absolute value of residuals is plotted in order to compare the negative and positive residuals. Figure 4.4 (c) represents the final model fit on a line of equality. Figures 4.4 (d) and 4.4 (g) show that the distribution of residuals is very close to normal; however, some outliers make it skew to the left. In Figure 4.4 (e), the range of the fitted values is higher than the residuals, which also proves the statistical strength of the model. Finally, Figure 4.4 (f) demonstrates the outliers encountered during model development.

The final plot demonstrating the measured resilient modulus versus predicted resilient modulus is given in Figure 4.5. The confidence intervals of the models are determined according to Equation 4.3 [Ang, 2007].

$$\left(\mu_{Y/x_i}\right)_{1-\alpha} = \bar{y}_i \pm t_{(1-\frac{\alpha}{2}), n-2} \cdot s_{Y/x} \sqrt{\frac{1}{n} + \frac{(x_i - \bar{x})^2}{\sum (x_i - \bar{x})^2}} \quad (4.3)$$

where

$s_{Y/x}$: conditional standard deviation of Y

$t_{(1-\frac{\alpha}{2}), n-2}$: the value of the t-distributed covariate at the probability of $(1-\frac{\alpha}{2})$ with

(n-2) degrees of freedom

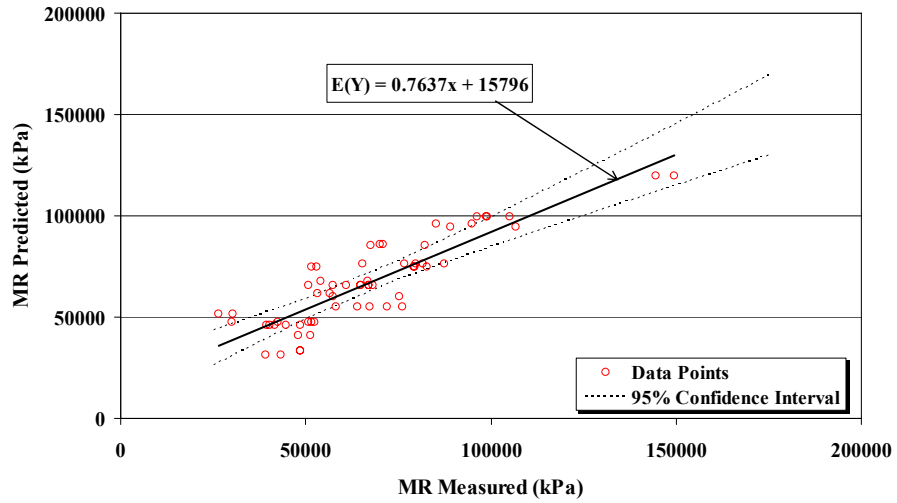


Figure 4.5 Comparison of Predicted and Measured Resilient Modulus for a Certain Stress State

4.4.2 Linear Model Correlating Resilient Modulus with Soil Index Properties and Stress Levels

The model development procedure explained in Section 4.4.1 is carried out for the estimation of resilient modulus of fine-grained soils from soil index properties and stress states. The ranges of independent stress state variables are given in Table 4.9.

Table 4.9 Ranges of Independent Stress State Variables

Variable Type	Symbols	Description	Range
Dependent	M _R	Laboratory resilient modulus for varying stress states	12823 – 198640 (kPa)
Independent	cp	Confining pressure	13.790 - 41.369 (kPa)
	bulk	Bulk stress	53.964 - 199.631 (kPa)
	dev	Deviator Stress	13.790 - 68.948
	Wvibr	Optimum water content (Vibratory compaction)	14.80 - 29.60 (%)
	DDvibr	Maximum dry – density (Vibratory compaction)	1.404 - 1.844 (Mg/m ³)

The independent variables with the highest statistical strengths are chosen in the model development according to the pairs plots, correlation matrix, ANOVA tables and Mallow’s C_p analysis. For this model type, the optimum water content and the maximum dry-density variables estimated from the vibratory compaction procedure are used since these variables are statistically more effective than W_{opt} and DD_{std}. In addition, statistical analyses suggest using the square of the W_{vibr} variable in order to improve the model performance. The resulting linear model correlating laboratory resilient modulus with soil index parameters and stress states is as follows:

$$M_R = \underset{(0.0000)}{-1342837.4659} + \underset{(0.0000)}{1310.4477} \cdot PI + \underset{(0.0000)}{409.9442} \cdot (W_{vibr})^2 + \underset{(0.0000)}{715230.5763} \cdot DD_{vibr} + \underset{(0.0053)}{65.3415} \cdot PP_{200} + \underset{(0.0000)}{604.6671} \cdot cp - \underset{(0.0000)}{7542.7057} \cdot W_{c1} + \underset{(0.0000)}{10986.1211} \cdot W_{c2} \quad (R^2 = 0.7723)$$

where,

cp: confining pressure

Figure 4.6 demonstrates the deviation between the predicted and the measured resilient modulus. The results indicate that the statistical strength of the model is

satisfactory for low resilient modulus levels. However, at higher resilient modulus levels the model is not capable of representing the laboratory test results. Thus, this model is not a reliable one for laboratory resilient modulus estimation at values higher than 130000 kPa.

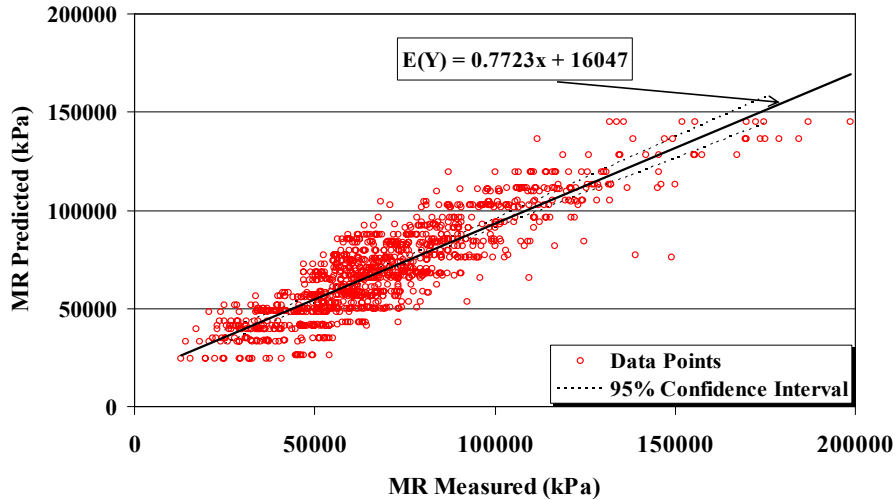


Figure 4.6 Comparison of Predicted and Measured Resilient Modulus for Varying Stress State

4.4.3 Linear Model Correlating Universal Constitutive Model Regression Coefficients with Soil Index Properties

The effects of seasonal variations in the resilient modulus based on the soil index properties can be estimated using the linear model presented in Section 4.4.1. However, it is not possible to determine the effects of stress sensitivity according to this model since it is only capable of representing the effects of stress states for a typical pavement section. On the other hand, models correlating the constitutive model regression coefficients with the soil index properties can result in more

successful estimates to capture the effects of stress sensitivity. In this section, the universal constitutive model is used for the estimation of the regression coefficients since the statistical strength of this model is higher than the other conventional correlation functions. The coefficients determined according to the universal constitutive model are given in Appendix B for each resilient modulus test. The model selection procedure described in Section 4.4.1 is used in developing satisfactory regression models for each constitutive model coefficient. The resulting models are as follows:

k1 Model:

$$k_1 = 1279.4092 - 54.5643 \cdot W_{opt} + 11.9323 \cdot LL - 60.8926 \cdot W_{c1} + 114.7914 \cdot W_{c2}$$

(0.0000) (0.0000) (0.0000) (0.0078) (0.0000)

(R² = 0.7095)

k2 Model:

$$k_2 = 1.0516 - 0.0088 \cdot LL + 0.0167 \cdot W_{opt} - 0.0082 \cdot PP10 - 0.0243 \cdot W_{c1}$$

(0.0000) (0.0000) (0.0047) (0.0000) (0.2266)

$$- 0.0267 \cdot W_{c2} \quad (R^2 = 0.6923)$$

(0.0435)

k3 Model:

$$k_3 = -1.0152 + 0.0037 \cdot Comp + 0.0005 \cdot PI + 0.0014 \cdot PP10 + 0.2613 \cdot DD_{std}$$

(0.2573) (0.6732) (0.7601) (0.2180) (0.0740)

$$+ 0.0098 \cdot W_{c1} + 0.0148 \cdot W_{c2} \quad (R^2 = 0.1567)$$

(0.6468) (0.2557)

Models for the estimation of k1 and k2 coefficients are statistically reliable. On the other hand, the residual errors for the model correlating k3 coefficient with the soil index properties are higher than the acceptable ranges. The final model in the constitutive equation form is obtained using Equation 2.4 and regression results. Figure 4.7 and 4.8 demonstrate the final model fitting results for constant and varying stress states, respectively.

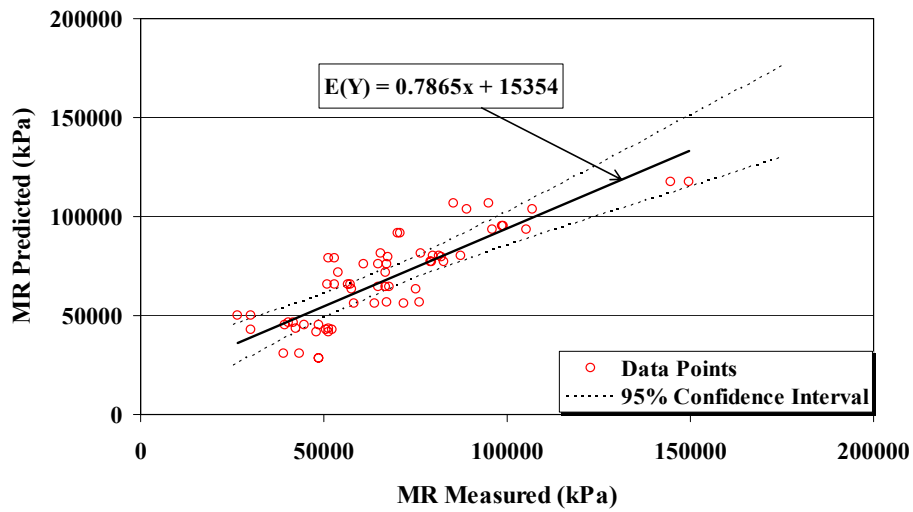


Figure 4.7 Comparison of Predicted and Measured Resilient Modulus for Constant Stress State (Based on Universal Constitutive Model Coefficients) ($R^2 = 0.7010$)

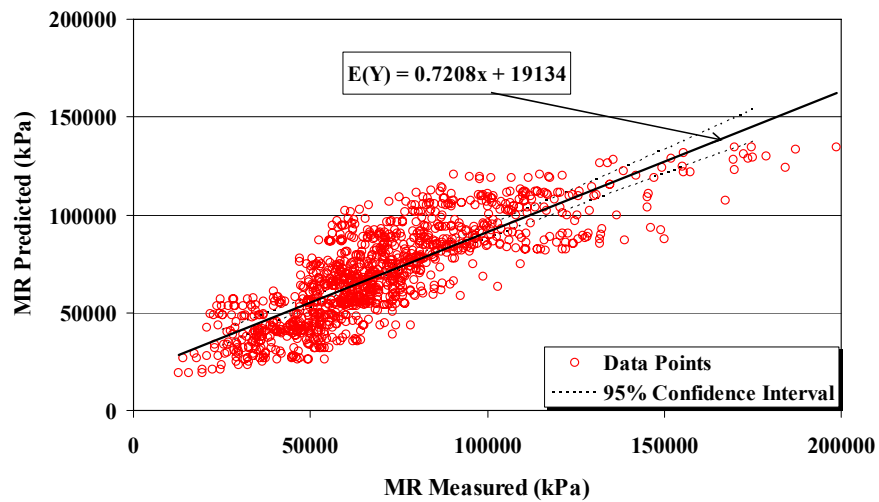


Figure 4.8 Comparison of Predicted and Measured Resilient Modulus for Varying Stress State (Based on Universal Constitutive Model Coefficients) ($R^2 = 0.6660$)

4.4.4 Nonlinear Model Correlating Resilient Modulus with Soil Index Properties

The statistical approach for developing nonlinear models is different from linear regression analysis. Iterative algorithms are used in the estimation of the effects between independent variables. The most important tools used for nonlinear model development are: 1) more general formulas, 2) extended data frames, 3) starting values, 4) derivatives. The criteria considered for model development is based on the minimum sum and the minimum sum of squares analyses. The minimum sum minimizes the total contributions from statistically ineffective variables. The minimum sum of squares minimizes the squared residual errors in order to decrease deviation. The nonlinear S-PLUS “*nls*” function is utilized for model development. The final nonlinear model correlating the soil index parameters with the resilient modulus is as follows:

$$M_R = 27.4079 \left(\left(\frac{(LL + 28.5) \times (DD_{std} + 19.5)}{W_{cc}} \right)^{1.79706} + \left(\frac{PP_{200}}{100} \right)^{-0.166677} \right)$$

$$(R^2 = 0.8120)$$

Residual standard error: 10641.3 on 58 degrees of freedom

where

LL: liquid limit

DD_{std}: maximum dry-density (Mg/m³)

W_{cc}: compaction water content (%)

PP₂₀₀: percent passing No. 200 sieve (%)

M_R = resilient modulus (kPa)

The final plot comparing the predicted and the measured resilient modulus is given in Figure 4.9.

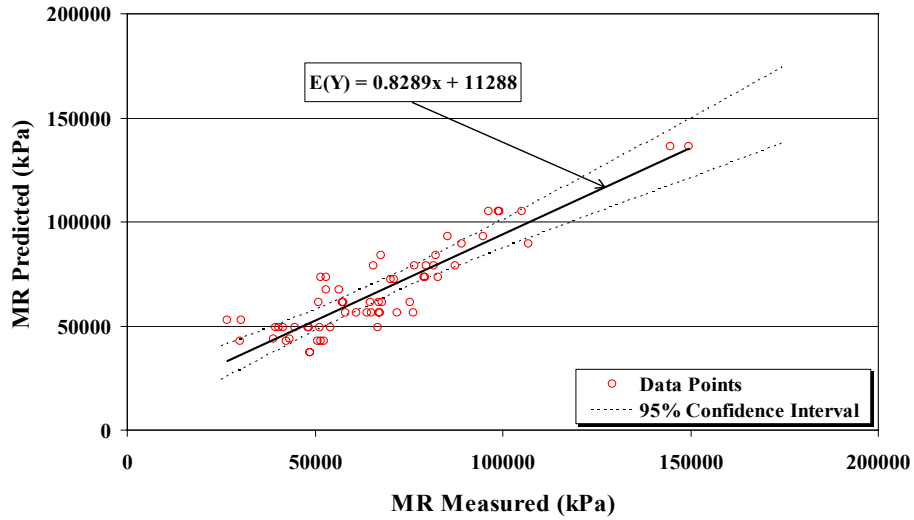


Figure 4.9 Comparison of Nonlinear Model Predicted and Measured Resilient Modulus

The final plot demonstrates a good fit for the estimation of the resilient modulus for fine-grained soils using the nonlinear model. The reliability of the model is also presented using the residual plot in Figure 4.10. Since the residuals are randomly distributed along the fitted values, there is no collinearity between the independent variables. In addition, the accumulation of the residuals at the zero level, according to the residual histogram plot in Figure 4.11, presents the statistical strength of the nonlinear model.

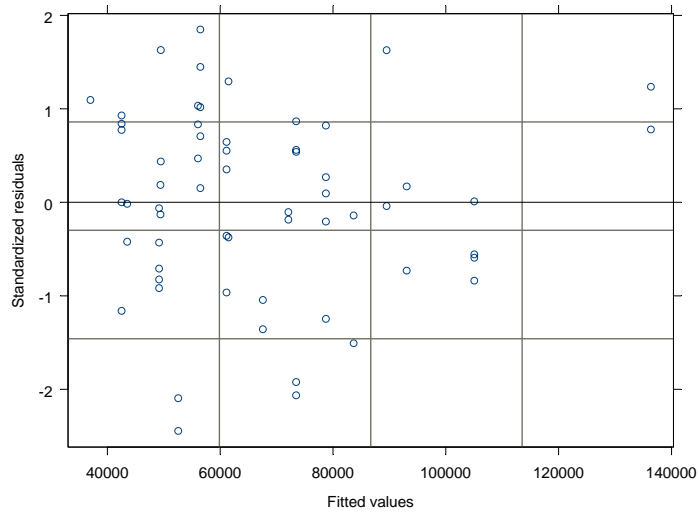


Figure 4.10 Residuals versus Fitted Values for the Developed Nonlinear Model

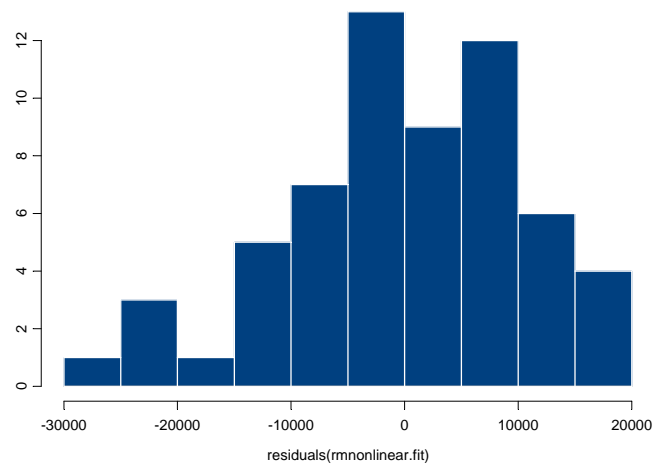


Figure 4.11 Residuals Histogram for the Estimation of the Deviation from Measured Resilient Modulus (Developed Nonlinear Model)

4.4.4.1 Model Validation Using an Independent Data Set

The reliability of the derived nonlinear model should also be validated by using the results of the tests other than the data set used for model development in order to be effectively used in design specifications. The summary of the data set developed for this purpose is given in Table 4.10. The fitting results for the nonlinear model developed in this study are given in Figure 4.12. The results of the analysis validate the success of the nonlinear model developed in this study since the R^2 for the final fits based on the independent data set is close to the model R^2 ($R^2_{\text{independent}} = 0.8102$, $R^2_{\text{model}} = 0.8121$). Thus, the nonlinear model developed in this study can be effectively used for resilient modulus prediction for the soil types which have the soil index parameters in the specified ranges given in Table 4.4.

Table 4.10 Summary of the Data Set Used for the Validation of the Developed Nonlinear Model

City	Region	AASHTO	PP10	PP40	PP200	LL	PI	W_{opt}	γ_{dr}
Bursa	14//8	A-6	95.5	81.6	48.8	40.2	11.6	23.6	1.521
	14//11	A-6	99.7	97.9	67.5	36.0	14.3	19.8	1.655
Kastamonu	4//145	A-2-6	77.0	54.6	35.1	34.6	18.3	13.6	1.872
Diyarbakır	9//8	A-6	99.9	99.7	97.9	67.2	37.2	28.8	1.430
	9//20	A-7-6	98.3	94.0	78.5	43.2	17.5	23.0	1.564

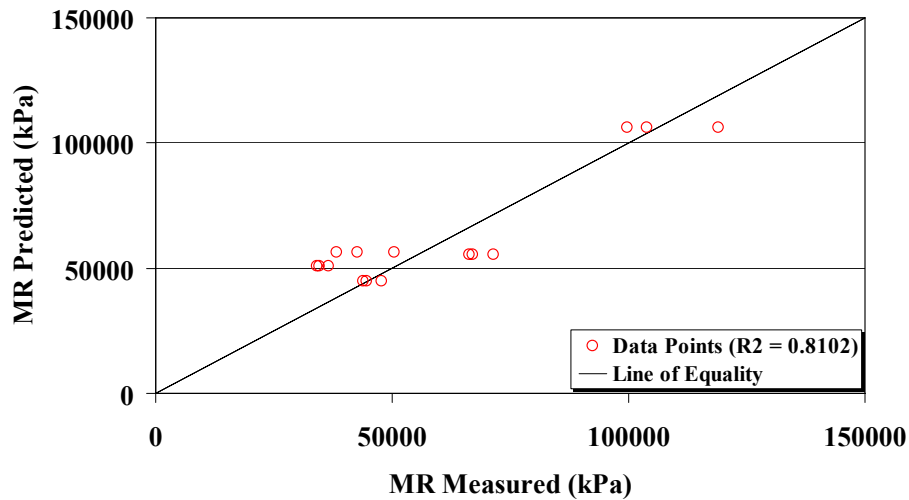


Figure 4.12 Comparison of Nonlinear Model Predicted and Measured Resilient Modulus (Based on the Independent Data Set)

4.5 Application of Genetic Algorithm and Curve Shifting Methodology as an Alternative to Constitutive Nonlinear Models (Experiment Set 1)

The deviator stress vs. resilient modulus curves obtained from the resilient modulus tests are considered as effective tools to characterize the elastic response of unbound layers under repeated loads. Resilient modulus tests were conducted at three different confining pressure levels, 13.79, 27.579 and 41.369 kPa, which constitute three different curves. Figure 4.13 presents these curves for a single test conducted for the specimen k67100opt1. In this study, a genetic algorithm is used to estimate feasible horizontal shift amounts for the deviator stress – resilient modulus curves in order to obtain a final gamma (stress softening) or polynomial curve (stress hardening) which describes the resilient response as a function of deviator stress. The main purpose in conducting the nonlinear fitting of data is to find a suitable mathematical function that can systematically represent the relationship between the

resilient modulus and the deviator stress at various confining pressures. The genetic algorithm program written in S-PLUS for this analysis is given in Appendix C.

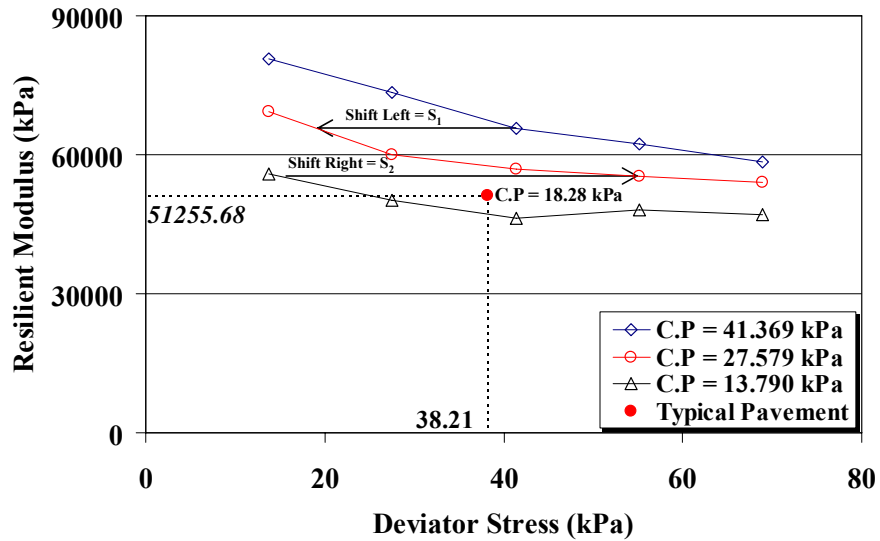


Figure 4.13 Deviator Stress vs. Resilient Modulus Curves at Three Different Confining Pressure Levels for a Certain Test

The general procedure for the application of the genetic algorithm is as follows:

1. Interval Prediction: Potential shift amounts (S_1 and S_2) are determined by using the plots of deviator stress vs. resilient modulus. As the uncertainty about the possible shift amounts increases, the length of the intervals should be extended while increasing the number of iterations in order to decrease the estimation error. Figure 4.14 illustrates the results of the initial shift amount estimation with a set of shift parameters $\{-8, 16\}$. The R^2 value between the shifted test results and the gamma fitting curve based on the estimated initial shift amounts is 0.76.

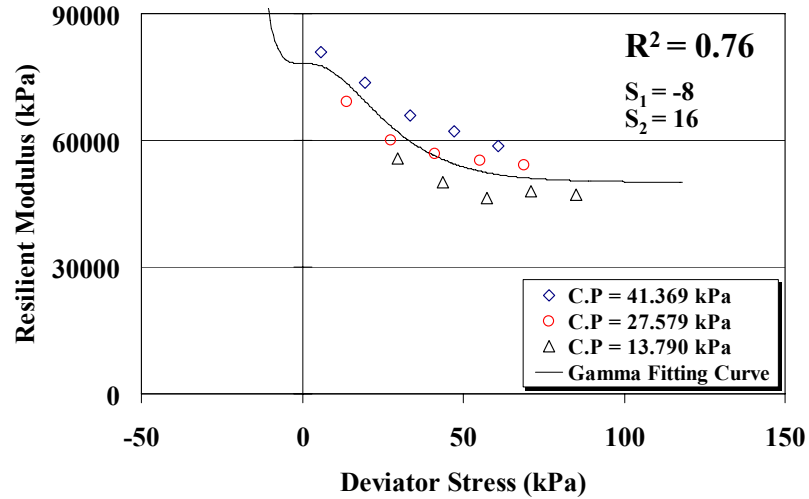


Figure 4.14 Initial Shift Amount Estimation

2. Gene Pool Generation: Gene pools are obtained by generating uniformly distributed random variables within the estimated shift intervals (80 numbers are generated for the S_1 and S_2 prediction intervals).

3. Fitting: For each gene in a gene pool, the derivative quantities S_1 and S_2 are determined and then the deviations of the predicted values from the measured data are evaluated using the fitness function. Fitted resilient modulus values are estimated based on the gamma or polynomial functions. The reason for using two different function types is a result of the different trends of the test results for different soil types. The fitness function of the genetic algorithm for the estimation of the shift amounts is basically the residual sum of squares (RSS) function which expresses the goodness of fit between the measured (test results) and predicted (fitting function) data points.

$$RSS = (y_i - \hat{y}_i)^2 \quad (4.4)$$

where y_i is the measured resilient modulus and \hat{y}_i is the predicted resilient modulus.

4. Ranking: The genes in the gene pool are ranked according to their RSS values.

5. Mating and Discarding: The ranked genes are mated in order to decrease the effects of bad genes. The last half of the genes with higher RSS is discarded. These discarded genes are then replaced with the new genes by returning to step 2. The required number of iterations depends on the level of uncertainty about the possible shifting amounts in the data set and the required accuracy of the test parameters.

The most important advantage of the genetic algorithm is that an experienced engineer can specify the appropriate parameter range while a novice can use larger intervals with higher number of iterations. The results of the applications will be the same for both users since the deviation decreases as the number of iterations increases (Figure 4.15). However, increasing the number of iterations will increase the computational time. The general flow-chart for the application of the genetic algorithm is given in Figure 4.16.

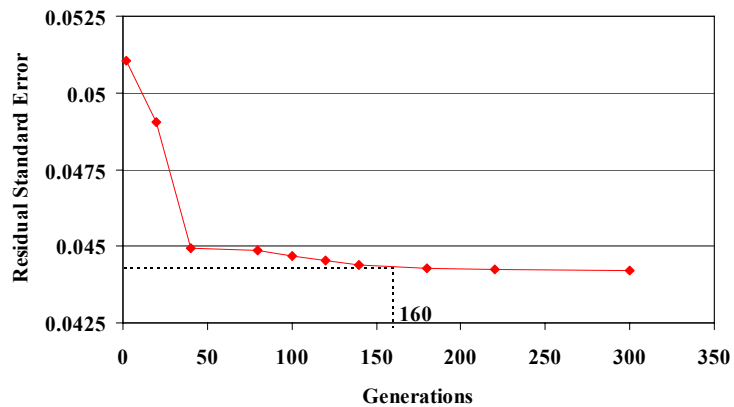


Figure 4.15 The Residual Standard Error Convergence Trend for Increasing Generations

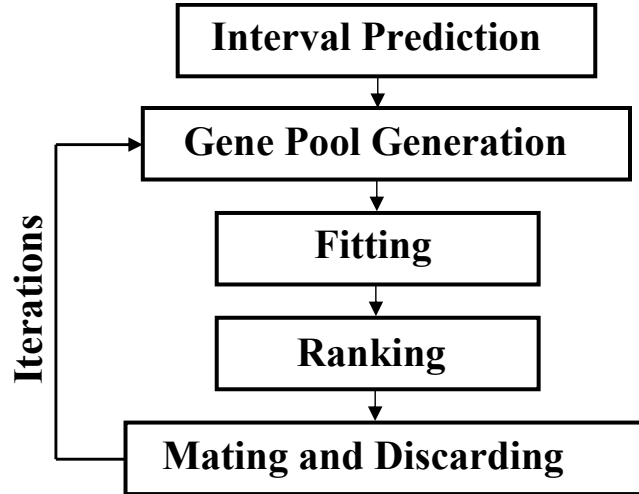


Figure 4.16 General Flow Chart for the Application of the Genetic Algorithm

The following gamma and polynomial fitting functions are used for the correction of the deviator stress and confining pressure effects for unbound materials:

Gamma fitting equation: (for the stress softening soil types)

$$M_R = C + A \cdot \left(1 - \exp\left(-\frac{(x)}{B}\right) \cdot \sum_{m=0}^{n-1} \frac{(x)^m}{B^m \cdot m!} \right) \quad (4.5)$$

Polynomial fitting equation: (for the stress hardening soil types)

$$M_R = A(x)^2 + B(x) + C \quad (4.6)$$

Confining pressure shift relationship for the fitting functions:

$$a_T = D \cdot \left(1 - \exp\left(-\frac{(C.P - C.P_{ref})}{E}\right) \right) \quad (4.7)$$

where $C.P_{ref} = 27.579$ kPa and a_T is the confining pressure shift factor.

$$x = DS + a_T \quad (4.8)$$

where x is the reduced deviator stress.

The parameters of the gamma fitting function are determined based on the “nls” function of S-PLUS. Since “nls” function performs iterations in order to determine the most feasible parameters, successful initial estimates result in more reliable output values for the parameters. Figures 4.17, 4.18 and 4.19 display how the scale and the shape parameters affect the curves of gamma distribution function. In Figure 4.17, the scale parameter B is assumed to be constant at 10 and the effect of the change in parameter A is monitored. Since parameter C is the intercept of the gamma function, initial estimate for these parameters is performed by using the minimum resilient modulus of the test results. Since the shape of the gamma fitting curves with $A = -0.4$ and $A = -0.6$ are close to the measured data points, the average of these two estimates (-0.5) is used as the initial iteration estimate. In Figure 4.18, the scale parameters are extended from 3 to 15 for constant A (-0.5) and C (10.76). The shape of the curves with B values 12 and 15 present similar trends with the test results. Thus, the average of these values (13.5) is used as the initial estimate of the “nls” function. Finally, the estimated gamma fitting curves are shifted to higher values by increasing the parameter C in order to converge to the measured test points. The final initial estimation curves and the corresponding parameters are given in Figure 4.19. The shape parameter $n = 3$ is used during the analysis.

The final parameters determined using the initial estimates and the “nls” function are as follows:

```
> EMod.fit<-nls(log(RM)~C+A*(1-exp(-(DS)/B)
*(1+((DS)/B)+((DS)^2)/((B^2)*2))),EMod,start=list(A=-0.5,B=13.5,C=11.2))
> summary(EMod.fit)
```

Formula: $\log(RM) \sim C + A * (1 - \exp(- (DS)/B) * (1 + ((DS)/B) + ((DS)^2)/((B^2) * 2)))$

Parameters:

	Value	Std. Error	t value
A	-0.39782	0.032714	-12.1606
B	13.91460	1.328400	10.4747
C	11.18780	0.020173	554.5940

Residual standard error: 0.0443806 on 12 degrees of freedom

Correlation of Parameter Estimates:

	A	B
B	-0.421	
C	-0.646	-0.191

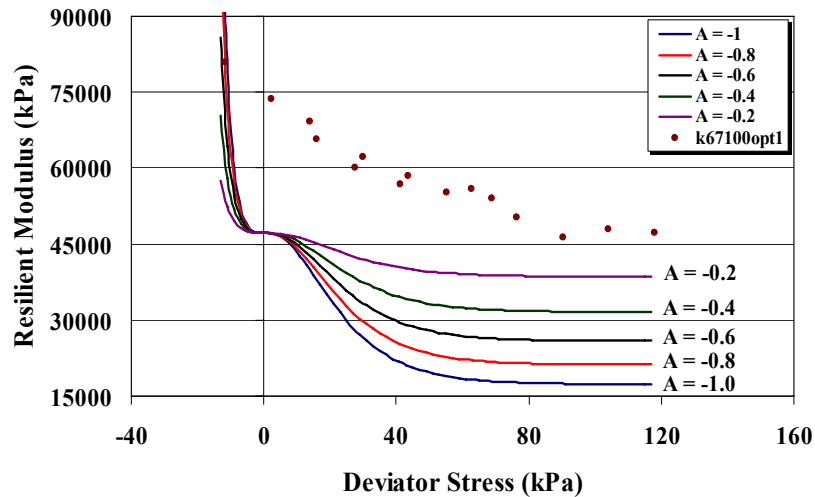


Figure 4.17 Gamma Fitting Curves with the Shape Parameter $n = 3$, Scale Parameter (B) = 10 , A = -0.2, -0.4, -0.6, -0.8, -1.0, C = $\ln(47139) = 10.76$

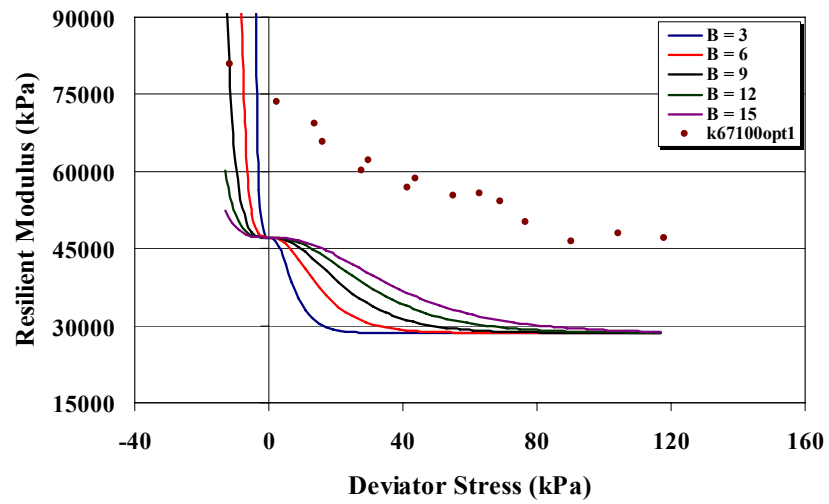


Figure 4.18 Gamma Fitting Curves with the Shape Parameter $n = 3$, Scale Parameters $(B) = 3, 6, 9, 12, 15$, $A = -0.5$, $C = \ln(47139) = 10.76$

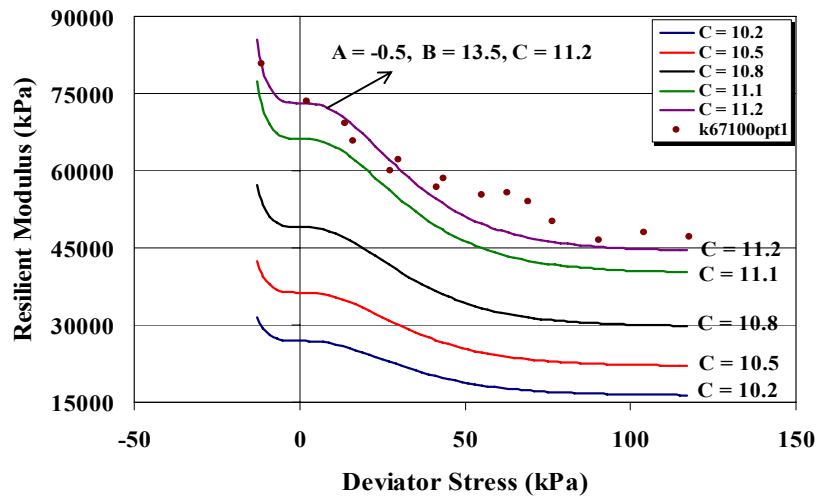


Figure 4.19 Gamma Fitting Curves with the Shape Parameter $n = 3$, Scale Parameter $(B) = 13.5$, $A = -0.5$ and $C = 11.2$

The parameters of the Equations 4.5, 4.6 and 4.7 determined by using the genetic algorithm and the master curve application method are given in Table 4.11. The final fitting results for the specimen k67100opt1 based on the genetic algorithm shift amounts are given in Figure 4.20. The increase in the R^2 value demonstrates the improvement in fitting curves after the application of the genetic algorithm. The relationship between confining pressure and confining pressure shift factor based on the Equation 4.7 is also given in Figure 4.21.

Table 4.11 Resilient Modulus Master Curve Parameters

City	Class	PP 200	LL	PI	D.D	M.C (%)	M.L	Comp. (%)	Gamma Fitting					C.P Shift		
									n	T	A	B	C	R ²	D	E
Kayseri 6/2	A -7-5	48.3	44.7	13.8	1.702	19.2	opt-2	100	G	-0.27472	18.18010	11.54010	0.95	47.90	-36.67	1
							opt+2	100	G	-0.23931	14.12520	11.14800	0.88	-57.33	20.79	1
							opt	95	G	-0.24896	24.71200	11.45130	0.75	-0.37	2.81	1
Kayseri 6/5	A -2-4	33.0	NP	NP	1.780	15.8	opt-2	100	G	-0.55330	30.95340	11.28450	0.88	-300.48	74.00	1
							opt+2	100	P	-3.56828	651.55326	9410	0.93	-29.98	-13.07	1
							opt	100	P	0.26041	232.30436	37838	0.96	27065.2	6835.9	1
Kayseri 6/6	A -2-7	18.3	59.2	21.2	1.436	28.4	opt-2	100	G	-0.36536	28.85560	11.36300	0.81	-178.22	44.21	1
							opt+2	100	P	0.11149	199.99256	40181	0.95	574.71	138.40	1
							opt	100	G	-0.65539	32.28570	10.98170	0.91	-723.15	179.57	1
Kayseri 6/7	A -5	48.5	42.0	9.7	1.478	24.8	opt-2	95	P	-0.06006	211.89534	41756	0.94	-1186.4	-292.65	1
							opt+2	100	G	-0.41923	24.81320	11.34170	0.93	-38.47	16.38	1
							opt	100	G	-0.47630	38.58680	10.96480	0.91	310.70	-82.49	1
									G	-0.39782	13.91460	11.18780	0.94	-52.40	20.90	1
									G	-0.46052	24.21530	10.94070	0.89	-318.54	110.53	1

Table 4.11 Resilient Modulus Master Curve Parameters (Continued)

City	Class	PP 200	LL	PI	D.D	M.C (%)	M.L	Comp. (%)	Gamma Fitting					C.P Shift		
									n	T	A	B	C	R ²	D	E
A.C	A -6	56.3	39.9	21.6	1.844	14.8	opt-2	100	-4.43001	850.97068	139646	0.84	0.22	2.63	1	
							opt+2	100	-0.47617	14.33980	11.54790	0.90	-14.27	10.79	1	
							opt	100	-0.43201	14.19350	11.92520	0.86	-20.95	10.50	1	
D.S	A -7-6	76.1	50.4	24.9	22.8	opt-2	95	-0.21986	23.92660	11.67380	0.58	-6.00	5.87	1		
						opt+2	100	-0.38316	55.97220	11.24940	0.70	563.39	-144.79	1		
						opt	100	-0.66043	16.59400	10.56200	0.98	-1355.8	1323.7	1		
D.K.V	A -7-6	94.2	57.2	28.8	25.8	opt-2	95	-0.34742	13.12560	11.35860	0.93	55.13	-43.34	1		
						opt+2	100	-0.34288	10.96070	11.27090	0.95	-94.70	57.48	1		
						opt	100	-0.21822	6.48359	11.91050	0.61	-9.85	7.27	1		
D.B	A -7-6	83.7	61.1	37.3	22.5	opt-2	100	-0.40475	12.34690	11.12770	0.95	26.39	-26.34	1		
						opt+2	100	-0.24605	5.32702	11.45730	0.91	-34.12	18.00	1		
						opt	95	-0.16572	15.61720	11.25380	0.80	-5.80	7.35	1		
D.B	A -7-6	83.7	61.1	37.3	22.5	opt-2	100	1.26415	143.78376	89284.9	0.71	70.24	44.98	1		
						opt+2	100	-0.23193	39.52750	11.03810	0.76	296.14	-82.29	1		
						opt	100	-0.26625	15.07510	11.55610	0.97	-3.52	5.10	1		
								95	-0.80173	10.06140	11.94800	0.93	-1.08	5.54	1	

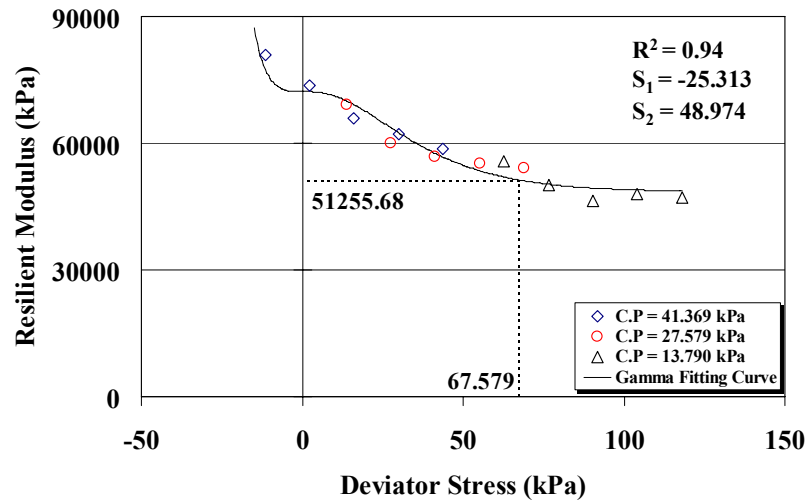


Figure 4.20 Final Gamma Fitting Curve for the Representation of the Shifted Test Results ($A = -0.39782$, $B = 13.91460$, $C = 11.18780$ (Eqn. 4.5))

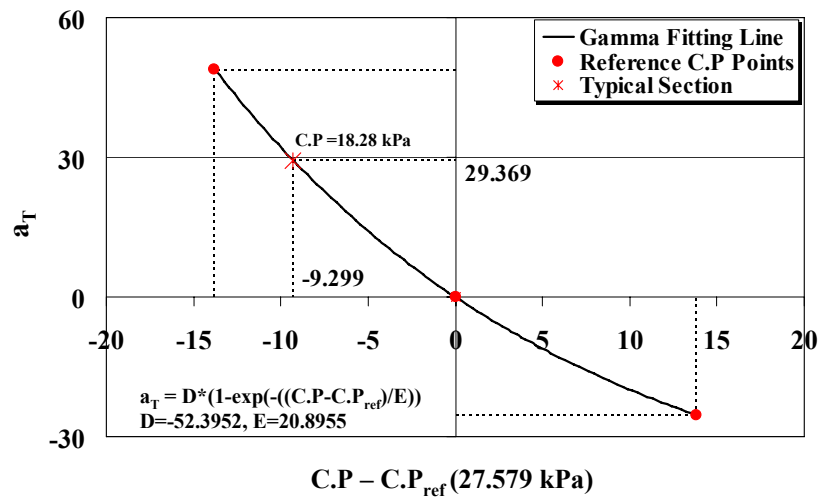


Figure 4.21 The Relationship between Confining Pressure and Confining Pressure Shift Factor (Eqn. 4.7)

Resilient modulus values are only associated with the confining pressure where the effect of deviator stress is also considered during the analysis. The procedure for the estimation of the resilient modulus related to confining pressure and deviator stress is quite promising since the effects of other parameters on the resilient modulus variation are relatively small when compared with the confining pressure and deviator stress effect for a single test.

4.5.1 Demonstration Example

The deviator stress and the confining pressure for a typical pavement section is determined in Section 4.3. For fine-grained (subgrade) soil types, deviator stress is estimated to be 38.21 kPa where the confining pressure is 18.28 kPa. The deviator stress and the confining pressure effects are corrected by the application of the following procedure for specimen K67100opt1:

1. Determine the difference between the reference (27.579 kPa) and the test confining pressures.

$$C.P - C.P_{ref} = 18.28 - 27.579 = -9.299$$

2. Obtain the confining pressure shift factor.(Equation 4.7) (Figure 4.20)

$$a_T = D \cdot \left(1 - \exp \left(- \frac{(C.P - C.P_{ref})}{E} \right) \right) = -52.3952 \cdot \left(1 - \exp \left(- \frac{(-9.299)}{20.8955} \right) \right) = 29.369$$

3. Determine reduced deviator stress. (Equation 4.8)

$$x = DS + a_T = 38.21 + 29.369 = 67.579 \text{ kPa}$$

4. Determine the resilient modulus at a certain confining pressure and deviator

stress using the calculated reduced deviator stress. (Equation 4.5 or 4.6)

$$M_R = 11.18780 - 0.39782 \cdot \left(1 - \exp\left(-\frac{(67.579)}{13.9146}\right) \cdot \sum_{m=0}^2 \frac{(67.579)^m}{(13.9146)^m \cdot m!} \right) = 51255.68$$

The final estimation results are shown in Figure 4.13.

Constitutive models, which represent the results of a single resilient modulus test with a single equation, may result in statistically inadequate estimates for fine-grained soils. On the other hand, application of genetic algorithm and curve shifting methodology gives more reliable results for resilient modulus estimation for a constant stress state. The results of the analysis present that the general gamma and polynomial fitting functions determined using the genetic algorithm and curve shifting methodology can be satisfactorily used for the simulation of the resilient characteristics of the unbound pavement layers.

4.6 Models Correlating Resilient Modulus with CBR Test Results (Experiment Set 2)

Statistical analysis procedure described in Section 4.4.1 is performed for developing models correlating resilient modulus with CBR test results. Three different correlations are developed in order to estimate resilient modulus. In Section 4.6.1, one-to-one correlation between resilient modulus and CBR is investigated based on the experiment set 2 test results. The effect of the category covariate “TYPE” on the regression results is also analyzed in Section 4.6.2. In Section 4.6.3, the effect of soil index properties on regression model performance is monitored using the related statistical analysis. In addition, applicability of tree-based approach for resilient modulus prediction is investigated in Section 4.6.4. All dependent and independent variables and their numerical ranges used for experiment set 2 model development are presented in Table 4.12.

**Table 4.12 Independent and Dependent Variables Used for Model
Development (Experiment Set 2)**

Variable Type	Symbols	Description	Range
Dependent	M_R	Laboratory resilient modulus for a certain stress state	26963 – 359442 kPa
Independent	CBR_w	CBR tests conducted with soaked specimens	5.5 – 128 %
	CBR_d	CBR tests conducted with unsoaked specimens	13.5 – 137 %
	Comp	Compaction Percentage	100 %
	LL	Liquid Limit	0 – 67.2
	PI	Plasticity Index	0 – 37.3
	W_{opt}	Optimum water content	4.8 – 28.8 %
	DD_{std}	Maximum dry-density	1.335 – 2.348 Mg/m ³
	PP4	Percent passing no. 4 sieve	37.4 – 100 %
	PP10	Percent passing no. 10 sieve	29 – 99.9 %
	PP40	Percent passing no. 40 sieve	14.9 – 99.7 %
PP200	Percent passing no. 200 sieve	1.1 – 97.9 %	
Category independent	TYPE	Type of Soil	TYPE1, TYPE2

In this study, CBR tests were conducted for soaked and unsoaked specimens for each soil type. Correlation matrix results for the complete data set show high positive correlations between soaked and unsoaked CBR test results. Thus, soaked CBR test results can be estimated based on a simple regression model with a reliable R^2 of 0.9857 without performing the soaked tests. Figure 4.22 illustrates the regression results for the soaked and unsoaked CBR test results. The final regression model which correlates the soaked CBR test results with the unsoaked CBR test results is as follows:

$$CBR_w = -4.5165 + 0.9972 \cdot CBR_d \quad (R^2 = 0.9857)$$

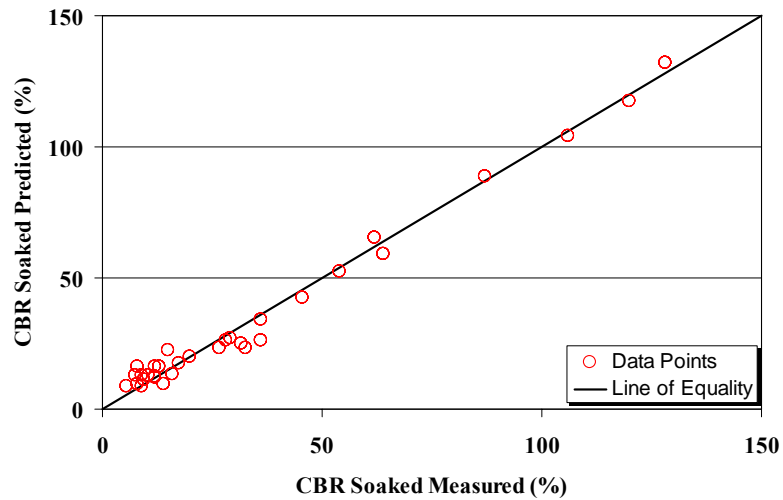


Figure 4.22 Comparison of Predicted and Measured Soaked CBR

4.6.1 One-to-one Correlation between Resilient Modulus and CBR Test Results

Granular soils have different physical properties when compared to the fine-grained soils. However, separation of the data set according to the soil type does not result in reliable prediction models since the independent variable CBR_d reflects this classification in the regression analysis. The regression result for the estimation of the one-to-one correlation between resilient modulus and CBR_d is as follows:

$$M_R = 51226.2745 + 1447.2894 \cdot CBR_d \quad (R^2 = 0.4619)$$

(0.0000) (0.0000)

The low correlation between the results of these two tests is a result of the different characteristics of the test methods. Resilient modulus tests measure the resilient response of the specimen where CBR tests measure the strength of the material under plastic deformations. Thus, CBR test results should be only used as a soil index property with the other soil index test results which presents the strength of the material. The plot showing the measured resilient modulus versus predicted

resilient modulus is given in Figure 4.23. It should be noted that the model loses its statistical strength at resilient modulus higher than 150000 kPa.

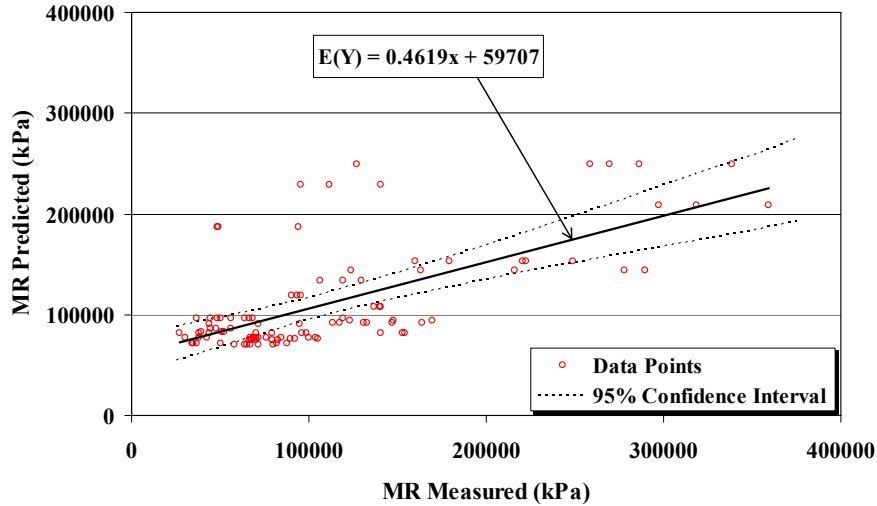


Figure 4.23 Comparison of Predicted and Measured Resilient Modulus based on One-to-one M_R vs. CBR Model

4.6.2 Correlation between Resilient Modulus and CBR Test Results Considering the Category Covariate “TYPE”

The statistical strength of the one-to-one correlation between resilient modulus and CBR_d can be improved by considering the variation of soil types. For this purpose, category covariate “TYPE” is included to the one-to-one correlation which is given in Section 4.6.1. The regression result for the estimation of the correlation between resilient modulus and CBR_d based on the soil type classification is as follows:

$$M_R = \exp \left(\underset{(0.0000)}{11.2828} + \underset{(0.0003)}{0.0047} \cdot CBR_d - \underset{(0.0000)}{0.3728} \cdot TYPE \right) \quad (R^2 = 0.6143)$$

The results of the analysis indicate that the prediction capability of the model improves for the resilient modulus ranging from 100000 to 180000 kPa when compared to the one-to-one correlation described in Section 4.6.1. The zero Pr values imply that all the independent variables are significant in representing the variation in the resilient modulus. Figure 4.24 presents the comparison between predicted and measured resilient modulus.

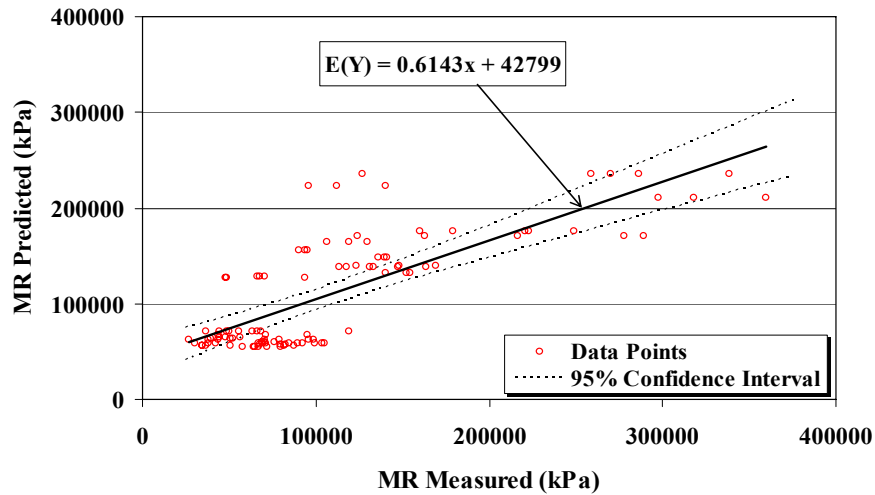


Figure 4.24 Comparison of Predicted and Measured Resilient Modulus based on M_R vs. CBR + TYPE Model

4.6.3 Correlation between Resilient Modulus and CBR Test Results Considering the Soil Index Properties

Resilient modulus prediction models can be further improved by including soil index parameters. The statistical analysis procedure described in Section 4.4.1 is followed for the model development in order to minimize residual errors and avoid numerical noise. The most effective parameters which have high significance in representing the resilient modulus variation are CBR_d, liquid limit (LL) and optimum water content (Wopt). In addition, the interaction between the independent variables LL and Wopt is also considered according to the statistical analysis. The regression model for the prediction of the resilient modulus based on the CBR_d and soil index variables is as follows:

$$M_R = 228376.7946 - 1479.8978 \cdot LL - 12381.4217 \cdot Wopt + 689.5002 \cdot CBR_d + 152.9164 \cdot LL \cdot Wopt \quad (R^2 = 0.7089)$$

(0.0000)
(0.0353)
(0.0000)
(0.0001)

(0.0000)

The low Pr values indicate that all the independent variables are significant in representing the variation in the resilient modulus. In addition, the improvement in the R² validates the effects of index test results on model performance. Although the data set for model development is not separated based on the soil types, this resilient modulus prediction model has high statistical strength when compared to the other models in the literature. The comparison of the predicted and measured resilient modulus is presented in Figure 4.25. The plot indicates that resilient modulus prediction according to the developed model results in reliable estimates for resilient modulus ranging from 0 to 250000 kPa.

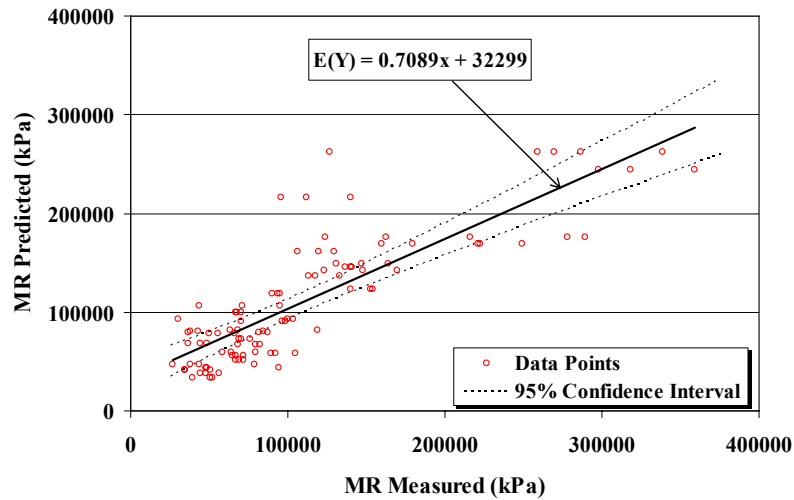


Figure 4.25 Comparison of Predicted and Measured Resilient Modulus based on M_R vs. CBR + Soil Index Parameters Model

4.6.4 Tree-Based Approach for Model Development

During the development of the resilient modulus prediction models for different soil types, the most effective variables which can be used for the classification of the data set should be determined in order to improve the regression models. Tree-Based modeling, which was developed by Breiman et al. (1984), is used in this analysis. Tree-based models provide an alternative to linear and additive models for regression problems. The rules for the constitution of a tree-based model are determined by an algorithm known as recursive partitioning. During the development of a tree-based model, the binary partitioning algorithm recursively splits the data into nodes until the nodes are homogenous or they contain too few observations.

The experiment set 2 resilient modulus test results are classified according to this approach using the independent variables; soil type, CBR_d , CBR_w , liquid limit,

plasticity index, optimum water content, and percent passing number 4, 10, 40 and 200 sieves. It should be noted that the independent variables CBR_w , plasticity index, liquid limit and soil type are not included in the model since they do not have significant effects for classification. The initial form of the regression tree dendrogram is given in Figure 4.26. The length of the vertical lines in the dendrogram points out the importance of each parent split. Since the dendrogram is complicated with many terminal nodes, the length of the vertical lines should be uniform for better observation. Figure 4.27 presents the dendrogram with uniform vertical lines and independent variables. The importance of each parent split can be determined by referring to Figure 4.26.

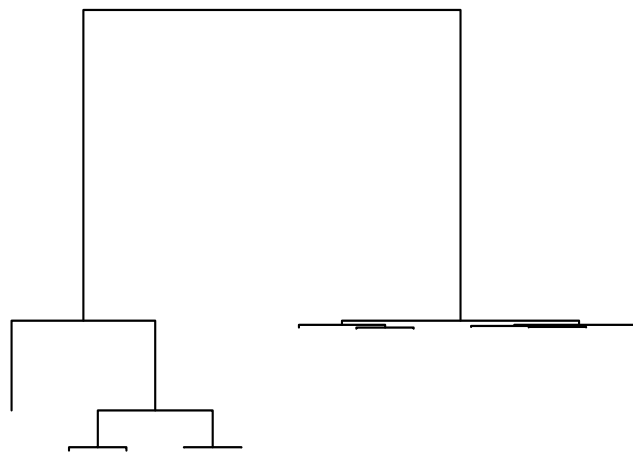


Figure 4.26 Initial Form of a Regression Tree

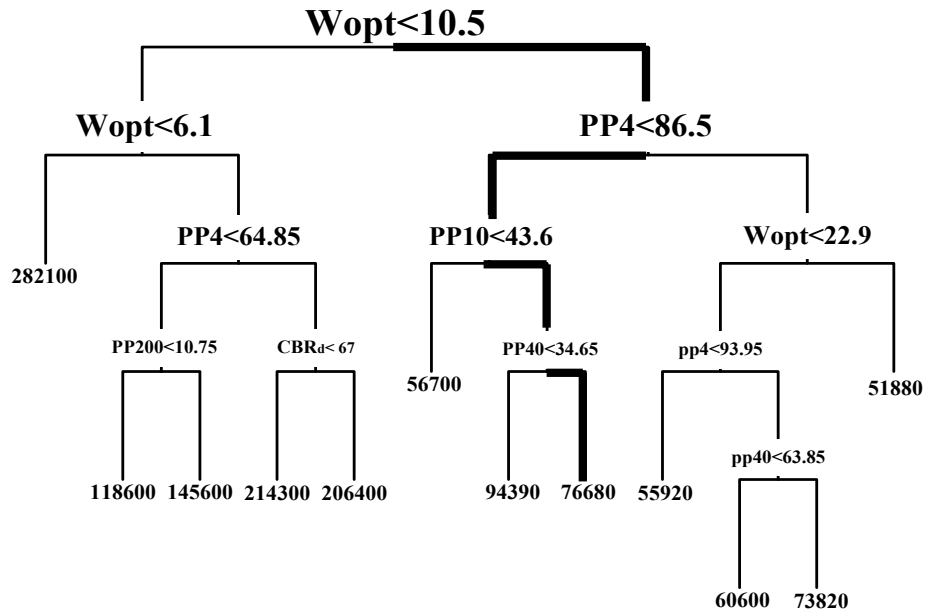


Figure 4.27 Uniform Regression Tree with the Corresponding Independent Variables

Resilient modulus of a certain soil can be determined according to Figure 4.27. For example, specimen KON3/13 has an optimum water content of 17.4 % which is higher than 10.5 in the dendrogram. The soil percentage passing number 4 sieve is 67.7 % which is smaller than 86.5. Since the percent passing number 10 and 40 sieves are higher than the ranges stated in the dendrogram, the estimated resilient modulus for that specimen is 76680 (Figure 4.27). The maximum of the resilient modulus test results for that specimen is calculated to be 76066 kPa which is closer to the estimated value. Resilient modulus ranges for different soil types can be estimated based on this dendrogram without using complicated regression equations. The reliability of the regression tree can be determined based on the residual plots given in Figure 4.28.

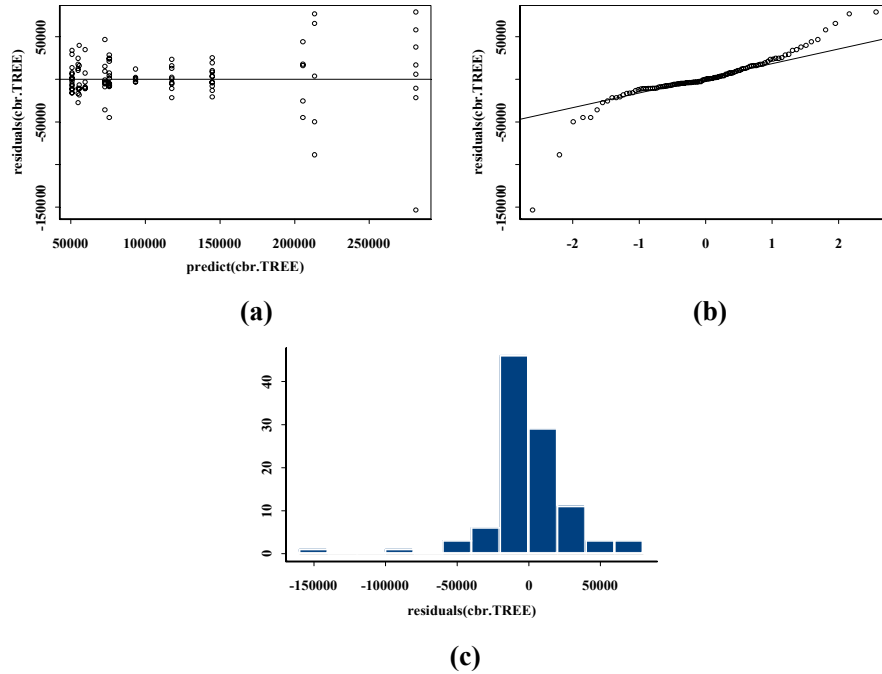


Figure 4.28 Tree model residual plots: (a) residuals vs. fitted values, (b) normal propability plot of residuals, (c) histogram of residuals

In Figure 4.28 (a), there is not any strong pattern in the predicted vs. residuals. This validates the reliability of the tree-model in terms of statistical analysis. In addition, since the normal probability plot of residuals are close to the line in Figure 4.28 (b), there is not much deviation in the model which is caused by the outliers. The histogram in Figure 4.28 (c) also presents a symmetrical shape with one peak value which validates the success of the tree-based model.

Experiment set 2 test results can be divided into groups by using the tree-based approach. For this purpose, the general regression tree should be pruned from terminal nodes (bottom) to the root (top) of the tree for simplification. Since the goodness of fit for the regression tree decreases due to the pruning, new dendrogram should not be used for resilient modulus prediction. However, regression analysis can be performed for each data group in order to obtain separate models for different

soil index properties. For this purpose, experiment set 2 is divided into three nodes by pruning. Since there are only two soil types with optimum water content lower than 6.1, the model developed for that group does not give reliable results. However, models developed for the other two groups result in successful estimates since soil index properties homogenously split these data groups. The regression results for each node of the pruned tree are as follows:

$$Wopt < 6.1 : M_R = 593661.2527 - 2463.3088 \cdot CBR_d \quad (R^2 = 0.2514)$$

(0.0361) (0.2055)

$$6.1 < Wopt < 10.5 : M_R = -913407.4317 - 468.8265 \cdot CBR_d - 24582.5480 \cdot LL$$

(0.0612) (0.1807) (0.2837)

$$+ 5282.4861 \cdot PP10 + 411850.6808 \cdot DDstnd + 286.3373 \cdot CBR_d \cdot LL$$

(0.0000) (0.0613) (0.2270)

$$+ 337.6624 \cdot LL \cdot PP10 \quad (R^2 = 0.5936)$$

(0.3516)

$$Wopt > 10.5 : M_R = 33099.7941 + 311.5712 \cdot CBR_w + 1521.5192 \cdot LL$$

(0.4607) (0.1497) (0.0000)

$$- 722.9403 \cdot PP200 + 21012.3714 \cdot DDstnd + 0.0960 \cdot LL \cdot PP200$$

(0.0085) (0.3065) (0.9837)

$$- 63.2045 \cdot LL \cdot CBR_w \quad (R^2 = 0.4491)$$

(0.0000)

The pruned tree for the estimation of the data groups is given with the final model fitting plots in Figure 4.29.

4.7 Models Correlating Resilient Modulus with LFWD Test Results (Experiment Set 3)

Statistical analysis procedure described in Section 4.4.1 is performed for developing models correlating resilient modulus with LFWD test results. LFWD tests determine the elastic response of the unbound pavement layers during the construction period. Since laboratory resilient modulus tests are conducted in order to determine a similar characteristic of the test specimens, the correlations based on this independent variable should result in satisfactory resilient modulus estimates. However, the differences in compaction type, water content and loading frequency may cause a variation between field and laboratory test results. Thus, the results of the tests should be analyzed in order to develop a reliable prediction model. Three different correlation functions are developed in order to estimate resilient modulus. In Section 4.7.1, one-to-one correlation between resilient modulus and LFWD is investigated based on experiment set 3 data set. The effect of the category covariate “TYPE” on the regression results is also analyzed in Section 4.7.2. In Section 4.7.3, the effect of soil index properties on regression model performance is monitored using the related statistical analysis. All dependent and independent variables and their numerical ranges used for experimental set 3 model development are presented in Table 4.13.

**Table 4.13 Independent and Dependent Variables Used for Model
Development (Experiment Set 3)**

Variable Type	Symbols	Description	Range
Dependent	M_R	Laboratory resilient modulus for a certain stress state	26963 – 249186 kPa
Independent	LFWD	LFWD test results	56000 – 214000 kPa
	Comp	Compaction Percentage	100 %
	LL	Liquid Limit	0 – 55.9
	PI	Plasticity Index	0 – 21.7
	Wopt	Optimum water content	7.3 – 26 %
	DDstd	Maximum dry-density	1.485 – 2.210 Mg/m ³
	PP4	Percent passing no. 4 sieve	46.4 – 100 %
	PP10	Percent passing no. 10 sieve	38.1 – 99.7 %
	PP40	Percent passing no. 40 sieve	16.3 – 97.9 %
PP200	Percent passing no. 200 sieve	8.1 – 67.5 %	
Category independent	TYPE	Type of Soil	TYPE1, TYPE2

4.7.1 One-to-one Correlation between Resilient Modulus and LFWD Test Results

The primary purpose of developing a statistical model to predict resilient modulus from LFWD test results is to use the correlation in asphalt pavement design and rehabilitation. The thickness of the overlays and unbound pavement layers can be determined based on these correlation functions and LFWD test results without conducting laboratory tests. For this purpose, one-to-one correlations between resilient modulus and LFWD test results can be practically used during the construction stages. The model developed for the estimation of the resilient modulus from LFWD test results is as follows:

$$M_R = 3599.1125 + 0.8563 \cdot \text{LFWD} \quad (R^2 = 0.5665)$$

(0.8265) (0.0000)

The statistical strength of the LFWD one-to-one correlation function is higher than the CBR one-to-one correlation. This is a result of the similar characteristics of the LFWD and resilient modulus tests. Although the statistical strength of the model is higher than the CBR model, the reliability of the model must be improved in order to use in asphalt pavement design stages. The plot presenting the measured vs. predicted resilient modulus is given in Figure 4.30.

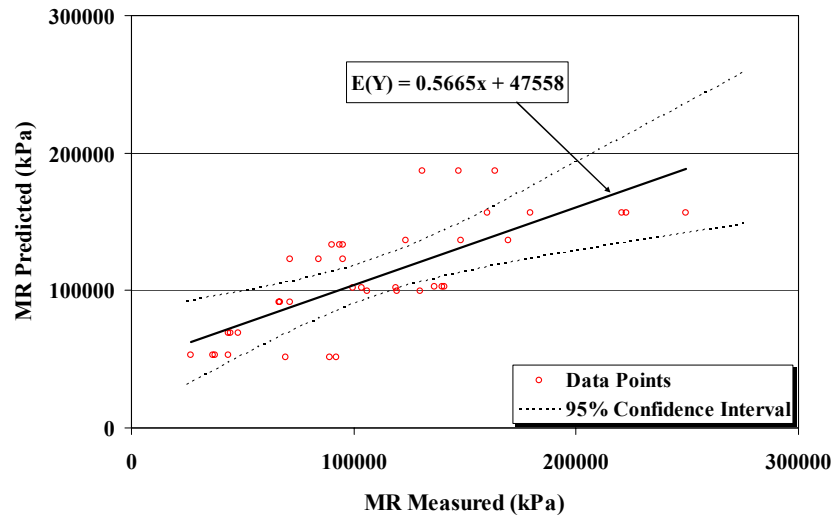


Figure 4.30 Comparison of Predicted and Measured Resilient Modulus based on One-to-one M_R vs. LFWD Model

4.7.2 Correlation between Resilient Modulus and LFWD Test Results Considering the Category Covariate “TYPE”

Category covariate “TYPE” is included to the one-to-one model in order to improve the statistical significance of the model. Since the number of the tests conducted with type 1 and type 2 specimens are nearly equal to each other, the statistical reliability of the model is anticipated to increase by the inclusion of this category

covariate. The regression result for the estimation of the correlation between resilient modulus and LFW D based on the soil type classification is as follows:

$$M_R = 46195.7064 + 0.5079 \cdot \text{LFW D} - 22594.1810 \cdot \text{TYPE} \quad (R^2 = 0.6536)$$

(0.0302)
(0.0032)
(0.0048)

The results of the analysis indicate that the developed model does not give satisfactory results for the estimation of the resilient modulus higher than 200000 kPa. The Pr values smaller than 0.05 imply that all the independent variables are significant in representing the variation in the resilient modulus. Figure 4.31 presents the comparison between predicted and measured resilient modulus.

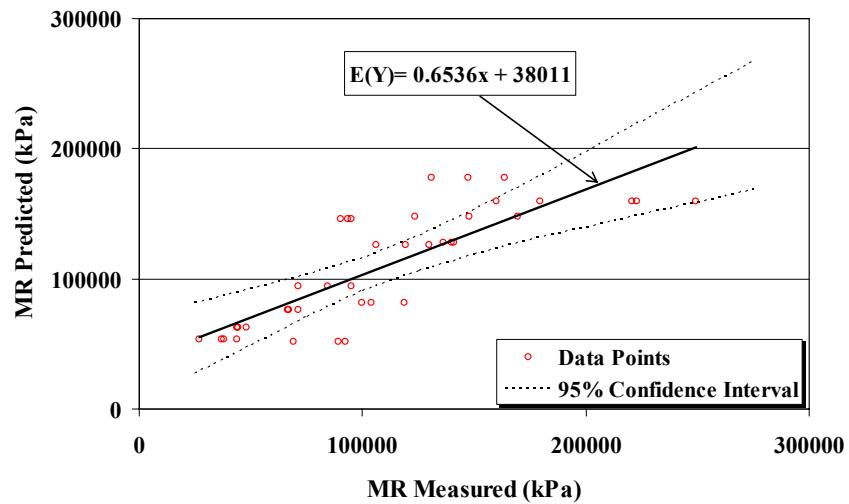


Figure 4.31 Comparison of Predicted and Measured Resilient Modulus based on M_R vs. LFW D + TYPE Model

4.7.3 Correlation between Resilient Modulus and LFWD Test Results Considering the Soil Index Properties

The statistical analysis procedure described in Section 4.4.1 is followed for the estimation of the correlations between resilient modulus and soil index properties. Plasticity index and the maximum dry-density are the variables which have high significance in representing the resilient modulus variation. In addition, the interactions between the LFWD test results and the plasticity index levels are considered in order to improve the reliability of the model according to the statistical analysis. The regression model for the prediction of the resilient modulus based on the LFWD test results and the soil index variables is as follows:

$$M_R = \exp\left(\underset{(0.0000)}{6.1810} + \underset{(0.0000)}{0.0000067} \cdot \text{LFWD} + \underset{(0.0000)}{0.1216} \cdot \text{PI} + \underset{(0.0000)}{2.2343} \cdot \text{DDstnd} - \underset{(0.0000)}{0.0000009} \cdot \text{LFWD} \cdot \text{PI}\right) \quad (R^2 = 0.8449)$$

The zero Pr values imply that all the independent variables are significant in representing the variation in the resilient modulus. The comparison of the predicted and measured resilient modulus is presented in Figure 4.32. The statistical reliability of the model is quite impressive with an R^2 of 0.8449. However, the plot indicates that resilient modulus prediction according to the developed model results in unreliable estimates for resilient modulus higher than 200000 kPa.

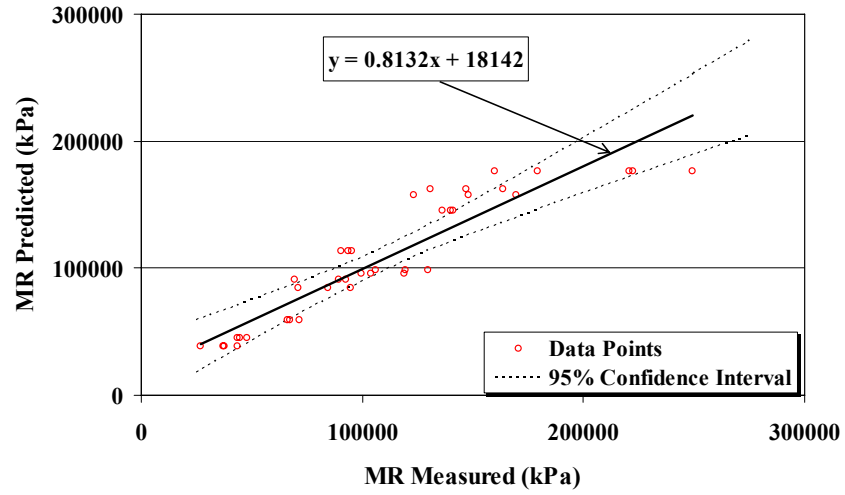


Figure 4.32 Comparison of Predicted and Measured Resilient Modulus based on M_R vs. LFWD + Soil Index Parameters Model

CHAPTER 5

SUMMARY AND CONCLUSIONS

5.1 Summary

This thesis discusses the effectiveness of soil index properties, simple strength and field strength test results on the estimation of the resilient response of unbound pavement layers. For this purpose, a total of 155 resilient modulus, 132 CBR and 232 LFWD tests were conducted in order to monitor the effects of different variables on the resilient modulus. In addition, soil index tests were also conducted for 32 different soil types. Three experiment sets are developed in order to investigate the effects of these parameters on resilient modulus. In experiment set 1, the effects of the variation in moisture content, compaction percentage and soil index properties were monitored. In addition, the effects of stress sensitivity were determined by evaluating the changes in the general characteristics of the materials at different stress states. Furthermore, applicability of genetic algorithm and curve shifting methodology to estimate a single representative resilient modulus for a constant stress state were investigated. The results of the analysis indicate that, for fine-grained soils, genetic algorithm and curve shifting methodology is a powerful technique for resilient modulus estimations when compared to the nonlinear constitutive models. In experiment set 2, the correlations between resilient modulus and simple strength test (CBR) results were determined in order to propose a one-to-one correlation. In addition, correlation functions were further improved by including soil index parameters as independent variables. The applicability of tree-

based approach for the classification of the resilient modulus test results and understanding the relative significance of the soil index parameters for resilient modulus estimations was also investigated based on the statistical analysis. Finally, correlations between resilient modulus and field strength test (LFWD) results were analyzed in order to determine a single correlation function for resilient modulus estimation using experiment set 3 test results. In addition, developed models were improved by including the soil index parameters as independent variables. Tables 5.1 and 5.2 present a summary of the developed models for the prediction of the resilient modulus at various conditions.

TABLE 5.1 Summary of Developed Models for Resilient Modulus Prediction Based on Soil Index Properties

Soil Type	Number of Tests			Model	R ²
	M _R	CBR	LFWD		
2	75	0	0	$M_R = 155670.8879 + 752.7832 \cdot PI - 4262.4089 \cdot W_{opt} - 107.9602 \cdot PP40$ $- 7183.4191 \cdot W_{c1} + 9073.0600 \cdot W_{c2}$	0.7637
2	75	0	0	$M_R = -1342837.4659 + 1310.4477 \cdot PI + 409.9442 \cdot (W_{vibr})^2 + 715230.5763 \cdot DD_{vibr}$ $+ 65.3415 \cdot PP200 + 604.6671 \cdot cp - 7542.7057 \cdot W_{c1} + 10986.1211 \cdot W_{c2}$	0.7723
				$k1 = 1279.4092 - 54.5643 \cdot W_{opt} + 11.9323 \cdot LL - 60.8926 \cdot W_{c1} + 114.7914 \cdot W_{c2}$	0.7095
2	75	0	0	$k2 = 1.0516 - 0.0088 \cdot LL + 0.0167 \cdot W_{opt} - 0.0082 \cdot PP10 - 0.0243 \cdot W_{c1}$ $- 0.0267 \cdot W_{c2}$	0.6923
				$k3 = -1.0152 + 0.0037 \cdot Comp + 0.0005 \cdot PI + 0.0014 \cdot PP10 + 0.2613 \cdot DD_{std}$ $+ 0.0098 \cdot W_{c1} + 0.0148 \cdot W_{c2}$	0.1567
2	75	0	0		0.8120

TABLE 5.2 Summary of Developed Models for Resilient Modulus Prediction Based on Strength Test Results and Soil Index Properties

Soil Type	Number of Tests		Model	R ²
	M _R	CBR LFWD		
1-2	104	132	$M_R = 51226.2745 + 1447.2894 \cdot CBR_d$ (0.0000)	0.4619
1-2	104	132	$M_R = \exp(11.2828 + 0.0047 \cdot CBR_d - 0.3728 \cdot TYPE)$ (0.0000) (0.0003) (0.0000)	0.6143
1-2	104	132	$M_R = 228376.7946 - 1479.8978 \cdot LL - 12381.4217 \cdot W_{opt} + 689.5002 \cdot CBR_d$ (0.0000) (0.0353) (0.0000) (0.0001)	0.7089
1-2	39	0	$M_R = 3599.1125 + 0.8563 \cdot LFWD$ (0.8265) (0.0000)	0.5665
1-2	39	0	$M_R = 46195.7064 + 0.5079 \cdot LFWD - 22594.1810 \cdot TYPE$ (0.0302) (0.0032) (0.0048)	0.6536
1-2	39	0	$M_R = \exp(6.1810 + 0.0000067 \cdot LFWD + 0.1216 \cdot PI + 2.2343 \cdot DDstd)$ (0.0000) (0.0000) (0.0000) (0.0000)	0.8449
			$- 0.0000009 \cdot LFWD \cdot PI$ (0.0000)	
			$W_{opt} < 6.1 : M_R = 593661.2527 - 2463.3088 \cdot CBR_d$ (0.0361) (0.2055)	0.2514
			$6.1 < W_{opt} < 10.5 : M_R = -913407.4317 - 468.8265 \cdot CBR_d - 24582.5480 \cdot LL$ (0.0612) (0.1807) (0.2837)	
			$+ 5282.4861 \cdot PP10 + 411850.6808 \cdot DDstd + 286.3373 \cdot CBR_d \cdot LL$ (0.0000) (0.0613) (0.2270)	0.5936
	104	132	$+ 337.6624 \cdot LL \cdot PP10$ (0.3516)	
			$W_{opt} > 10.5 : M_R = 33099.7941 + 311.5712 \cdot CBR_w + 1521.5192 \cdot LL$ (0.4607) (0.1497) (0.0000)	
			$- 722.9403 \cdot PP200 + 21012.3714 \cdot DDstd + 0.0960 \cdot LL \cdot PP200$ (0.0085) (0.3065) (0.9837)	0.4491
			$- 63.2045 \cdot LL \cdot CBR_w$ (0.0000)	

5.2 Conclusions

The following conclusions are drawn based on the results presented:

1. Resilient modulus of fine-grained soils is highly stress dependent and presents large variations depending on their soil index properties.
2. Models based on stress and soil index covariates result in reliable estimates with a R^2 of 0.7723. It is also possible to determine the effects of stress sensitivity based on this model since it is capable of representing the effects of different stress states. On the other hand, models predicting universal model coefficients based on the soil index properties do not present reliable results for resilient modulus estimations.
3. Resilient modulus test results do not depend much on compaction percentages. In contrast, the effect of water content ($W_{opt} \pm 2$) variation on resilient modulus test results is immensely high.
4. For fine-grained soils, plasticity index (PI), liquid limit (LL) and optimum water content (W_{opt}) covariates affect the resilient modulus considerably.
5. For granular soils, liquid limit (LL) and maximum dry-density (DD_{std}) of fine content are the most significant covariates in representing the variation in the resilient modulus.
6. Since fine-grained soils have high liquid limits and plasticity indexes, the effect of moisture content variation on these specimens is higher. Thus, the results of the CBR tests conducted with soaked specimens have high correlations with resilient modulus test results. On the other hand, the results of the CBR tests

conducted with unsoaked specimens have high correlations with the resilient modulus test results for granular soils.

7. The nonlinear model developed to predict resilient modulus based on the soil index properties results in the most successful estimates with an R^2 of 0.8120 for fine-grained soils. In addition, the high statistical performance of the model for an independent data set validates the applicability of this function for design resilient modulus estimations.

8. Genetic algorithm and curve shifting methodology is a reliable and effective tool to characterize unbound layers' elastic response under repeated loads. Since there are certain deficiencies in predicting resilient modulus for a certain stress state according to the constitutive nonlinear models for fine-grained soils, genetic algorithm and curve shifting methodology is highly recommended for successful estimations.

9. The models correlating resilient modulus with CBR test results are not statistically reliable due to the different characteristics of these two tests. However, models can be improved by including the soil index properties as independent variables.

10. Resilient modulus and LFWD tests have similar characteristics in terms of resilient response prediction. However, the differences in test conditions, such as loading frequency, compaction type and water content levels, provide differences in the test results. However, models correlating resilient modulus with soil index parameters and LFWD test results can be effectively used in design resilient modulus estimations.

11. Tree-Based approach is an effective method in understanding the relative significance of the soil index parameters in resilient modulus estimations. In addition, separating the test results based on this approach and performing

regression analysis for each split result in reliable prediction models for certain soil index parameter intervals.

5.3 Recommendations

In this study, tests are conducted with the materials which have different characteristics in order to develop general resilient modulus prediction models. However, further tests should be conducted to improve and validate the statistical reliability of these models before their use in pavement design.

A general design specification should be developed by also analyzing the asphalt test results. Elastic modulus of the asphalt layers can be determined by using the flexural frequency test results or applying back-calculation procedures for the standard falling weight deflectometer (FWD) test results. Pavement layer thicknesses and binder structures can be designed using these elastic properties according to the layered elastic analysis.

REFERENCES

AASHTO (1993), *Guide for Design of Pavement Structure*, Washington, D.C., American Association of State Highway and Transportation Officials, 1993.

AASHTO T193-99, *Standard Method of Test for the California Bearing Ratio Test*, AASHTO, Washington D.C., 2003.

AASHTO T224-01, *Correction for Coarse Particles in the Soil Compaction Test*, Standard Method of Test, AASHTO, Washington D.C., 2004.

AASHTO T274, *Standard Method of Test for Resilient Modulus of Subgrade Soils*, Standard Method of Test, 1982.

AASHTO T27-99, *Sieve Analysis of Fine and Coarse Aggregate*, Standard Method of Test, AASHTO, Washington D.C., 2006.

AASHTO T292-91, *Standard Method of Test for Resilient Modulus of Subgrade Soils and Untreated Base/Subbase Materials*, Standard Method of Test, AASHTO, Washington D.C., 2000.

AASHTO T294-94, *Resilient Modulus of Unbound Granular Base/Subbase Materials and Subgrade*, Standard Method of Test, AASHTO, Washington D.C., 1995.

AASHTO T307-99, *Determining the Resilient Modulus of Soils and Aggregate Materials*, Standard Specifications for Transportation Materials and Methods of Sampling and Testing, 20th Edition, AASHTO, Washington D.C., 2000.

AASHTO T89, *Determining the Liquid Limit of Soils*, Standard Method of Test, AASHTO, Washington D.C., 2000.

AASHTO T-90-00, *Determining the Plastic Limit and Plasticity Index of Soils*, Standard Method of Test, AASHTO, Washington D.C., 2004.

AASHTO T99-01, *Moisture-Density Relations of Soils Using a 2.5 kg (5.5 lb) Rammer and a 305 mm (12 in) Drop*, Standard Method of Test, AASHTO, Washington D.C., 2004.

AASHTO TP46-94, *Standard Test Method for Determining the Resilient Modulus of Soils and Aggregate Materials*, AASHTO, Washington D.C., 1994.

Alshibli, K.A., Abu-Farsakh M., and Seyman E., *Laboratory Evaluation of the Geogauge and Light Falling Weight Deflectometer as Construction Control Tools*, Journal of Materials in Civil Engineering, ASCE / September/October 2005.

Ang, H.S., Tang W.H., *Probability Concepts in Engineering*, John Wiley and Sons, 2nd Edition, 2007.

ASTM M145-82, American Association of State Highway and Transportation Officials. Standard Method of Test, *The Classification of Soils and Soil-Aggregate Mixtures for Highway Construction Purposes*, AASHTO Designation: M145-82, Part I Specifications, 14th Edition, 1986.

Atkins, H., *Highway Materials, Soils, and Concretes*, Prentice Hall; 4 edition, June 25, 2002.

Attoh-Okine, N.O. *Predicting Roughness Progression Models in Flexible Pavements – An Evolutionary Algorithm Approach*. Intelligent Engineering Systems Through Neural Networks, Vol. 8, 1998, pp.845-853.

Bandara, N. (Dynatest Consulting Inc., Box 1510), Rowe, G.M., *Design Subgrade Resilient Modulus for Florida Subgrade Soils*, ASTM Special Technical Publication, n 1437, 2002, p 85-96.

Brieman, L., Friedman, J. H., Olshen, R., & Stone, C. J., *Classification and regression trees*, Belmont, CA: Wadsworth International Group, 1984.

Clegg, B. (Univ of West Aust, Aust), *Impact Soil Test as Alternative To California Bearing Ratio*, Environmental Conference, Proceedings of the Technical Association of the Pulp and Paper Industry, 1980, p 1225-1230, May 12-16 1980, Wellington, NZ.

Franco, C.A. (Rhode Island DOT, Providence, RI, USA); Lee, K.W., *Improved California Bearing Ratio Test Procedure*, Transportation Research Record, 1987, p 91-97.

Geocomp Corporation, *Load-Trac II Resilient Modulus Testing User's Manual*, 2005.

George, K.P., *Falling Weight Deflectometer for Estimating Subgrade Resilient Moduli*, Final Report by the Department of Civil Engineering, University of Mississippi, October 2003.

George K.P., *Prediction of Resilient Modulus from Soil Index Properties*, Final Report, Conducted by the Department of Civil Engineering at University of Mississippi, Mississippi, November 2004.

Hardcastle, J.H., *Subgrade Resilient Modulus for Idaho Pavements*, Final Report of ITD Research Project RP 110-D, Agreement No. 89-47, Department of Civil Engineering, University of Idaho, 1992, 252 pp.

Heukelom, W., and Klomp, A.J.G., *Dynamic Testing as a Means of Controlling Pavement during and after Construction*, Proceedings of the 1st international Conference on the Structural Design of Asphalt Pavement, University of Michigan, Ann Arbor, MI., 1962.

Hicks, R. and Monismith C.L., *Factors Influencing the Resilient Response of Granular Materials*, Highway Research Record 345, Highway Research Board, Washington, D.C., 1971.

Huang, Y.H., *Pavement Analysis and Design*, Englewood Cliffs, New Jersey, Prentice Hall, 1993.

Johnson, T., Berg R., and DiMillio A., *Frost Action Predictive Techniques: An Overview of Research Results*, TRR 1089, TRB, Washington, D.C., 1986.

Kameyama, S., K. Himeno, A. Kasahara, and T. Maruyama., *Backcalculation of Pavement Layer Moduli Using Genetic Algorithms*, Proc., 8th International Conference on Asphalt Pavement, Seattle, Wash., Aug. 1997, pp. 1375-1385.

Liu, M.-Y., and S.-Y. Wang., *Genetic Optimization Method of Asphalt Pavement Based on Rutting and Cracking Control*, Journal of Wuhan University of Technology, Materials Science Edition, Vol. 18, No. 1, 2003, pp.72-75.

Livneh, M., Greenstein, J., *Modified California Bearing Ratio Test for Granular Materials*, Geotechnical Testing Journal, v 1, n 3, sep, 1978, p 141-147.

Lotfi, H. A., Schwartz, C. W., and Witczak, M. W., *Compaction Specification for the Control of Subgrade Rutting*, Transportation Research Record: 1196, Transportation Research Board, Washington D.C., 1988.

Maier, A. , Bennert, T. and Gucunski, N., *Resilient Modulus Properties of New Jersey Subgrade Soils*, Final Report, The State of New Jersey Department of Transportation, September 2000.

Mehta, Y., and Roque R., *Evaluation of FWD Data for Determination of Layer Moduli of Pavements*, ASCE Journal of Materials in Civil Engineering / January/February 2003.

Mohammad, L.N., Huang, B., Puppala, A., and Allen, A., *A Regression Model for Resilient Modulus of Subgrade Soils*, National Research Council Journal of the Transportation Research Board, No. 1687, 1999, pp. 47-54.

Monismith, C.L., *MR Testing-Interpretation of Laboratory Results for Design Purposes*, Workshop on Resilient Modulus Testing, Oregon State University, Corvallis, 1989.

Monismith, C.L., J.T. Harvey, F. Long, S. Weissman, *Tests to Evaluate the Stiffness and Permanent Deformation Characteristics of Asphalt/Binder-Aggregate Mixes*, Technical Memorandum, TM-UCB PRC-2000-1, 2000.

Nataatmadja, A., and Parkin, A., *Characterization of Granular Materials for Pavements*, Canadian Geotechnical Journal, Vol.26, No. 4, 1989.

National Cooperative Highway Research Program (NCHRP), *Research Results Digest*, Number: 285, January 2004.

Nazarian, S., and Feliberti, M., *Methodology for Resilient Modulus Testing of Cohesionless Subgrades*, In Transportation Research Record 1406, Washington, D.C. 1993, pp.108-115., 1993.

Pezo, R.F., Kim, D.S., Stokoe, K.H., and Hudson, W.R., *A Reliable Resilient Modulus Testing System*, Transportation Research Record 1307, TRB, National Research Council, Washington D.C., 1991, pp. 90 - 98.

Pezo, R., *A General Method of Reporting Resilient Modulus Tests of Soils, A Pavement Engineer's Point of View*, 72nd Annual Meeting of Transportation Research Board, Jan. 12-14, Washington, D.C., 1993.

Pezo, R and Hudson, W. R., *Prediction Models of Resilient Modulus for Nongranular Materials*, Geotechnical Testing Journal, GTJODJ, Vol. 17, No. 3, 1994, pp. 349 ~ 355.

Ping, W.V., Yang Z., and Gao Z., *Field and Laboratory Determination of Granular Subgrade Moduli*, Journal of Performance of Constructed Facilities / November 2002.

Rada, G. and M.W. Witzak, *Comprehensive Evaluation of Laboratory Resilient Moduli Results for Granular Materials*, Transportation Research Record 810, Transportation Research Board, National Academy of Sciences, Washington, D.C., 1981, pp. 23-33.

Rahim, A., and George K. P., *Falling Weight Deflectometer for Estimating Subgrade Elastic Moduli*, Journal of Transportation Engineering / January/February 2003.

Rahim, A.M., *Subgrade Soil Index Properties to Estimate Resilient Modulus for Pavement Design*, The International Journal of Pavement Engineering, 2005.

Ross, S.M., *Introduction to Probability and Statistics for Engineers and Scientists*, University of California, Berkeley, Wiley Series in Probability and Mathematical Statistics, John Wiley and Sons, 1987.

Seber, G.A.F., *Linear Regression Analysis*, John Wiley & Sons, 1977.

Seed, H.B., Chan, C.K., and Lee, C.E., *Resilience Characteristics of Subgrade Soils and Their Relation to Fatigue Failures in Asphalt Pavements*, Proc. 1st International Conference on the Structural Design of Asphalt Pavements, Ann Arbor, Michigan, 1962.

Shekharan, A.R., *Solution of Pavement Deterioration Equations by Genetic Algorithms*, In Transportation Research Record: Journal of the Transportation Research Board, No. 1699, TRB, National Research Council, Washington D.C., 2000, pp. 101-106.

Sousa, J. B., J. A. Deacon, S. Weissman, J. T. Harvey, C. L. Monismith, R. B. Leahy, G. Paulsen, and J. S. Coplantz., *Permanent Deformation Response of Asphalt-Aggregate Mixes*, Report No. SHRP-A-415, Strategic Highway Research Program, National Research Council, Washington, D.C., 1994.

Tanyu, B.F. (Geological Engineering Program, University of Wisconsin-Madison), Kim, W.H., Edil, T.B., Benson, C.H., *Comparison of Laboratory Resilient Modulus with Back-Calculated Elastic Moduli from Large-Scale Model Experiments and FWD Tests on Granular Materials*, ASTM Special Technical Publication, n 1437, 2002, p 191-208.

Thompson, M.R., and Q. L. Robnett, *Pressure Injected Lime for Treatment of Swelling Soils*, Transportation Research Record, No.568, 24-34, 1976.

Tsai, B.W., J.T. Harvey, C.L. Monismith, *Two-Stage Weibull Approach for Asphalt Concrete Fatigue Performance Prediction*, Journal, Association of Asphalt Paving Technologists, 2004, Vol. 73, pages 623-656.

Tsai, B. W., M.O. Bejarano, J.T. Harvey , C.L. Monismith., *Prediction and Calibration of Pavement Fatigue Performance Using Two-Stage Weibull Approach, Journal*, Association of Asphalt Paving Technologists, 2005, Vol. 74, pages 697-732.

Tsai, B. W., J.T. Harvey , C.L. Monismith., *Application of Weibull Theory in Prediction of Asphalt Concrete Fatigue Performance*, Journal, Transportation Research Board, 2003, No. 1832.

Tsai, B.W., V.N. Kannekanti, and J.T. Harvey, *Application of Genetic Algorithm in Asphalt Pavement Design*, Journal, Transportation Research Board, 2004, No.1891.

Tsai, B.W. J.T. Harvey, and C.L. Monismith, *Using the Three-Stage Weibull Equation and Tree-Based Model to Characterize the Mix Fatigue Damage Process*, Journal, Transportation Research Board, 2005, No. 1929.

Uzan, J., *Characterization of Granular Materials*, TRR 1022, TRB, Washington, D.C., 1985.

Zaman, M. (Univ of Oklahoma), Chen, D.H, Laguros, J., *Resilient Moduli of Granular Materials*, Journal of Transportation Engineering, v 120, n 6, Nov-Dec, 1994, p 967-988.

APPENDIX A

CIRCLY Results for the Typical Pavement Section

Table A1 Typical CIRCLY Output

```

*****
*
* PROGRAM- CIRCLY
*
* VERSION- 2.0 UPDATE- 10 (1989)
*
* SERIAL NUMBER:
*
* REGISTERED OWNER:
*
* LAYERS BLOCK WORKSPACE (MLYBLK)... 10000
* COORDINATES BLOCK WORKSPACE (MCOORD)... 4000
* LOADS BLOCK WORKSPACE (MLOADS)... 1000
*
* CONVERGENCE TOLERANCE (EPS)... 1.0E-02
* MAXIMUM INTEGRATION RANGE (RKNMTR)... 1.0E+01
* MAXIMUM EXPONENTIAL FN. ARG.(EXPMAX)... 2.0E+01
* MAXIMUM NODES IN QUADRATURE (MXKNOD)... 127
*
*****

```

```

ODetails OF LAYERED SYSTEM . . . DGAC daggat 4 layers SIMULATIONS UNITS U.S
-----
NUMBER OF LAYERS..... 4
0

```

LAYER	TYPE	ELASTIC CONSTANTS	THICKNESS	INTERFACE
0	ISOTROPIC	MODULUS = 0.5118E+05	0.4489E+01	ROUGH
0	ISOTROPIC	MODULUS = 0.8370E+05	0.3425E+01	ROUGH
0	ISOTROPIC	MODULUS = 0.1886E+05	0.1075E+02	ROUGH
0	ISOTROPIC	MODULUS = 0.6808E+04	INFINITE	

Table A1 Typical CIRCLY Output (Continued)

```

0DETAILS OF LOADS      dual single (6745 lb each; 105 psi tire pressure; radius 3.7 in; c.t.c
-----
0NUMBER OF LOAD GROUPS..... 2
0NUMBER OF NON-DEFAULT LOAD LOCATIONS.... 1

0 LOAD GROUP LOAD TYPE RADIUS REFERENCE AVERAGE LOAD/MOMENT
  NO.          (1) VERTICAL FORCE 0.3700E+01 0.1568E+03 0.1568E+03 0.6745E+04 0.0000E+00
  2          (1) VERTICAL FORCE 0.3700E+01 0.1568E+03 0.1568E+03 0.6745E+04 0.0000E+00

NON-DEFAULT LOAD LOCATION DATA
-----
LOAD GROUP X Y THETA SCALING
  NO.          (DEGREES) FACTOR

1 2 0.1417E+02 0.0000E+00 0.000 0.1000E+01

DGAC daggat 4 layers SIMULATIONS UNITS U.S
dual single (6745 lb each; 105 psi tire pressure; radius 3.7 in; c.t.c
0 *** WARNING - RESULTS FOR POINTS INDICATED BY * MAY NOT HAVE CONVERGED

POINT COORDINATES DISPLACEMENTS
-----
NO. X Y Z L UX UY UZ
0* 1 0.1122E+02 0.0000E+00 0.2000E+01 1 0.2015E-02 0.6698E-10 -0.4689E-01
0 2 0.1122E+02 0.0000E+00 0.6200E+01 2 -0.9486E-05 0.7276E-10 -0.4335E-01
0 3 0.1122E+02 0.0000E+00 0.1579E+02 3 -0.1261E-02 0.6601E-10 -0.3560E-01
0 4 0.1122E+02 0.0000E+00 0.2400E+02 4 -0.1257E-02 0.5174E-10 -0.2876E-01

```

Table A1 Typical CIRCLY Output (Continued)

POINT NO.	C O O R D I N A T E S			N O R M A L S T R A I N S			S H E A R S T R A I N S				
	X	Y	Z	L	XX E1	YY E2	ZZ E3	XX GAM1	YZ GAM2	XY GAM3	
0*	1	0.1122E+02	0.0000E+00	0.2000E+01	1	0.3648E-04	-0.1484E-03	0.1229E-02	-0.3891E-03	-0.4276E-10	0.2132E-10
0	2	0.1122E+02	0.0000E+00	0.6200E+01	2	0.1344E-02	-0.1484E-03	-0.7922E-04	0.7463E-03	0.7118E-03	-0.3456E-04
0	3	0.1122E+02	0.0000E+00	0.1579E+02	3	-0.1387E-03	-0.3571E-03	0.5363E-03	-0.2030E-03	-0.2707E-10	0.6673E-11
0	4	0.1122E+02	0.0000E+00	0.2400E+02	4	0.5927E-03	-0.3571E-03	-0.1950E-03	0.4749E-03	0.3939E-03	-0.8105E-04
						-0.3040E-03	-0.4356E-03	0.7404E-03	0.9071E-04	-0.9519E-11	0.1402E-11
						0.7483E-03	-0.4356E-03	-0.3118E-03	0.5919E-03	0.5300E-03	-0.6191E-04
						-0.2949E-03	-0.3655E-03	0.7529E-03	0.1083E-03	-0.5522E-11	0.5572E-12
						0.7640E-03	-0.3655E-03	-0.3060E-03	0.5647E-03	0.5350E-03	-0.2975E-04

POINT NO.	C O O R D I N A T E S			N O R M A L S T R E S S E S			S H E A R S T R E S S E S				
	X	Y	Z	L	XX S1	YY S2	ZZ S3	XX TAU1	YZ TAU2	XY TAU3	
0*	1	0.1122E+02	0.0000E+00	0.2000E+01	1	0.5078E+02	0.4377E+02	0.9597E+02	-0.1475E+02	-0.1621E-05	0.8084E-06
0	2	0.1122E+02	0.0000E+00	0.6200E+01	2	0.1004E+03	0.4377E+02	0.4639E+02	0.2830E+02	0.2699E+02	-0.1310E+01
0	3	0.1122E+02	0.0000E+00	0.1579E+02	3	-0.5663E+01	-0.1921E+02	0.3619E+02	-0.1259E+02	-0.1678E-05	0.4137E-06
0	4	0.1122E+02	0.0000E+00	0.2400E+02	4	0.3968E+02	-0.1921E+02	-0.9158E+01	0.2944E+02	0.2442E+02	-0.5025E+01
						-0.3905E+01	-0.5617E+01	0.9676E+01	0.1180E+01	-0.1238E-06	0.1824E-07
						0.9778E+01	-0.5617E+01	-0.4007E+01	0.7698E+01	0.6893E+01	-0.8051E+00
						0.5707E+00	0.2394E+00	0.5490E+01	0.5083E+00	-0.2593E-07	0.2616E-08
						0.5542E+01	0.2394E+00	0.5188E+00	0.2651E+01	0.2512E+01	-0.11397E+00

APPENDIX B

Universal Model Coefficients for Experiment Set 1

Table B1 Universal Model Coefficients for Experiment Set 1

Region	Test	AASHTO	Wc	Comp. (%)	LL	PI	Wstnd	DDstnd	Universal Model Coefficients			
									K _a	K _i	K _s	R ²
Kayseri 6/2	k6295opt1	A-7-5	opt	95	44.7	13.8	19.2	1.702	493.80	0.223	-0.0787	0.93
Kayseri 6/2	k6295opt2	A-7-5	opt	95	44.7	13.8	19.2	1.702	453.99	0.222	-0.135	0.86
Kayseri 6/2	k62100opt1	A-7-5	opt	100	44.7	13.8	19.2	1.702	708.43	0.286	-0.17	0.64
Kayseri 6/2	k62100opt2	A-7-5	opt	100	44.7	13.8	19.2	1.702	768.23	0.095	-0.0291	0.66
Kayseri 6/2	k62100opt3	A-7-5	opt	100	44.7	13.8	19.2	1.702	693.05	0.236	-0.144	0.87
Kayseri 6/2	k62100opt-21	A-7-5	opt-2	100	44.7	13.8	19.2	1.702	779.04	0.113	-0.134	0.86
Kayseri 6/2	k62100opt-22	A-7-5	opt-2	100	44.7	13.8	19.2	1.702	987.99	0.144	-0.0792	0.78
Kayseri 6/2	k62100opt-21	A-7-5	opt+2	100	44.7	13.8	19.2	1.702	512.73	0.151	-0.117	0.43
Kayseri 6/2	k62100opt+23	A-7-5	opt+2	100	44.7	13.8	19.2	1.702	637.35	0.025	-0.159	0.86
Kayseri 6/5	k6595opt1	A-2-4	opt	95	0	0	15.8	1.78	351.81	0.745	-0.111	0.97
Kayseri 6/5	k6595opt2	A-2-4	opt	95	0	0	15.8	1.78	360.52	0.752	-0.186	0.99
Kayseri 6/5	k65100opt1	A-2-4	opt	100	0	0	15.8	1.78	426.72	0.705	-0.0712	0.97
Kayseri 6/5	k65100opt2	A-2-4	opt	100	0	0	15.8	1.78	368.98	0.829	-0.0838	0.98
Kayseri 6/5	k65100opt3	A-2-4	opt	100	0	0	15.8	1.78	320.33	0.563	0.141	0.93
Kayseri 6/5	k65100opt4	A-2-4	opt	100	0	0	15.8	1.78	306.78	0.976	-0.261	0.98
Kayseri 6/5	k65100opt-21	A-2-4	opt-2	100	0	0	15.8	1.78	551.76	0.547	-0.234	0.92
Kayseri 6/5	k65100opt-22	A-2-4	opt-2	100	0	0	15.8	1.78	438.93	0.740	-0.329	0.98
Kayseri 6/5	k65100opt+21	A-2-4	opt+2	100	0	0	15.8	1.78	347.34	0.759	0.0349	0.96
Kayseri 6/5	k65100opt+22	A-2-4	opt+2	100	0	0	15.8	1.78	384.14	0.313	0.336	0.97
Kayseri 6/5	k65100opt+23	A-2-4	opt+2	100	0	0	15.8	1.78	328.49	0.337	0.338	0.95
Kayseri 6/6	k6695opt1	A-2-7	opt	95	59.2	21.2	28.4	1.436	356.22	0.756	-0.182	0.99
Kayseri 6/6	k6695opt2	A-2-7	opt	95	59.2	21.2	28.4	1.436	369.12	0.698	-0.171	0.94
Kayseri 6/6	k66100opt1	A-2-7	opt	100	59.2	21.2	28.4	1.436	408.21	0.669	-0.222	0.96
Kayseri 6/6	k66100opt2	A-2-7	opt	100	59.2	21.2	28.4	1.436	357.55	0.877	-0.29	0.92

Table B1 Universal Model Coefficients for Experiment Set 1 (Continued)

Region	Test	AASHTO	Wc	Comp. (%)	LL	PI	Wstd	DDstd	Universal Model Coefficients			
									K ₀	K ₁	K ₂	R ²
Kayseri 6/6	k66100opt-21	A-2-7	opt-2	100	59.2	21.2	28.4	1.436	551.57	0.525	-0.2000	0.89
Kayseri 6/6	k66100opt-22	A-2-7	opt-2	100	59.2	21.2	28.4	1.436	573.49	0.548	-0.1950	0.95
Kayseri 6/6	k66100opt-23	A-2-7	opt-2	100	59.2	21.2	28.4	1.436	546.81	0.514	-0.1450	0.95
Kayseri 6/6	k66100opt+21	A-2-7	opt+2	100	59.2	21.2	28.4	1.436	355.26	0.783	-0.1520	0.99
Kayseri 6/6	k66100opt+22	A-2-7	opt+2	100	59.2	21.2	28.4	1.436	422.10	0.738	-0.0788	0.95
Kayseri 6/7	k6795opt1	A-5	opt	95	42.0	9.7	24.8	1.478	425.39	0.271	-0.2060	0.73
Kayseri 6/7	k6795opt2	A-5	opt	95	42.0	9.7	24.8	1.478	353.09	0.463	-0.2180	0.94
Kayseri 6/7	k67100opt1	A-5	opt	100	42.0	9.7	24.8	1.478	417.01	0.417	-0.2250	0.95
Kayseri 6/7	k67100opt2	A-5	opt	100	42.0	9.7	24.8	1.478	435.83	0.436	-0.2140	0.95
Kayseri 6/7	k67100opt3	A-5	opt	100	42.0	9.7	24.8	1.478	242.46	0.626	-0.2660	0.96
Kayseri 6/7	k67100opt-21	A-5	opt-2	100	42.0	9.7	24.8	1.478	602.25	0.231	-0.1130	0.59
Kayseri 6/7	k67100opt-22	A-5	opt-2	100	42.0	9.7	24.8	1.478	513.81	0.297	-0.0658	0.84
Kayseri 6/7	k67100opt+21	A-5	opt+2	100	42.0	9.7	24.8	1.478	446.46	0.367	-0.1070	0.92
Kayseri 6/7	k67100opt+22	A-5	opt+2	100	42.0	9.7	24.8	1.478	413.67	0.343	-0.1830	0.86
A.C	ac95opt1	A-6	opt	95	39.9	21.6	14.8	1.844	940.23	0.235	-0.0574	0.50
A.C	ac95opt2	A-6	opt	95	39.9	21.6	14.8	1.844	899.03	0.243	-0.1080	0.92
A.C	ac100opt3	A-6	opt	100	39.9	21.6	14.8	1.844	886.88	0.500	-0.1130	0.85
A.C	ac100opt4	A-6	opt	100	39.9	21.6	14.8	1.844	998.28	0.257	-0.0624	0.66
A.C	ac100opt-21	A-6	opt-2	100	39.9	21.6	14.8	1.844	1686.9	0.047	0.1330	0.64
A.C	ac100opt-22	A-6	opt-2	100	39.9	21.6	14.8	1.844	1575.8	0.232	0.0809	0.86
A.C	ac100opt+21	A-6	opt+2	100	39.9	21.6	14.8	1.844	539.66	0.447	-0.2570	0.87
A.C	ac100opt+22	A-6	opt+2	100	39.9	21.6	14.8	1.844	689.82	0.414	-0.2020	0.91
D.S	ds9395opt1	A-7-6	opt	95	50.4	24.9	22.8	1.590	434.98	0.261	-0.1700	0.86
D.S	ds9395opt2	A-7-6	opt	95	50.4	24.9	22.8	1.590	467.21	0.338	-0.2260	0.83
D.S	ds93100opt1	A-7-6	opt	100	50.4	24.9	22.8	1.590	537.42	0.195	-0.2300	0.91

Table B1 Universal Model Coefficients for Experiment Set 1 (Continued)

Region	Test	AASHTO	Wc	Comp. (%)	LL	PI	Wstnd	DDstnd	Universal Model Coefficients			
									K ₀	K ₁	K ₂	R ²
D.S	ds93100opt2	A-7-6	opt	100	50.4	24.9	22.8	1.590	611.88	0.1690	-0.0616	0.74
D.S	ds93100opt3	A-7-6	opt	100	50.4	24.9	22.8	1.590	648.59	0.1430	-0.0477	0.51
D.S	ds93100opt-21	A-7-6	opt-2	100	50.4	24.9	22.8	1.590	648.99	0.2100	-0.0845	0.89
D.S	ds93100opt-22	A-7-6	opt-2	100	50.4	24.9	22.8	1.590	746.67	0.0966	0.0570	0.52
D.S	ds93100opt+21	A-7-6	opt+2	100	50.4	24.9	22.8	1.590	186.62	0.2980	-0.3740	0.93
D.S	ds93100opt+22	A-7-6	opt+2	100	50.4	24.9	22.8	1.590	200.94	0.3010	-0.4330	0.94
D.K.V	dkv9695opt1	A-7-6	opt	95	57.2	28.8	25.8	1.527	625.33	0.1210	-0.0729	0.72
D.K.V	dkv9695opt2	A-7-6	opt	95	57.2	28.8	25.8	1.527	729.95	0.2050	-0.0481	0.75
D.K.V	dkv96100opt1	A-7-6	opt	100	57.2	28.8	25.8	1.527	589.54	0.1440	-0.0838	0.79
D.K.V	dkv96100opt2	A-7-6	opt	100	57.2	28.8	25.8	1.527	552.73	0.1670	-0.0525	0.82
D.K.V	dkv96100opt3	A-7-6	opt	100	57.2	28.8	25.8	1.527	603.80	0.2670	-0.1890	0.82
D.K.V	dkv96100opt-21	A-7-6	opt-2	100	57.2	28.8	25.8	1.527	1158.4	0.1790	-0.00157	0.66
D.K.V	dkv96100opt-22	A-7-6	opt-2	100	57.2	28.8	25.8	1.527	1046.9	0.3120	-0.0730	0.67
D.K.V	dkv96100opt+21	A-7-6	opt+2	100	57.2	28.8	25.8	1.527	430.47	0.1790	-0.1840	0.71
D.K.V	dkv96100opt+22	A-7-6	opt+2	100	57.2	28.8	25.8	1.527	434.02	0.2370	-0.1110	0.77
D.B	db91795opt1	A-7-6	opt	95	61.1	37.3	22.5	1.599	674.79	0.0850	0.0369	0.72
D.B	db91795opt2	A-7-6	opt	95	61.1	37.3	22.5	1.599	535.54	0.3100	-0.3800	0.79
D.B	db917100opt1	A-7-6	opt	100	61.1	37.3	22.5	1.599	823.71	0.2630	-0.0713	0.87
D.B	db917100opt2	A-7-6	opt	100	61.1	37.3	22.5	1.599	758.05	0.2120	-0.0808	0.66
D.B	db917100opt3	A-7-6	opt	100	61.1	37.3	22.5	1.599	912.60	0.1550	0.1380	0.82
D.B	db917100opt-21	A-7-6	opt-2	100	61.1	37.3	22.5	1.599	913.16	0.2740	0.0594	0.88
D.B	db917100opt-22	A-7-6	opt-2	100	61.1	37.3	22.5	1.599	947.89	0.1880	-0.00405	0.71
D.B	db917100opt+21	A-7-6	opt+2	100	61.1	37.3	22.5	1.599	505.95	0.1880	-0.0531	0.78
D.B	db917100opt+22	A-7-6	opt+2	100	61.1	37.3	22.5	1.599	526.92	0.2150	-0.0762	0.94

APPENDIX C

Genetic Algorithm Code for Curve Shifting (S-PLUS)

```
#GENETIC ALGORITHM#

# Input data : deviator stress, confining pressure, measured resilient
modulus
# The data set must be from lowest confining pressure to the highest
# Deviator stress is always from low to high
# pref: position of the reference confining pressure
# cb: a vector of left side endpoints of parameters
# ce: a vector of right side endpoints of parameters
# nn: number of genes
# nt: number of confining pressures
# ndisc: number of discarded genes
# iter: number of iterations
# epsilon: allowance to prevent the parameter out of range
# Output data: horizontal shifts, fitted final curve, residual deviance

#-----
#Subroutine general
#-----

gamc2_function(data,pref,cb,ce,nn,ndisc,iter,A,epsilon)
{
  x<-split(data$Col2,data$Col2)
  nt<-length(as.numeric(names(x)))
  gen<-gene(nn,nt,cb,ce)
  yy<-NULL
  for (i in 1:nn){
    cp<-mcf2(data,pref,gen[i, ])
    yy<-c(yy, cp$resdev)
  }
  newx<-rankf(gen,yy,0)
  child<-matef(newx,cb,ce,A,epsilon)
  count<-1
  result<-matrix(rep(0,nt*iter),ncol=nt)
  result[1, ]<-newx[1, ]
  count<-2
  while(count<=iter) {
    yy<-NULL
    for (i in 1:nn) {
      cp<-mcf2(data,pref,child[i, ])
      yy<-c(yy,cp$resdev)
    }
    newchild<-rankf(child,yy,ndisc)
    nnchild<-matef(newchild,cb,ce,A,epsilon)
    result[count, ]<-newchild[1, ]
    newgen<-gene(ndisc,nt,cb,ce)
    child<-rbind(newchild,newgen)
    count<-count+1
  }
}
```

```

}
result
}

#-----
#Subroutine gene
#-----

# generation of gene pool
# n: number of genes
# nv: number of parameters
# cb: a vector of left side end points of parameters
# ce: a vector of right side end points of parameters

gene_function(n,nv,cb,ce)
{
result<-NULL
for(i in 1:nv) {
result<-cbind(result,runif(n,cb[i],ce[i]))
}
result
}

#-----
#Subroutine rankf
#-----

# sorting the gene pool based on the fitness value
# and discard "ndisc" number of bad genes
# x: gene pool
# y: a vector of fitness value

rankf_function(x,y,ndisc)
{
xrow<-dim(x)[1]
xcol<-dim(x)[2]
newx<-matrix(rep(0,xrow*xcol),ncol=xcol)
j<-1
for(i in rank(y)){
newx[i, ] <-x[j, ]
j<-j+1
}
n<- length(y)
newx<-newx[1:(n-ndisc), ]
newx
}

#-----
#Subroutine matef
#-----

# mate the nearest ranked pairs
# newx: a ranked parameter matrix

```

```

# epsilon: if parameter is out of range, then endpoint+-epsilon

matef_function(newx,cb,ce,A,epsilon)
{
  xrow<-dim(newx)[1]
  xcol<-dim(newx)[2]
  child<-matrix(rep(0,xrow*xcol),ncol=xcol)
  oddset<-seq(1,xrow,2)
  for(i in oddset) {
    cp1<-runif(1,0,1)*A
    cp2<-runif(1,0,1)*A
    child[i, ] <-cp1*newx[i, ]+(1-cp1)*newx[i+1, ]
    child[i+1, ] <-cp2*newx[i, ]+(1-cp2)*newx[i+1, ]
  }

  for(i in 1:xcol) {
    for(j in 1:xrow){
      if(child[j, i] >= ce[i])
        child[j, i]<-ce[i]-epsilon
      else if(child[j, i]<-cb[i])
        child[j, i]<-cb[i]+epsilon
    }
  }
  child
}

#-----
#Subroutine mcfit2
#-----

# gamma type curve fitting
# pref: position of the reference confining pressure
# shift: shifting vector
# nt: number of tested confining pressures
# Output to the general subroutine: fitted master curve, residual deviance
# of fitting
# IMPORTANT NOTE:FOR STRESS HARDENING SOIL TYPES(TYPE 1) CHANGE THE "sign"
# VECTORS TO POZITIVE AND NEGATIVE

mcfit2_function(data,pref,shift)
{
  sgn<-NA
  xf<-NULL
  x<-split(data$Col2,data$Col2)
  data.spl<-split(data,data$Col2)
  nt<-length(as.numeric(names(x)))
  for(i in 1:nt) {
    if(i<pref)
      sgn[i]<- -1

# (If Stress Hardening, Type 1 then)   sgn[i]<- 1

    else if(i==pref)
      sgn[i]<-0
    else sgn[i]<- 1
  }
}

```

```

# (If Stress Hardening Type 1 then)     else sgn[i]<- -1
}
for(i in 1:nt){
  subdata<-data.spl[[i]]$Col1
  xf<-c(xf, (subdata)+sgn[i]*shift[i])
}
xy.gam<-gam(data$Col3~s(xf))
dev<-xf
fitted<-xy.gam$fitted
measured<-data$Col3
resdev<-sum((xy.gam$res)^2)
return(dev,fitted,measured,resdev)
}

#-----
#subroutine: findfs (nonlinear gamma fitting)
#-----

findfs1_function(data,a,b,m){
  dev<-data$Col1
  n<-length(dev)
  xx<-dev
  lnw<-xx-xx[1]
  yy<-data$Col2
  yyy<-yy-yy[1]
  xy<-data.frame(x=lnw,y=yyy)
  param(xy,"A")<-a
  param(xy,"B")<-b
  if(m==1){
    xy.nls<-nls(y~A*(1-exp(-x/B))*(1)),xy,trace=T)
  }
  else if (m==2) {
    xy.nls<-nls(y~A*(1-exp(-x/B))*(1+x/B)),xy,trace=T)
  }
  else if (m==3) {
    xy.nls<-nls(y~A*(1-exp(-x/B))*(1+x/B+(x/B)^2/2)),xy,trace=T)
  }
  else if (m==4) {
    xy.nls<-nls(y~A*(1-exp(-x/B))*(1+x/B+(x/B)^2/2+(x/B)^3/6)),xy,trace=T)
  }

  xnls<-xy.nls
  aa<-coef(xnls) [1]
  bb<-coef(xnls) [2]
  xf<-xx

  if(m==1) {
    yf<-yy[1]+aa*(1-exp(-lnw/bb))*(1)
  }
  else if (m==2) {
    yf<-yy[1]+aa*(1-exp(-lnw/bb))*(1+lnw/bb)
  }
  else if (m==3) {
    yf<-yy[1]+aa*(1-exp(-lnw/bb))*(1+lnw/bb+(lnw/bb)^2/2)
  }
  else if (m==4) {
    yf<-yy[1]+aa*(1-exp(-lnw/bb))*(1+lnw/bb+(lnw/bb)^2/2+(lnw/bb)^3/6)
  }
  return(xnls,xf,yf)
}

```

```

}

findfs2_function(data,a,b,m){
  dev<-data$Col1
  n<-length(dev)
  yy<-data$Col2
  xy<-data.frame(x=dev,y=yy)
  param(xy,"A")<-a
  param(xy,"B")<-b
  param(xy,"C")<-dev[1]
  param(xy,"D")<-yy[1]

  if(m==1){
    xy.nls<-nls(y~D+A*(1-exp(-(x-C)/B)*(1)),xy,trace=T)
  }
  else if (m==2) {
    xy.nls<-nls(y~D+A*(1-exp(-(x-C)/B)*(1+(x-C)/B)),xy,trace=T)
  }
  else if (m==3) {
    xy.nls<-nls(y~D+A*(1-exp(-(x-C)/B)*(1+(x-C)/B+((x-
C)/B)^2/2)),xy,trace=T)
  }
  else if (m==4) {
    xy.nls<-nls(y~D+A*(1-exp(-(x-C)/B)*(1+(x-C)/B+((x-C)/B)^2/2+((x-
C)/B)^3/6)),xy,trace=T)
  }

  xnls<-xy.nls
  aa<-coef(xnls) [1]
  bb<-coef(xnls) [2]
  cc<-coef(xnls) [3]
  dd<-coef(xnls) [4]
  xf<-dev
  lnw<-dev-cc

  if(m==1) {
    yf<-dd+aa*(1-exp(-lnw/bb)*(1))
  }
  else if (m==2) {
    yf<-dd+aa*(1-exp(-lnw/bb)*(1+lnw/bb))
  }
  else if (m==3) {
    yf<-dd+aa*(1-exp(-lnw/bb)*(1+lnw/bb+(lnw/bb)^2/2))
  }
  else if (m==4) {
    yf<-dd+aa*(1-exp(-lnw/bb)*(1+lnw/bb+(lnw/bb)^2/2+(lnw/bb)^3/6))
  }
  return(xnls,xf,yf)
}

cb<-c(0.1,1e-20,0.1)
ce<-c(90,1e-15,90)
gamc2(g9dgfs,2,cb,ce,40,20,20,2^0.5,1e-5)

xx<-mcfits2(g9dgfs,2,c(24.60858,0, 52.24893))
yy<-cbind(xx$dev,xx$measured)

xxx_findfs2(yy,-0.3,18,3)

```

```
plot(yy$Col1,yy$Col2)
lines(xxx$xf,xxx$yf)
xxx
```